

SERI/STR-255-3040
DE87001167

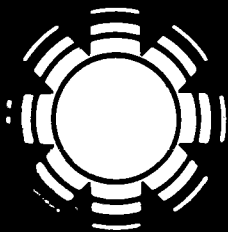
March 1987

**Evaluation of Cermet
Selective Absorber
Coatings Deposited by
Vacuum Sputtering**

Final Subcontract Report

J. A. Thornton
J. A. Lamb
Telic Company
Santa Monica, California

Prepared under Subcontract No. XP-9-8260-1



SERI

Solar Energy Research Institute

A Division of Midwest Research Institute

1617 Cole Boulevard
Golden, Colorado 80401-3393

Operated for the

U.S. Department of Energy

under Contract No. DE-AC02-83CH10093

SERI/STR-255-3040
UC Categories: 59a, 62b,c
DE87001167

Evaluation of Cermet Selective Absorber Coatings Deposited by Vacuum Sputtering

Final Subcontract Report

J. A. Thornton
J. A. Lamb
Telic Company
Santa Monica, California

March 1987

SERI Technical Monitor: James M. Lefferdo

Prepared under Subcontract No. XP-9-8260-1

Solar Energy Research Institute

A Division of Midwest Research Institute

1617 Cole Boulevard
Golden, Colorado 80401-3393

Prepared for the
U.S. Department of Energy
Contract No. DE-AC02-83CH10093

NOTICE

This report was prepared as an account of work sponsored by the United States Government. Neither the United States nor the United States Department of Energy, nor any of their employees, nor any of their contractors, subcontractors, or their employees, makes any warranty, expressed or implied, or assumes any legal liability or responsibility for the accuracy, completeness or usefulness of any information, apparatus, product or process disclosed, or represents that its use would not infringe privately owned rights.

Printed in the United States of America
Available from:
National Technical Information Service
U.S. Department of Commerce
5285 Port Royal Road
Springfield, VA 22161

Price: Microfiche A01
Printed Copy A05

Codes are used for pricing all publications. The code is determined by the number of pages in the publication. Information pertaining to the pricing codes can be found in the current issue of the following publications, which are generally available in most libraries: *Energy Research Abstracts (ERA)*; *Government Reports Announcements and Index (GRA and I)*; *Scientific and Technical Abstract Reports (STAR)*; and publication, NTIS-PR-360 available from NTIS at the above address.

PREFACE

The research and development described in this document was conducted within the U.S. Department of Energy's (DOE) Solar Thermal Technology Program. The goal of this program is to advance the engineering and scientific understanding of solar thermal technology and to establish the technology base from which private industry can develop solar thermal power production options for introduction into the competitive energy market.

Solar thermal technology concentrates the solar flux using tracking mirrors or lenses onto a receiver where the solar energy is absorbed as heat and converted into electricity or incorporated into products as process heat. The two primary solar thermal technologies, central receivers and distributed receivers, employ various point and line-focus optics to concentrate sunlight. Current central receiver systems use fields of heliostats (two-axis tracking mirrors) to focus the sun's radiant energy onto a single, tower-mounted receiver. Point focus concentrators up to 17 meters in diameter track the sun in two axes and use parabolic dish mirrors or Fresnel lenses to focus radiant energy onto a receiver. Troughs and bowls are line-focus tracking reflectors that concentrate sunlight onto receiver tubes along their focal lines. Concentrating collector modules can be used alone or in a multimodule system. The concentrated radiant energy absorbed by the solar thermal receiver is transported to the conversion process by a circulating working fluid. Receiver temperatures range from 100°C in low-temperature troughs to over 1500°C in dish and central receiver systems.

The Solar Thermal Technology Program is directing efforts to advance and improve each system concept through solar thermal materials, components, and subsystems research and development and by testing and evaluation. These efforts are carried out with the technical direction of DOE and its network of field laboratories that works with private industry. Together they have established a comprehensive, goal-directed program to improve performance and provide technically proven options for eventual incorporation into the Nation's energy supply.

To successfully contribute to an adequate energy supply at reasonable cost, solar thermal energy must be economically competitive with a variety of other energy sources. The Solar Thermal Technology Program has developed components and system-level performance targets as quantitative program goals. These targets are used in planning research and development activities, measuring progress, assessing alternative technology options, and developing optimal components. These targets will be pursued vigorously to ensure a successful program.

This report documents the work performed by an industrial organization, Telic, Inc., to build upon the ideas developed at Cornell University. Although selective absorber coatings are of primary interest in low-concentration, line focus systems operating at temperatures of up to 350°C, the performance of the Cermet coating described in this report may allow its use at higher temperatures, perhaps up to 600°C, and in higher concentration systems including cen-

tral receivers and dish technologies. The tests performed at the Solar Energy Research Institute during the course of this research support the data obtained and reported here.

The coatings were not subjected to thermal cycling for extended duration as a part of this effort. The work was completed in 1982, and since then, funding limitations did not allow further work to evaluate the coating performance in a line focus solar collector system nor to evaluate its high-temperature performance. The report is being published without such additional information.

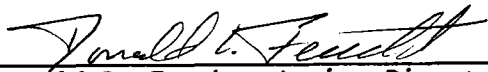
We appreciate the effort of James Lefferdo, Georgia Tech Research Institute; Craig Tyner, Sandia National Laboratories-Albuquerque; and Jacques Hull, Accurex, in reviewing the report; their constructive comments were helpful.

Approved for

SOLAR ENERGY RESEARCH INSTITUTE



B. P. Gupta, Leader
Solar Thermal Program



Donald L. Feucht, Acting Director
Solar Heat Research Division

SUMMARY

In a preliminary investigation at Cornell University it was shown that Pt/Al₂O₃ cermet coatings with graded Pt composition profiles could be deposited by co-evaporation in forms that yielded excellent selective absorber properties and thermal stability at 600°C in air. The co-evaporation method is difficult to apply to the variety of substrates that are of interest for medium and high temperature solar thermal receivers.

Accordingly, this project was undertaken to investigate the use of sputtering. Three coating configurations were examined: (1) cermets with graded Pt composition and Al₂O₃ antireflection layers; (2) cermets with uniform Pt compositions and Al₂O₃ antireflection layers; and (3) Al₂O₃-M-Al₂O₃ type coatings with Pt/Al₂O₃ M-layers. Sputter co-deposition was used to form the cermet layers. Direct rf sputtering of alumina and dc reactive sputtering of aluminum were investigated as methods for depositing the Al₂O₃. The rf sputtered Al₂O₃ was found to yield coatings with superior thermal stability. Thus, when deposited with rf-sputtered Al₂O₃ onto Pt base layers at elevated temperatures, all three of the coating configurations listed above were stable in air at 600°C. Absorptances were in the range 0.90 to 0.95.

The graded cermet coatings appear to be the generally most useful of the three types examined. Optimized coatings on Pt coated glass substrates have yielded absorptances of 0.97 and room temperature emittances of about 0.08. Alternative IR reflector layer materials such as Cr, Mo, Ta, W and ZrB₂ were investigated and concluded to be limited to low temperature (~400°C) applications. Substrate surface polishing is concluded to be an important consideration affecting the optical properties and thermal stability of coatings deposited onto engineering substrates such as stainless steel and Incoloy. An Al₂O₃ diffusion barrier, between the substrate and the IR reflector layer, was required to achieve maximum thermal stability for coatings deposited onto the engineering substrates. Experiments are described in which 24 inch long receiver tubes were coated with Pt/Al₂O₃ graded cermet coatings by sputtering.

TABLE OF CONTENTS

	Page
1. PROJECT DESCRIPTION.....	1
1.1 Overall Objective.....	1
1.2 Project Status.....	5
2. COATING DEPOSITION AND EVALUATION PROCEDURES.....	10
2.1 Deposition Apparatus and Procedures.....	10
2.2 Coating Optical Measurements.....	14
2.3 Thermal Stability Tests.....	15
3. GRADED CERMET OPTIMIZATION STUDIES.....	16
3.1 Introduction.....	16
3.2 Specification of Deposition Conditions.....	16
3.3 Results of Optimization Experiments.....	20
3.4 Thermal Stability Studies.....	42
3.5 Cermet Microstructure.....	42
4. ALTERNATE IR REFLECTOR LAYER MATERIALS.....	45
5. EXAMINATION OF ENGINEERING SUBSTRATES.....	55
6. TUBE COATING EXPERIMENTS.....	62
6.1 Objective and Apparatus Design.....	62
6.2 Considerations Relating to Coating Uniformity.....	64
6.3 Coating Experiments.....	77
7. SUMMARY.....	82
REFERENCES.....	87

LIST OF TABLES AND FIGURES

	Page
FIG. 1. Schematic representation of graded cermet type coating investigated at Cornell University.....	2
FIG. 2. Schematic representation of basic Pt/Al ₂ O ₃ cermet coating configurations investigated on present program.....	4
FIG. 3. Apparatus configuration used to deposit Pt/Al ₂ O ₃ cermet coatings during Phase III Research.....	11
FIG. 4. Photograph of deposition apparatus.....	12
FIG. 5. Shape of Pt volume fraction versus depth profile that is expected for coating deposited with Pt deposition rate that is graded linearly with time.....	19
FIG. 6. Correlation between Pt volume fraction estimated from deposition conditions and Pt composition (atomic percent) measured by Auger depth profiling.....	22
TABLE I Optical properties of graded cermet coatings deposited during optimization study and tested at Battelle.....	23
FIG. 7. Dependence of the absorptance on the substrate drum rotational speed for coatings deposited using both direct rf and reactive sputtered Al ₂ O ₃	26
FIG. 8. Auger depth profile composition analysis of graded cermet coating (sample 1241) with d _{Al₂O₃} thickness of 42 nm and F-value at cermet base of 0.67.....	27
FIG. 9. Auger depth profile composition analysis of graded cermet coating (sample 1373) with d _{Al₂O₃} thickness of 70 nm and F-value at cermet base of 0.55.....	28
FIG.10. Auger depth profile composition analysis of graded cermet coating (sample 1204) with d _{Al₂O₃} thickness of 140 nm and F-value at cermet base of 0.38.....	29
FIG.11. Spectral reflectance data for graded cermet coating (sample 1373) with d _{Al₂O₃} thickness of 70 nm and F-value at cermet base of 0.55. Auger depth profile data are given in Fig. 9..	30

LIST OF TABLES AND FIGURES

	Page
FIG.12. Spectral reflectance data for graded cermet coating (sample 1204) with $d_{Al_2O_3}$ thickness of 140 nm and F-value at cermet base of 0.38. Auger depth profile data are given in Fig. 10..	31
FIG.13. Spectral reflectance data for graded cermet coating (sample 1241) with $d_{Al_2O_3}$ thickness of 42 nm and F-value at cermet base of 0.67. Auger depth profile data are given in Fig. 8...	32
FIG.14. Spectral reflectance data for graded cermet coating (sample 1544) with $d_{Al_2O_3}$ thickness of 70 nm, F-value at base of cermet of 0.55, and near-optimum antireflection layer thickness.....	35
FIG.15. Spectral reflectance data for graded cermet coating (sample 1281) with $d_{Al_2O_3}$ thickness of 42 nm and F-value at the cermet base of 0.55.....	36
FIG.16. Spectral reflectance data for graded cermet coating (sample 1400) with $d_{Al_2O_3}$ thickness of 42 nm, F-value at base of cermet of 0.55, and near-optimum antireflection layer thickness.....	37
FIG.17. Spectral reflectance data for graded cermet coating (sample 1568) with $d_{Al_2O_3}$ thickness of 25 nm, F-value at base of cermet of 0.55, and near-optimum antireflection layer thickness.....	39
FIG.18. Hemispherical absorptance versus antireflection layer thickness for graded cermet coatings having cermet layers of various thicknesses.....	40
FIG.19. Spectral reflectance data for graded cermet coating (sample 1460) with $d_{Al_2O_3}$ thickness of 70 nm, F-value at base of cermet of 0.55, and near-optimum antireflection layer thickness.....	41
TABLE II Optical properties of graded cermet coatings with alternative IR reflector layers.....	47
FIG.20. Temperature dependence of emittance for graded cermet coatings with tungsten low emittance base layers (calculated from reflectance measurements).....	48

LIST OF TABLES AND FIGURES

	Page
TABLE III Results of thermal stability tests for graded cermet coatings with alternative IR reflector layer materials.....	50
FIG.21. Spectral reflectance data for graded cermet coating with tantalum low emittance base layer (sample 1270) after heat treatment in air for 800 hrs at 400°C.....	52
FIG.22. Spectral reflectance data for graded cermet coating with ZrB ₂ low emittance base layer (sample 1365) after heat treatment in air for 600 hrs at 400°C.....	53
TABLE IV Comparison of optical properties for graded cermet coatings on glass and engineering substrates.....	58
TABLE V Results of thermal stability tests for graded cermet coatings deposited onto engineering substrate materials.....	59
FIG.23. Schematic illustration of production apparatus for depositing Pt/Al ₂ O ₃ graded cermet coatings onto tubular substrates.....	63
FIG.24. Schematic illustration of bench scale apparatus that was used for depositing Pt/Al ₂ O ₃ graded cermet coatings onto tubular substrates.....	65
FIG.25. Photograph of bench scale apparatus that was used for depositing Pt/Al ₂ O ₃ graded cermet coatings onto tubular substrates...	66
FIG.26. Deposition rate profiles along the long axis of a 5 inch x 15 inch planar magnetron with an alumina (Al ₂ O ₃) target and a 5 inch x 12 inch planar magnetron with a platinum target...	68
FIG.27. Deposition rate profiles along the short axis of a 5 inch x 15 inch planar magnetron with an alumina (Al ₂ O ₃) target and a 5 inch x 12 inch planar magnetron with a platinum target....	69
FIG.28. Shield or mask configuration for producing uniform deposition onto moving substrates.....	70
FIG.29. Production coating configuration which uses a plurality of relatively short magnetron sputtering sources to deposit uniform coatings onto long tubular substrates.....	71

LIST OF TABLES AND FIGURES

	Page
FIG.30. Calculated Pt volume fraction as function of depth, showing the effect of the axial variations in the Pt and Al_2O_3 deposition profiles for a substrate element that makes one pass in the axial direction during the time that the F-value grading takes place.....	74
FIG.31. Calculated Pt volume fraction as function of depth for an element on the surface of a tube which is about equal in length to the deposition sources and makes six single passes (down or back) in front of the sources during the time that the F-value grading takes place.....	75
FIG.32. Approximate axial profiles for the cermet and antireflection layer thicknesses that were deposited in the final sequence of bench type tube coating experiments.....	79
FIG.33. Photograph showing several of the tubes that were coated during the bench type proof-of-concept experiments.....	80

1. PROJECT DESCRIPTION

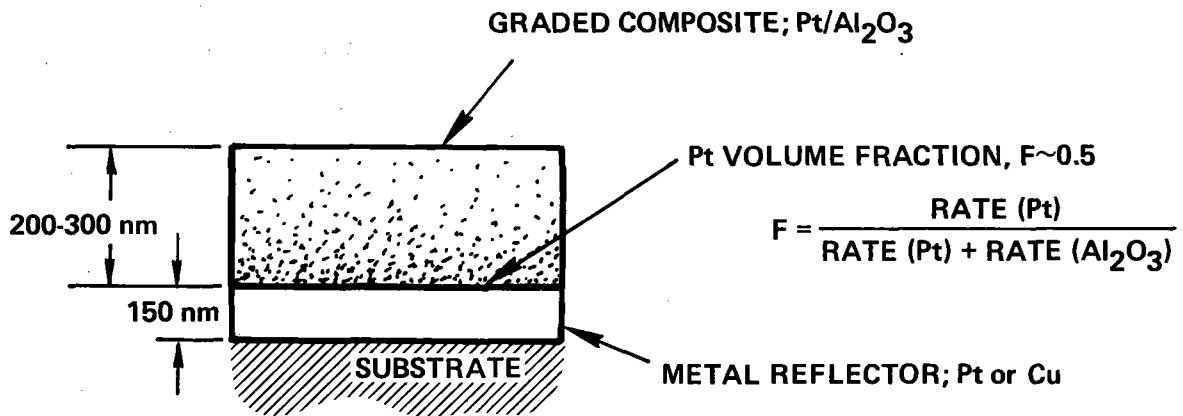
1.1 Overall Objective

A wide range of selective absorber coatings have been reported.¹⁻³ However, most of them degrade at temperatures above about 500°C. Higher temperature coatings are required for various types of receivers designed to be used with tracking concentrators and operating temperatures of 400°C or greater.

In 1979 a type of Pt-Al₂O₃ cermet coating with remarkable thermal stability was reported by a group at Cornell University.⁴⁻⁵ The coatings were typically about 200-300 nm thick and had graded platinum contents which varied from about 50 volume percent at the rear surface to zero at the front surface. See Fig. 1. They were deposited by electron beam co-evaporation onto copper, or platinum-coated quartz substrates maintained at about 500°C. Normal absorptances in the range from 0.80 to 0.94 with hemispherical emittances at 150°C of from 0.08 to 0.19 (the highest emittances corresponding to the highest absorptances) were reported for the coatings on copper base layers. Of particular importance was the observation that a coating on a platinum-coated quartz substrate showed no change in optical properties after being heated in air for 300 hrs at 600°C.

The co-evaporation method used in the Cornell work is difficult to apply to the variety of substrate shapes, such as large flat panels, long tubes, and the inside and outside surfaces of cylinders, hemispheres, and domes, which are of interest for high temperature solar collectors. Sputtering, by contrast, is applicable to such complex shapes, and magnetron sputtering⁶ in particular is capable of depositing uniform coatings over large surface areas.⁷ The purpose of this project was to investigate the use of magnetron sputtering to deposit Pt/Al₂O₃ cermet selective absorber coatings on a commercial scale (10⁴ to 10⁶ m²/yr).

The project was divided into three phases. The first phase consisted of confirming that Pt/Al₂O₃ cermet coatings comparable to those produced at Cornell could be deposited by sputtering. The first phase also included modeling studies to examine coating and apparatus configurations and the associated



$\alpha = 0.80$	$\epsilon (150^\circ\text{C}) = 0.08$
$= 0.89$	$= 0.12$
$= 0.94$	$= 0.19$

Pt/Al₂O₃ COATING

REFLECTOR - Pt

SUBSTRATE - QUARTZ

THERMAL STABILITY - 300 hr at 600°C in Air.

FIG. 1. Schematic representation of graded cermet type coating investigated at Cornell University.

production costs for the various classes of substrates listed below.

- Flat Panels
(2 ft x 10 ft)
- Outer Surface of Straight Tubes
(Up to 2 in. diam x 10 ft. long)
- Inner and Outer Surfaces of Domes
(Up to 12 in. diam)
- Inner and Outer Surfaces of Hemispheres
(Up to 12 in. diam)
- Inner and Outer Surfaces of Cylinders
(Up to 12 in. diam)

The second phase examined general deposition parameters such as coating thickness, platinum content, and substrate temperature for three different types of Pt/Al₂O₃ cermet coating configurations that were identified in the Phase I work as having promise for various applications. The configurations, which are shown in Fig. 2, were:

- The basic Cornell type Pt/Al₂O₃ cermet with a graded Pt content, as shown in Fig. 2b.
- A cermet layer with uniform Pt content overcoated with an Al₂O₃ antireflection coating, as shown in Fig. 2a. This type of coating was investigated for application to confined inner surfaces where co-deposition to produce a graded composition would be difficult.
- A multi-layer AMA-type coating which places a thin Pt/Al₂O₃ layer with a high Pt content (~80 volume percent) between two Al₂O₃ layers, as shown in Fig. 2c. The AMA type coating was examined as an alternative configuration which would require less platinum.

Most of the coatings were deposited by co-deposition from Pt and Al₂O₃ sources. Both direct rf sputtering of alumina, and dc reactive sputtering of aluminum in an argon-oxygen atmosphere, were investigated for depositing the Al₂O₃ component in all of the coating types. Direct sputtering from a Pt/Al₂O₃ cermet target was also investigated for depositing the uniform cermet coatings. Both cylindrical and planar magnetron sources were examined, because no single source type was convenient for coating all of the substrate shapes of interest.

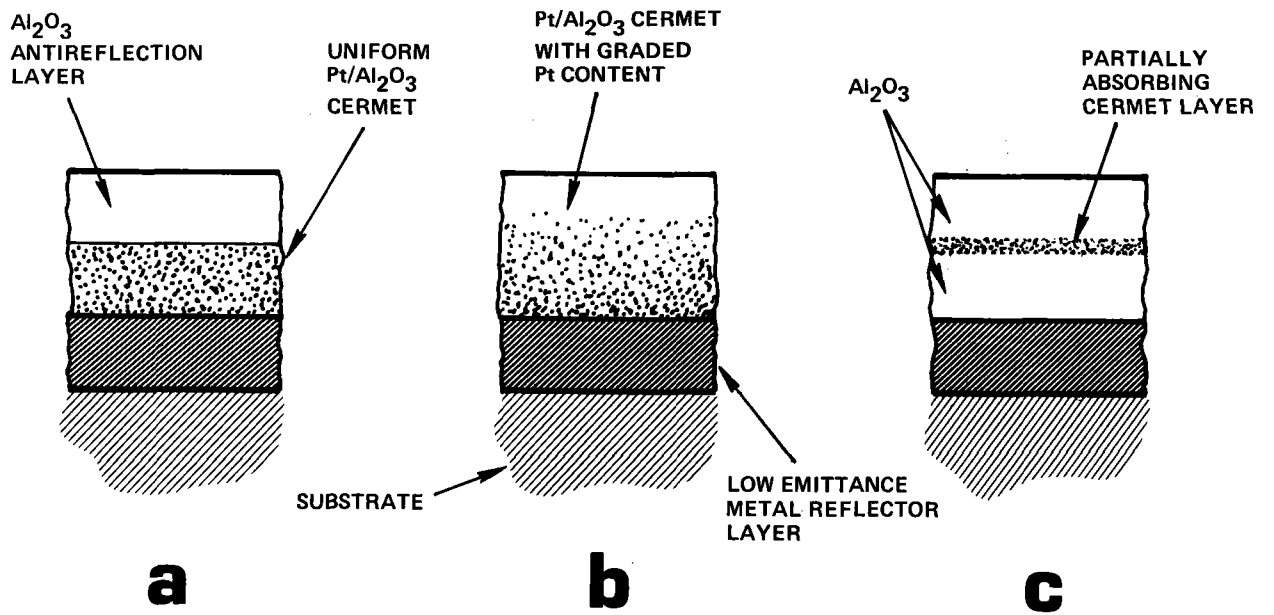


FIG. 2. Schematic representation of basic Pt/Al₂O₃ cermet coating configurations that were investigated on present program.

The use of platinum for the low emittance base layer causes this layer to become a major contributor to the overall coating cost. Therefore, molybdenum and chromium were also investigated as base layer materials for the uniform cermet and AMA type coatings.

The results of the Phase I and Phase II investigations were described in detail in an interim report (Ref. 8). Preliminary reports were given in Refs. 9 through 11. The Phase I/Phase II results are summarized in the following section. However, the primary emphasis in this report is on the results of the Phase III investigation. The objectives of this phase were to:

- Further optimize the graded cermet and AMA type coatings for use at operating temperatures of about 400°C.
- Examine tantalum, tungsten, and zirconium diboride as alternative low emittance (IR reflector) layers.
- Examine Pt/Al₂O₃ cermet coatings deposited onto engineering materials of potential interest. These are type 316 stainless steel, Incoloy 800, and low carbon steel.
- Deposit graded-cermet type Pt/Al₂O₃ coatings onto 1 1/4 inch outside diameter by 1 inch inside diameter by 24 inch long receiver tube sections.

1.2 Project Status

The Phase I investigation confirmed that Pt/Al₂O₃ cermet selective absorber coatings could be deposited by sputtering to achieve the same thermal stability that had been reported for the Cornell coatings. Coatings having graded Pt contents and direct rf sputtered Al₂O₃, which were deposited onto glass substrates with Pt base layers, exhibited no change in absorptance after tests of several hundred hours at 600°C in air. The Pt/Al₂O₃ cermet layers were typically about 100 to 200 nm thick, with a graded Pt content which varied from about 50% by volume at the rear surface, to zero at the top surface. This layer was overcoated by an approximately 30 nm thick Al₂O₃ antireflection layer. Hemispherical absorptances (α) were typically in the range 0.90 to 0.93, with room temperature emittances (ϵ) of about 0.08.

The coatings were estimated to cost about \$5/ft² when deposited over large

surface areas. The cost of such coatings is dominated by the cost of the Pt and therefore is relatively insensitive to the substrate shape (i.e., tubes versus flat plates). It is estimated that the coating cost would be reduced to about \$1-2/ft² if the Pt low emittance base layer were replaced with a lower cost material, and to about \$0.50/ft² if, in addition, the graded cermet layer were replaced by an AMA type coating with a Pt/Al₂O₃ M-layer.

During Phase II all three of the cermet coating configurations shown in Fig. 2 were investigated. Thus, in addition to the basic graded cermet configuration described above and shown in Fig. 2b, the uniform cermet configuration shown in Fig. 2a and the AMA type coating shown in Fig. 2c were also examined. Both direct rf sputtering from an alumina source, and dc reactive sputtering from an aluminum source in an Ar+O₂ atmosphere, were investigated as methods for depositing the Al₂O₃ component of the cermets and the antireflection layers.

The direct rf sputtering method yielded the most stable coatings. When deposited by rf sputtering onto substrates at elevated temperatures (300-500°C), all three of the coating configurations listed above appear to be stable at 600°C in air.

The graded cermet coatings appear to be the generally most useful of the three types examined. The work on the project has therefore concentrated on the graded cermet coatings. Graded cermet coatings with direct rf sputtered Al₂O₃, which were deposited onto Pt coated glass substrates at a temperature of 350°C during the Phase II research, showed no change in optical properties after being maintained at 600°C in air for 700 hrs. Similar coatings on type 316 stainless steel substrates with a 50 nm diffusion barrier between the stainless steel and the Pt base layer showed no change in optical properties after being exposed to 2800 suns--i.e., a radiation power density of 2.8 MW/m²--for 2 hrs.¹² It was shown that the graded cermet configuration permits high absorptances (0.93-0.94) to be consistently achieved, even on glass substrates. Furthermore, it was found that relatively sharp cut-off wavelengths could be

obtained. Thus it is possible to maintain high α/ϵ ratios, even at elevated operating temperatures. Typical room temperature α/ϵ values were in the range 10 to 17. Emittances for coatings on Pt-coated glass substrates varied from 0.06 to 0.08 at 20°C, to 0.15 to 0.20 at 500°C. The exact thickness, Pt content, or grading profile do not appear to be critical. This is an important advantage for the coating of complex shaped substrates.

The uniform cermet coatings consisted of a Pt/Al₂O₃ cermet about 100 nm thick, with a uniform Pt content of about 40% by volume, and a 70 nm thick antireflection layer. Hemispherical absorptances were typically about 0.90. However, long wavelength interference effects caused the emittances to be relatively high at room temperature (0.15 to 0.20) and to increase rapidly with increasing temperature. This limits the usefulness of these coatings for high temperature applications.

The multi-layer AMA type coatings consisted of a Pt layer about 5 nm thick, containing about 20% by volume Al₂O₃, which was sandwiched between two Al₂O₃ layers, about 40 nm thick. These coatings typically yielded hemispherical absorptances of about 0.92 with room temperature emittances of about 0.08. The low Pt content makes these coatings attractive for simple substrate shapes where the individual layer thicknesses could be controlled accurately. However, the critical nature of the coating layer thicknesses and interference effects makes these coatings less attractive for substrates of complex shape.

Reactive sputtering is desirable because of its potential for scaling to large production volumes at low cost. The cermet coatings deposited by both direct rf sputtering and reactive sputtering during the Phase II research appeared to have very similar integrated optical properties (absorptance and emittance). However, the reactive sputtered Al₂O₃ that we have deposited, at least thus far, is inferior to the direct rf sputtered Al₂O₃ as a diffusion barrier.^{13,14} In the case of graded cermet coatings on Pt coated glass substrates, Pt diffusion simply tends to change the Pt composition profile, and little change is seen in the absorptance or emittance, since these parameters

are relatively insensitive to this profile.⁴ However, for the cases of (1) coatings on metal substrates with an Al_2O_3 diffusion barrier between the substrate and the low emittance base layer, or (2) coatings which use a material other than Pt as a low emittance base layer, we found that the poor diffusion barrier properties of the reactive sputtered Al_2O_3 reduced the thermal stability of the coatings. Therefore, it is anticipated that reactive sputtering will find application primarily for coatings designed for low and medium rather than high temperature applications.

Elevated substrate temperatures in the range 350°C to 500°C was found to yield coatings with the greatest thermal stability. This was the case for all three of the coating types and for Al_2O_3 deposited by both direct rf sputtering and reactive sputtering.

The use of Cr or Mo as alternative low emittance base layer materials was investigated during the Phase II research. Base layers of these materials appeared to make the coatings more sensitive to the diffusion barrier quality of the Al_2O_3 and in general to compromise the thermal stability. Thus uniform cermet and AMA type coatings with rf sputtered Al_2O_3 deposited onto Cr and Mo at elevated substrate temperatures were found to be stable to about 500°C but to undergo changes in absorptance in the 550 to 600°C range.⁹ The use of lower substrate temperatures with these base layer materials yielded coatings that were stable at 400°C but subject to degradation in the 450 - 600°C range.

The work during Phase III has concentrated on a particular application: the use of graded cermet coatings for solar thermal receiver tubes operating at temperatures of about 400°C . Graded cermet coatings deposited by rf sputtering, at sufficiently low substrate temperatures ($\sim 150^\circ\text{C}$) to be suitable for large scale production, were shown to be stable in the 400 to 500°C range in tests lasting as long as 1100 hrs.

Optimization of the antireflection layer thickness has yielded graded cermet coatings on glass substrates with hemispherical absorptances as high as 0.97. The optimization studies have also shown that absorptances of about 0.95 can be

obtained for cermet layers that are sufficiently thin to reduce the cermet layer Pt cost to about \$1/ft² and therefore to vindicate earlier projections.

The use of Ta, W, and ZrB₂ was investigated as alternative reflector layer materials to replace Pt. Bare films of Ta and W underwent severe oxidation in tests at 400°C in air. Therefore, the long term stability of coatings incorporating these materials as base layers is in doubt. Zirconium diboride is more stable and shows promise for modest temperature (~400°C) applications. However, the sputtered ZrB₂ coatings tended to have relatively high emittances (~0.2).

An investigation of engineering substrates (type 316 stainless steel, Incoloy 800, and low carbon steel) reconfirmed the importance of the substrate surface roughness on the coating optical properties and thermal stability. Thus emittances of coatings deposited onto unpolished stainless steel and Incoloy substrates were typically a factor of two higher than for identical coatings deposited onto glass substrates or on relatively smooth cold rolled mild steel substrates. The substrate roughness is believed to affect the coating thermal stability through its influence on the porosity of the cermet layer, and particularly the Al₂O₃ diffusion barrier which is deposited between the substrate and the low emittance base layer.

A bench scale coating apparatus which had the same general design configuration that is envisioned for production coating of tubular collectors was assembled. The apparatus is capable of simultaneously depositing graded cermet coatings onto a load of twelve 1 1/4 inch diameter by 24 inch long tubes. A batch of ten type 316 stainless steel tubes, that were coated during the shake-down tests on the apparatus, has been sent to SERI for evaluation.

2. COATING DEPOSITION AND EVALUATION PROCEDURES

2.1 Deposition Apparatus and Procedures

During the Phase III research most of the Pt/Al₂O₃ cermet coatings were formed by co-deposition from an rf driven alumina source and a dc driven Pt source. The apparatus is shown schematically in Fig. 3. A photograph of the apparatus is shown in Fig. 4. Three planar magnetron sputtering sources¹⁵ were attached to a frame surrounding a substrate mounting drum. The target-to-substrate distance was 76 mm. The drum was configured to mount eight substrates (about 50 mm x 150 mm). A stationary array of eight quartz heating lamps was located within the drum assembly. The frame was mounted on wheels which permitted the assembly to be rolled on a pair of rails into a 1m diameter vacuum chamber.

Two of the magnetron sources were designed to mount 5x12 inch targets. They were driven by dc power supplies. One of these was used to sputter the Pt. The other was used to sputter Ta, W, and ZrB₂, which were investigated as alternative low emittance base layer materials to replace Pt. The third magnetron was designed to mount a 5x15 inch target. This source was used to deposit the Al₂O₃ layers by direct rf sputtering from an alumina target and, in a few cases, by reactive sputtering from an Al target.

The target specifications are listed below.

Platinum - Target was 30 mil thick Pt sheet of 99.99% purity which was solder bonded to a 5x12x3/8 inch Cu plate. Supplied by Engelhard Industries, Carteret, NJ.

Tantalum - Target was 10 mil thick Ta sheet of commercial purity, which was solder bonded to a 5x12x3/8 inch Cu plate. The Ta sheet was supplied by R.D. Mathis Company, Long Beach, CA. Solder bonding was performed by Sputtering Materials Inc., Santa Clara, CA.

Tungsten - Target was 1/8 inch thick plate of commercial purity which was solder bonded to a 5x12x3/8 inch Cu plate. The W plate was supplied by Teledyne Wah Chang, Huntsville, AL. Solder bonding was performed by Sputtering Materials Inc., Santa Clara, CA.

ZrB₂ - Target was 1/4 inch thick plate of 99% purity which was formed in two sections by powder metallurgy methods and solder bonded to a 5x12x1/4 inch Cu plate. Supplied by Cerac, Inc., Milwaukee, WI.

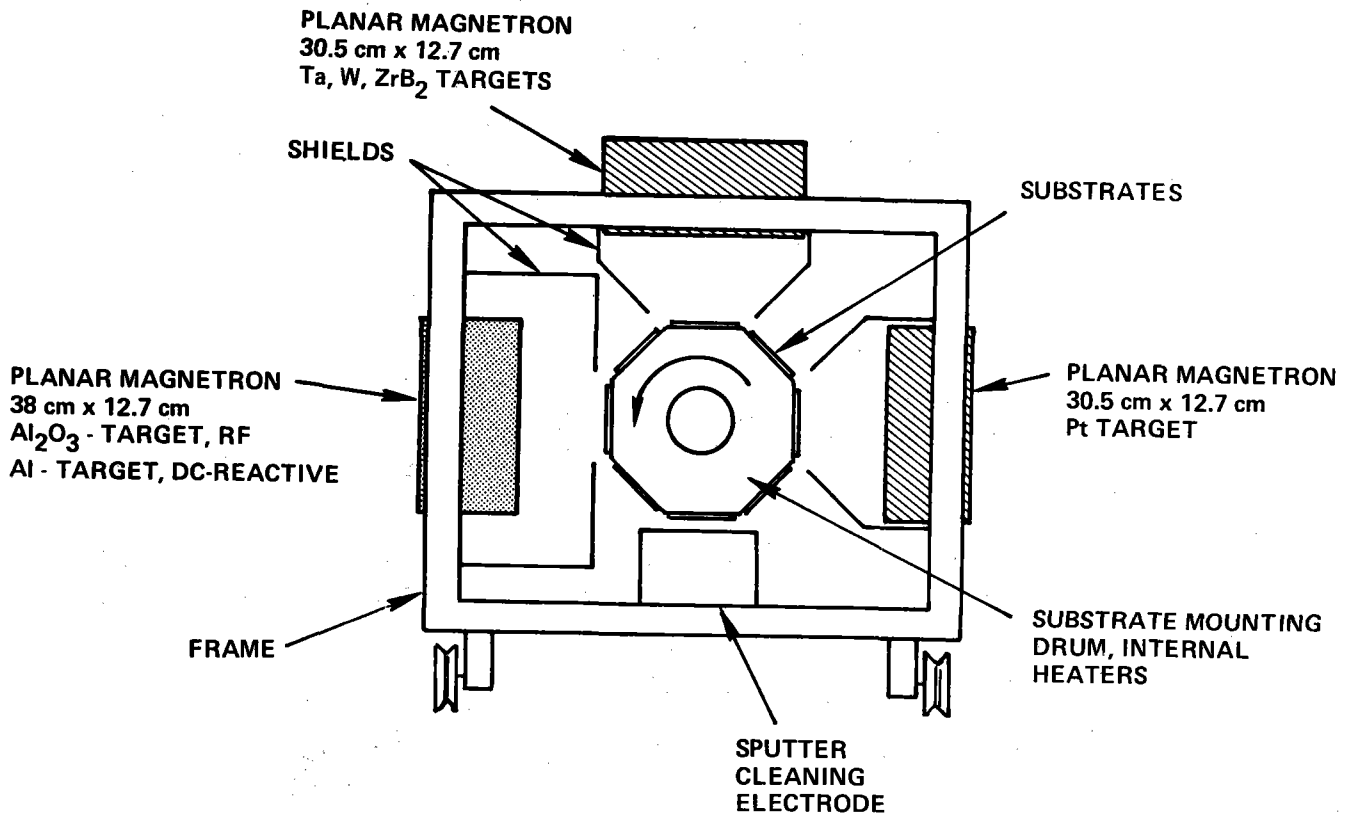


FIG. 3. Apparatus configuration used to form Pt/Al₂O₃ cermet coatings by sputter co-deposition during the Phase III Research.

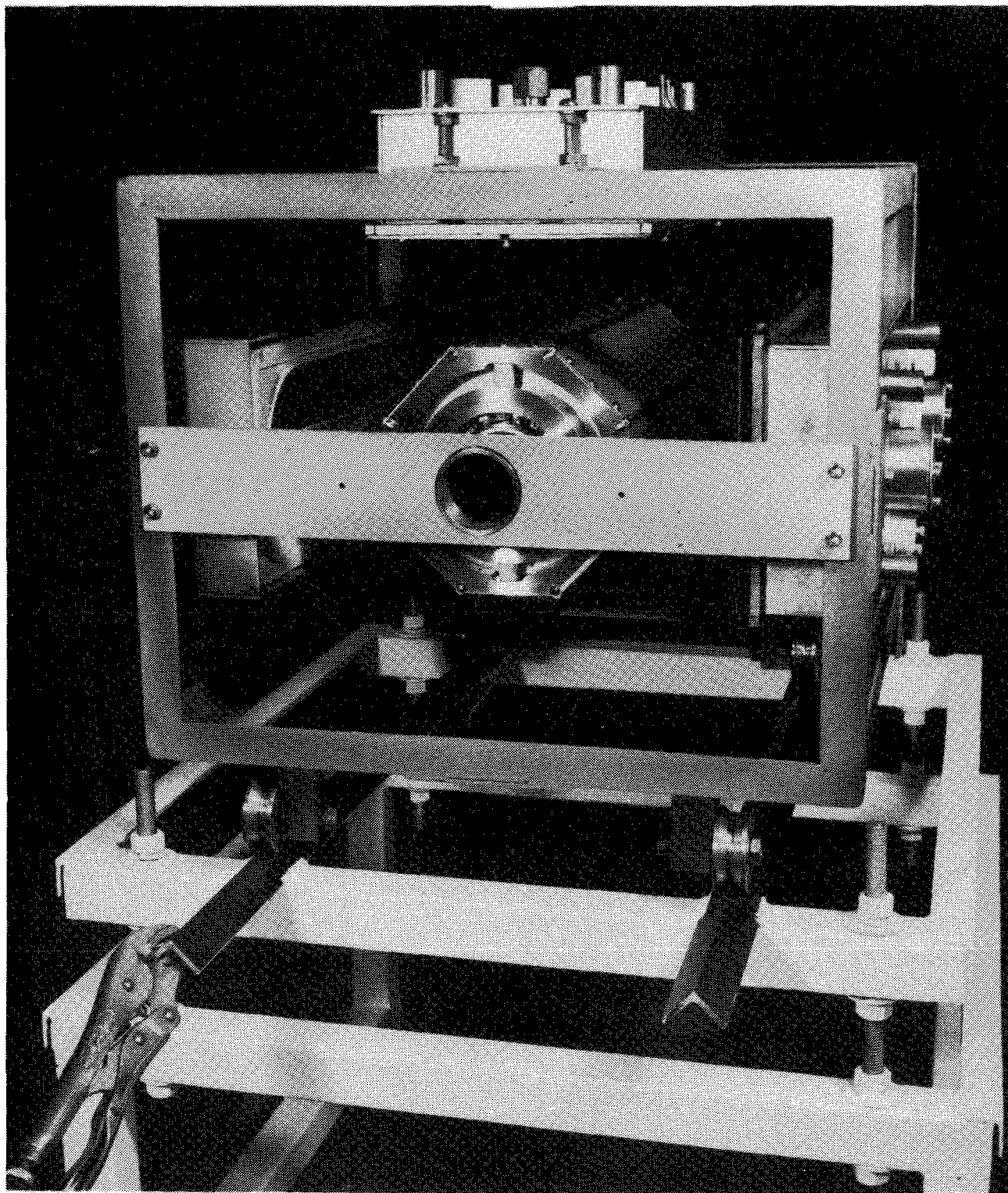


FIG. 4. Photograph of deposition apparatus shown schematically in Fig. 3.

Alumina - Target was 1/4 inch thick Coors type AD-995 alumina (99.5% Al_2O_3) plate which was formed in two sections with a lap joint. Supplied by Coors Porcelain, Golden, CO. The two sections were solder bonded to 5x15x1/4 inch Cu plate, by Sputtering Materials Inc., Santa Clara, CA.

Aluminum - Target was 1/4 inch thick plate of 99.99% Al which was solder bonded to a 5x15x1/4 inch thick Cu plate. Supplied by Varian Specialty Metals Division, Grove City, OH.

The chamber was evacuated to an initial pressure of about 5×10^{-4} Pa with a freon-trapped oil diffusion pump having a speed of about 700 liters/sec for air. Argon at a pressure of 0.16 Pa was used as a working gas for sputtering the metal and alumina. Working gas pressures were measured with a capacitive manometer.

Corning 7059 borosilicate glass plates (25 mm x 25 mm x 1.2 mm) were used as substrates for the optimization studies described in Section 3. The glass substrates were cleaned using a proprietary process and mechanically clamped to larger stainless steel plates which were attached directly to the substrate drum. The stainless steel plates are clearly visible in Fig. 4. These plates were fabricated from type 316 stainless steel. In most of the deposition runs at least one of the stainless steel plates was used directly as a substrate. In addition, type 1020 low carbon steel and Incoloy 800 were evaluated as engineering substrates. The cleaning and deposition procedures for these substrates are described in Section 5. In most cases the metal substrates were small 50 mm x 50 mm x 1 mm plates which were clamped to the larger stainless steel backing plates, following a procedure similar to that used for the glass.

Most of the coatings were deposited without substrate heating. The substrate temperature under typical deposition conditions is estimated to have been about 150°C. A few heated substrate depositions were made at glass substrate temperatures of about 250°C and 350°C. These estimates are based on (1) calibration experiments in which the heaters were operated at various power levels, with glass substrates containing embedded chromel-alumel thermocouples attached to the substrate mounting drum, and on (2) temperature measurements made with an Ircon optical pyrometer.

The deposition procedure was to rotate the drum so that the substrates faced the cathode in question, which was then operated for a prescribed time to deposit the base layer coating. Thus coatings with both Pt and an alternate base layer could be deposited in a given experiment. The Pt/Al₂O₃ cermet coatings were deposited by rotating the substrate drum at speeds of from 0.5 to 10 rpm while simultaneously operating both the Pt and Al₂O₃ sources. The rf driven Al₂O₃ source was operated at a relatively low power level of 500W to avoid target damage. The Al₂O₃ deposition rate was about 0.1 nm/s. The current to the Pt source was controlled with a fixed Al₂O₃ deposition rate to yield cermet coatings with controlled Pt composition profiles. The current to the Pt source was typically in the range between 10 and 60 mA. The Pt deposition rate at 60 mA was about 0.1 nm/s. Shields prevented the sputtered fluxes from the various sources from mixing except at the substrate surface.

A few coatings were deposited with reactive sputtered Al₂O₃ for comparative examinations by transmission electron microscopy. The deposition procedure was identical to that described above, except that the alumina target was replaced with an aluminum one which was operated at a dc discharge current of 6A in an Ar+O₂ mixture. The Ar partial pressure was 0.16 Pa. The oxygen injection rate was 37 sccm and the partial pressure with the discharge in operation was 0.05 Pa. The Al₂O₃ deposition rate was about 0.2 nm/s.

2.2 Coating Optical Measurements

Approximate absorptance and emittance measurements were made at Telic to assist in making day-to-day research decisions and to screen coatings. The measurements were made using an International Technology Wiley Alpha Meter and Ambient Emisometer.

Major coating optical measurements were made at the Battelle Pacific Northwest Laboratory and the Lawrence Berkeley Laboratory. Measurements on a few coatings were made at the Lockheed Palo Alto Research Laboratory. The procedures used in the Lockheed measurements are described in Ref. 8.

Hemispherical reflectance measurements were made at Battelle over the

wavelength range from 300 nm to 2500 nm using a Beckman UV5270 spectrophotometer equipped with an integrating sphere. Hemispherical absorptances were calculated from these measurements using the NASA Air Mass 1.5 solar insolation curve. The Battelle and Lockheed measurements on common test samples were in excellent agreement.

Approximate estimates of the room temperature emittance were made from specular reflectance measurements at 10.6 μm , which were performed at Battelle using a CO_2 laser source. More detailed long wavelength normal reflectance measurements were made on selected samples over the wavelength range from 2 to 50 μm at the Lawrence Berkeley Laboratory, using a Perkin-Elmer Model 283 monochrometer. Total normal emittances for various temperatures were calculated from these measurements using the Planck function.

2.3 Thermal Stability Tests

Thermal stability tests were conducted by placing the substrates on a stainless steel tray which slid between two large steel blocks spaced about 10 mm apart in an electric oven designed for ceramic annealing. The oven temperature was controlled by an on/off Schmidt trigger circuit having a dead band of about 5°C at 300°C, which was connected to an iron constantan thermocouple located within one of the blocks. Most of the tests were conducted at temperatures of 400°C and 500°C. Typical test times were between 100 and 2000 hrs. During the tests approximate absorptance measurements were made at about 100 hr intervals using the International Technology Inc. Alpha Meter. Selected samples were sent to Battelle for spectral reflectance measurements and more accurate determinations of the absorptance.

3. GRADED CERMET OPTIMIZATION STUDIES

3.1 Introduction

The original objective of this task was to further optimize both the graded cermet and AMA type coatings for use at operating temperatures of about 400°C. Our particular interest was on coatings that would be suitable for application to long tubular sections. As the program developed, we concluded that the optimization studies should be restricted to graded cermet coatings in which the Al₂O₃ component was deposited by rf sputtering from an alumina source. The reasons were: (1) the greater stability of coatings with rf sputtered Al₂O₃, and (2) the fact that the critical nature of the coating thicknesses and interference effects make the AMA type coatings less attractive than the graded coatings for substrates of complex shape (See Section 1.2). Particular attention was given in the optimization study to the thicknesses of the cermet and antireflection layers and the cermet Pt content. The layer thicknesses are important in determining the tolerance in deposition conditions that will provide coatings over large areas with uniform optical properties (absorptance and emittance). The Pt content is important in determining the coating cost (see Section 2 in Ref. 8).

3.2 Specification of Deposition Conditions

The optical properties of a graded Pt/Al₂O₃ cermet coating are determined by:

- 1) The surface roughness of the substrate.
- 2) The low emittance base or reflector layer material.
- 3) The thickness of the cermet layer.
- 4) The macroscopic Pt distribution; i.e., the variation of Pt content within the cermet layer.
- 5) The microscopic Pt distribution; i.e., the size and shape of the metal phase particles in the Al₂O₃ host.
- 6) The thickness of the Al₂O₃ antireflection layer.

The effects of the first two variables were eliminated from the present study by using glass substrates and Pt as the low emittance base layer. This also permitted the present work to be compared directly with the majority of

the deposition studies which were conducted during Phases I and II using Pt-coated glass substrates. The use of metal "engineering" substrates and the use of alternative low emittance base layer materials are discussed in Sections 4 and 5 respectively.

As noted above, particular attention was given in the optimization study to the thicknesses of the cermet and antireflection layers and to the cermet Pt content. The thickness and Pt content of the cermet layer are coupled in a rather complex way, both in terms of the mechanics of deposition and in terms of their influence on the coating optical properties as discussed below.

The general procedure when dealing with cermet or granular materials is to specify the metal component in terms of a volume fraction, F .^{4,16} For Pt/ Al_2O_3 cermets deposited by co-deposition from Pt and Al_2O_3 sources, it is convenient to define F in terms of the Pt and Al_2O_3 deposition rates (R)--

$$F = \frac{R_{Pt}}{R_{Pt} + R_{Al_2O_3}} \quad (1)$$

As described in Section 2.1, the procedure in our work was to deposit graded cermet coatings by varying the Pt deposition rate, R_{Pt} , while the Al_2O_3 deposition rate, $R_{Al_2O_3}$, was maintained constant. The effective Pt and Al_2O_3 thicknesses, d_{Pt} and $d_{Al_2O_3}$, which would be present if all the Pt and Al_2O_3 were isolated into independent layers, are useful parameters for estimating coating cost and for specifying the deposition conditions for the cermet layer.⁸ The effective Pt thickness can be estimated from the specified deposition parameters, $d_{Al_2O_3}$ and F , by the relation

$$d_{Pt} = d_{Al_2O_3} \left(\frac{F}{1-F} \right) \psi \quad (2)$$

The parameter ψ is unity for a uniform cermet. For graded cermet coatings we specify F at the base of the cermet layer. For the case of linear grading, $\psi = 1/2$. However, it is important to note that since F does not vary

linearly with R_{Pt} [see Eq.(1)], and since the Pt component contributes to the overall cermet thickness, a linear variation of the R_{Pt} with a fixed $R_{Al_2O_3}$ will not produce a linear variation of F with cermet thickness. The effect is small at low volume fractions but obviously can become very important at the larger F -values of about 50% that were typically used at the base of the cermets. Thus a linear grading of the Pt deposition rate would produce an F versus thickness profile of the form shown in Fig. 5. Theoretical work at Cornell University indicates that although the spectral reflectance is dependent on the volume fraction versus depth profile, the integrated optical properties (absorptance and emittance) are independent of the profile for linear sigmoid and quadratic profiles in which the total integrated Pt content is constant (25%).⁴

Theoretical studies predict that the microscopic metal distribution--i.e., the size and shape of the metal phase particles in the Al_2O_3 host--will have a significant effect on the coating optical properties.¹⁷ In general, we would expect the microscopic Pt distribution to depend on the Ar working pressure during deposition, the substrate temperature, and the Pt and Al_2O_3 deposition rates.¹⁸ Since the present work was conducted at a constant Ar working pressure and Al_2O_3 deposition rate, we expect the primary deposition variables which affect the microscopic Pt distribution to be the substrate temperature, the substrate drum rotation rate, and the Pt deposition rate.

Optimization studies during the second phase of the program yielded the following results for the graded cermet coatings of the type shown in Fig. 2b. See Ref. 8.

- 1) The best optical performance (hemispherical absorptance ~ 0.94 , room temperature emittance ~ 0.07) was generally obtained for coatings with $d_{Al_2O_3} \sim 70$ nm and a graded Pt content which varied from essentially 50 volume percent at the rear surface to zero at the top surface. The low emittance base layer was Pt (~ 100 nm thick). The Al_2O_3 antireflection coating thickness was about 70 nm. The cermet coatings were deposited at a substrate temperature of about 350°C using a substrate drum rotational speed of 1 rpm.

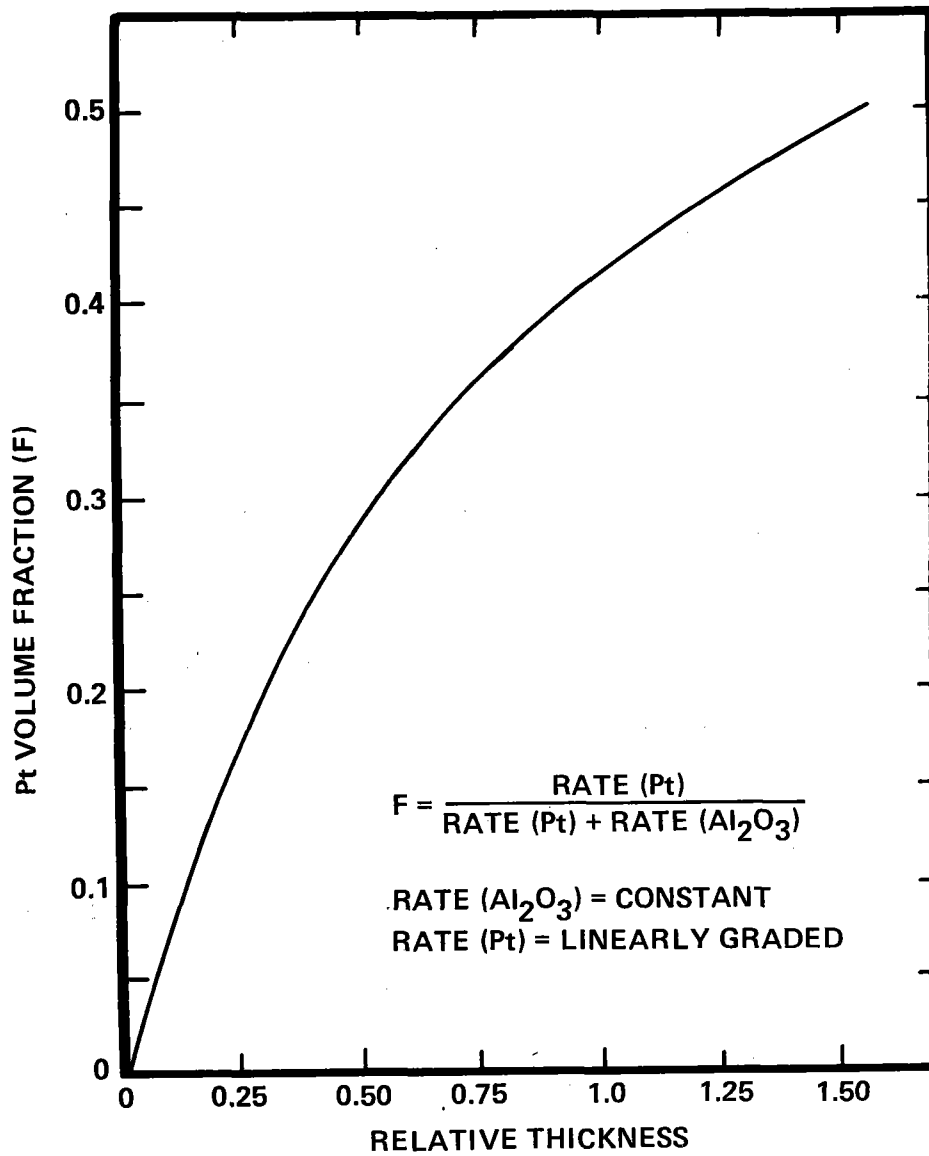


FIG. 5. Shape of Pt volume fraction versus depth profile that is expected for coating deposited with Pt deposition rate that is graded linearly with time, while Al₂O₃ deposition rate is held constant.

- 2) The integrated optical properties (absorptance and emittance) for coatings having the configuration described above were independent of whether the Al_2O_3 component was deposited by direct rf sputtering of alumina or by reactive sputtering from aluminum in an $\text{Ar}+\text{O}_2$ working gas.
- 3) The influence of variations in the substrate drum rotational speed on the absorptance and emittance was investigated over the rotational speed range from 1 to 10 rpm for coatings with reactive sputtered Al_2O_3 layers. Increasing the rotational speed decreased the absorptance and emittance by about 10%.
- 4) The use of a substrate temperature equal to or greater than about 350°C was consistently seen to reduce the emittance by about 40% from that of coatings deposited at about 150°C , although the absorptance was not affected.
- 5) The optical data for the graded and uniform cermet coatings were generally consistent with the proposition that a minimal Pt content, corresponding to an effective Pt thickness, d_{Pt} , of about 40 nm, is necessary to achieve a high absorptance.

Most of the data which provided the tentative conclusions cited above were obtained from coatings having antireflection layers of nearly identical thickness. Particular attention in the present optimization studies was given to further exploring the validity of statement five above in order to determine whether optimized antireflection layer thicknesses might reduce the amount of Pt required. A second objective was to determine the criticality of the antireflection thickness for various cermet layer configurations, in anticipation of depositing coatings with uniform integrated optical properties over large areas or substrates of complex shape (see Section 6).

3.3 Results of Optimization Experiments

The purpose of the optimization studies was to provide coatings suitable for operating temperatures of about 400°C and for application to tubular receivers. Item four above suggests that elevated substrate temperatures ($\sim 350^\circ\text{C}$) provide minimum emittances. In addition, our previous work has shown that, as a general rule, the coatings deposited at an elevated temperature possess the greatest thermal stability.⁸ However, most of the coatings in the present study were deposited without substrate heating at a deposition temperature of

about 150°C. This was done for two reasons: (1) the anticipated receiver operating temperatures (~400°C) are modest, and (2) the elimination of substrate heating greatly simplifies the coating apparatus and the deposition procedures which would be required for production applications (see Section 6). In summary, our goal was to optimize the coatings within a framework that was considered reasonable for large scale production. A few graded cermet coatings were deposited during the present work at a substrate temperature of about 250°C. These coatings, in fact, exhibited no significant difference in absorptance or emittance from coatings deposited under otherwise identical conditions at about 150°C.

Figure 6 compares atomic compositions based on Auger depth profile analysis to the F-values (volume percent) that were thought to be built into the coatings based on the deposition conditions. The large solid circular data points are from the current optimization studies. The other data are from our earlier work. The F-values for the graded coatings are based on the Pt content at the bottom of the cermet. Two groups of data from our previous work, corresponding to the reactive sputtered graded coatings and the rf sputtered uniform coatings, fell below the theoretical curve relating F to the atomic percent composition. Arguments were presented in the interim report which could explain these departures and which therefore indicate that the deposition condition can in fact be used to control the Pt content with reasonable accuracy. See Section 4.4 in Ref. 8. The data from our new coatings is based on Auger depth profile measurements made by the Lawrence Berkeley Laboratory. These data are within about 15% of the theoretical curve and clearly support the proposition that the co-sputtering process can be accurately controlled to produce cermets of specified composition.

Table I tabulates the coating configurations and optical properties for the coatings that were deposited during the optimization study and evaluated at the Battelle Northwest Laboratory. See Section 2.2.

In our previous work the effect of substrate drum rotational speed was

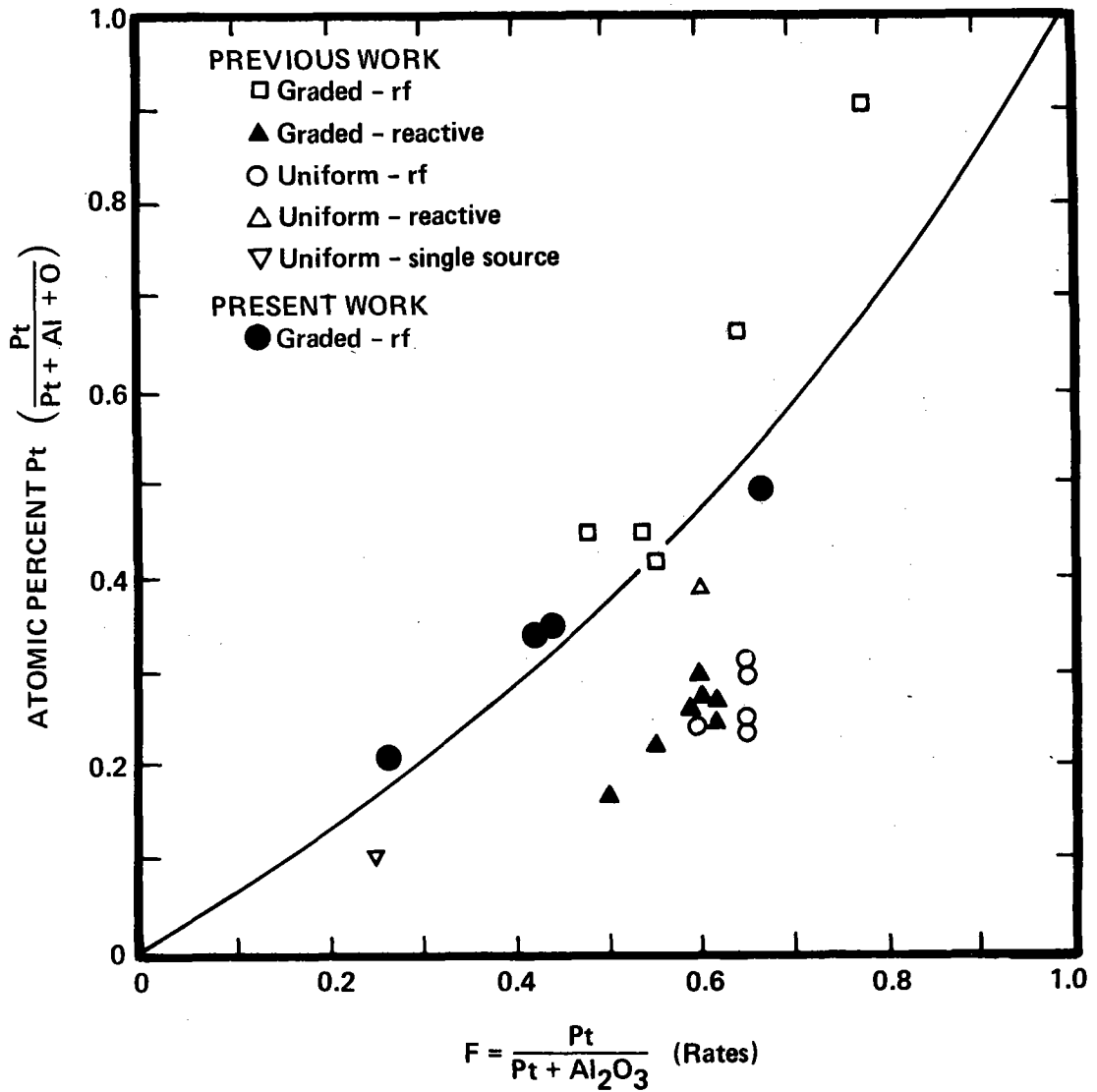


FIG. 6. Correlation between Pt volume fraction estimated from deposition conditions and Pt composition (atomic percent) measured by Auger depth profiling. Small data points from work conducted during Phase II. Curve is theoretical relation between volume fraction and composition in atomic percent.

TABLE I-A

OPTICAL PROPERTIES OF GRADED CERMET COATINGS DEPOSITED
DURING OPTIMIZATION STUDY AND TESTED AT BATTELLE

<u>Sample Number</u>	<u>AR Thickness</u>	<u>Cermet (1) Thickness</u>	<u>Pt (2) Content F</u>	<u>Rotation Speed (RPM)</u>	<u>Substrate Temperature</u>	<u>Absorptance</u>	<u>Emittance (3) (20°C)</u>
1121	70 nm	70 nm	0.55	1.0	250°C	0.96	0.10
1164	70 nm	70 nm	0.55	3.4	250°C	0.95	0.05
1204	70 nm	140 nm	0.38	1.0	150°C	0.86	0.09
1241	70 nm	42 nm	0.67	1.0	150°C	0.88	0.10
1261	70 nm	70 nm	0.55	1.0	150°C	0.95	0.08
1281	70 nm	42 nm	0.55	1.0	150°C	0.92	0.08
1319	70 nm	25 nm	0.55	1.0	150°C	0.86	0.04
1325	42 nm	70 nm	0.55	1.0	150°C	0.96	0.10
1373	70 nm	70 nm	0.55	1.0	150°C	0.94	0.07
1400	42 nm	42 nm	0.55	1.0	150°C	0.95	0.01

Substrate - Glass

IR reflecting layer - Platinum

- (1) Effective thickness of Al₂O₃ component of cermet layer. See Section 3.2.
- (2) F refers to Pt content at the base of the cermet layer. F-value is based on the deposition conditions.
- (3) Room temperature emittance estimated from $\epsilon(20^\circ\text{C}) = 1-R$, where R is normal reflectance at 10.6 μm measured with CO₂ laser. See Section 2.2.

TABLE I-B

OPTICAL PROPERTIES OF GRADED CERMET COATINGS DEPOSITED
DURING OPTIMIZATION STUDY AND TESTED AT BATTELLE

<u>Sample Number</u>	<u>AR Thickness</u>	<u>Cermet⁽¹⁾ Thickness</u>	<u>Pt⁽²⁾ Content F</u>	<u>Rotation Speed (RPM)</u>	<u>Substrate Temperature</u>	<u>Absorptance</u>	<u>Emittance (20°C)</u>
1454	0	70 nm	0.55	1.0	150°C	0.90	0.05
1460	30 nm	70 nm	0.55	1.0 ⁽⁴⁾	150°C	0.97	0.07
1463	55 nm	70 nm	0.55	1.0 ⁽⁴⁾	150°C	0.93	0.08
1478	0	45 nm	0.55	1.0	150°C	0.91	0.03
1487	55 nm	45 nm	0.55	1.0 ⁽⁴⁾	150°C	0.91	0.05
1499	20 nm	45 nm	0.55	1.0 ⁽⁴⁾	150°C	0.96	0.04
1502	0	25 nm	0.55	1.0	150°C	0.88	0.03
1505	10 nm	25 nm	0.55	1.0 ⁽⁴⁾	150°C	0.92	0.03
1511	55 nm	25 nm	0.55	1.0 ⁽⁴⁾	150°C	0.81	0.05
1544	40 nm	70 nm	0.55	1.0	150°C	0.96	0.08
1568	20 nm	25 nm	0.55	1.0	150°C	0.91	0.03

Substrate - Glass

IR reflecting layer - Platinum

- (1) Effective thickness of Al₂O₃ component of cermet layer. See Section 3.2.
- (2) F refers to Pt content at the base of the cermet layer. F-value is based on the deposition conditions.
- (3) Room temperature emittance estimated from $\epsilon(20^\circ\text{C}) = 1-R$, where R is normal reflectance at 10.6 μm measured with CO₂ laser. See Section 2.2.
- (4) A.R. layer deposited with no rotation.

investigated for coatings with reactively sputtered Al_2O_3 , at drum speeds of from 1 to 10 rpm (item three in above list). Our new work has investigated coatings with rf sputtered Al_2O_3 and extended the speed range down to 0.5 rpm. A substrate temperature of about 250°C was used. Absorptance data from these experiments are shown in Fig. 7 for both Pt and W (see Section 4) low emittance base layers and compared to the data for reactive sputtered coatings that were obtained previously. The new data are generally consistent with the previous results and show no additional improvement in absorptance at the very low rotational speeds. Transmission electron microscopy examinations over the 1 to 10 rpm speed range showed no evidence of rotational speed influence on the Pt phase microstructure. See Section 3.5.

Two groups of experiments were conducted to explore the influence of the coating Pt content and therefore to further explore the range of validity of statement five in the preceding section. In the first case, a group of three coatings, which had cermet layers of various thicknesses, were deposited. The effective Al_2O_3 thicknesses for the cermet layers were 42 nm, 70 nm, and 140 nm. The Pt sputtering rate was graded linearly with time to give a near linear composition variation and adjusted so that the total integrated Pt content of all the coatings was essentially the same, with a d_{Pt} value of about 42 nm. A constant antireflection layer thickness of 70 nm was used for all the coatings.

Figures 8 through 10 show Auger depth profiles of the three coatings. The pattern of differences in the Pt distributions is readily apparent along with the fact that the composition gradings (atomic percent) are nearly linear. Furthermore, integration under the Pt composition profiles verifies that the total Pt contents of the three cermet layers are nearly identical (within about 15%) and satisfy the condition given in statement five that $d_{\text{Pt}} \sim 40$ nm. The reason for the apparent lack of stoichiometry in the Al_2O_3 layer is not known.

Figures 11 through 13 gives spectral reflectance data for the three coatings. Figure 11 shows a coating with $d_{\text{Al}_2\text{O}_3} = 70$ nm and $F = 0.55$ which duplicates the near-optimum configuration that was established in our previous work. The

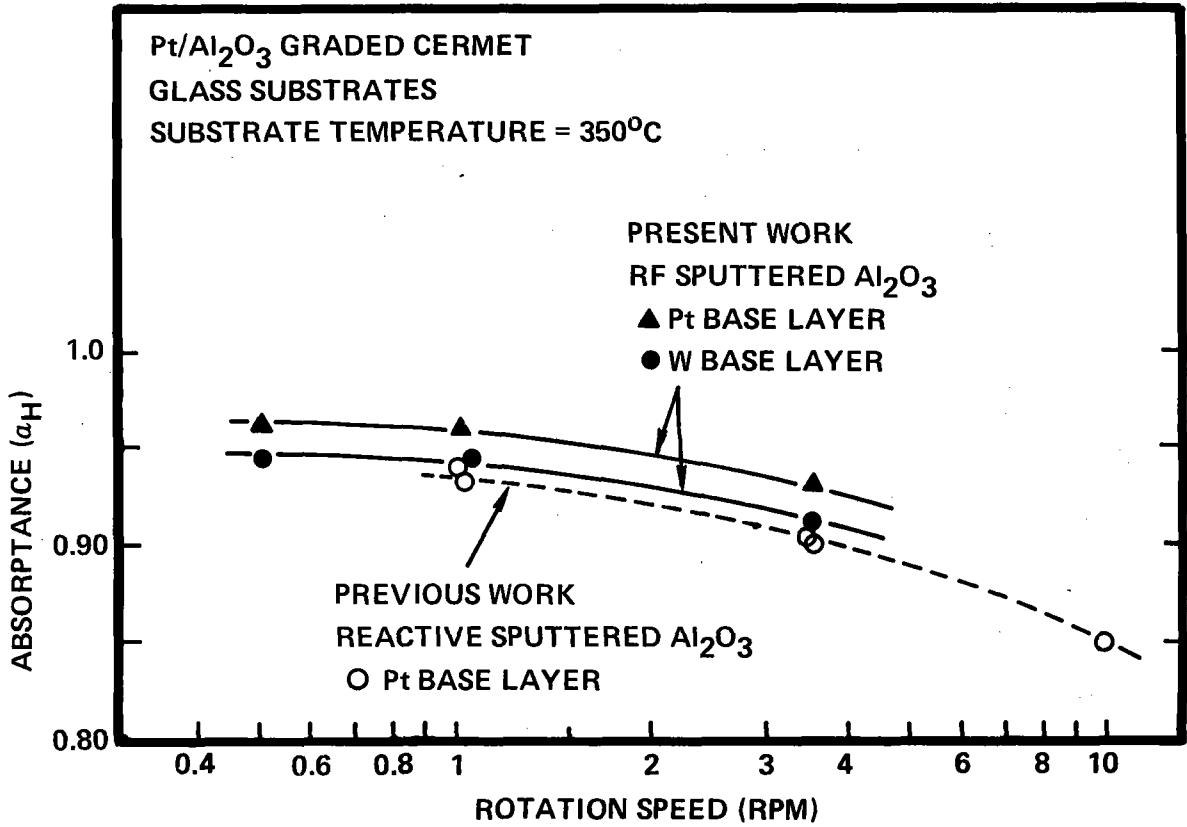


FIG. 7. Dependence of the hemispherical absorptance on the substrate drum rotational speed for coatings deposited using both direct rf and reactive sputtered Al₂O₃.

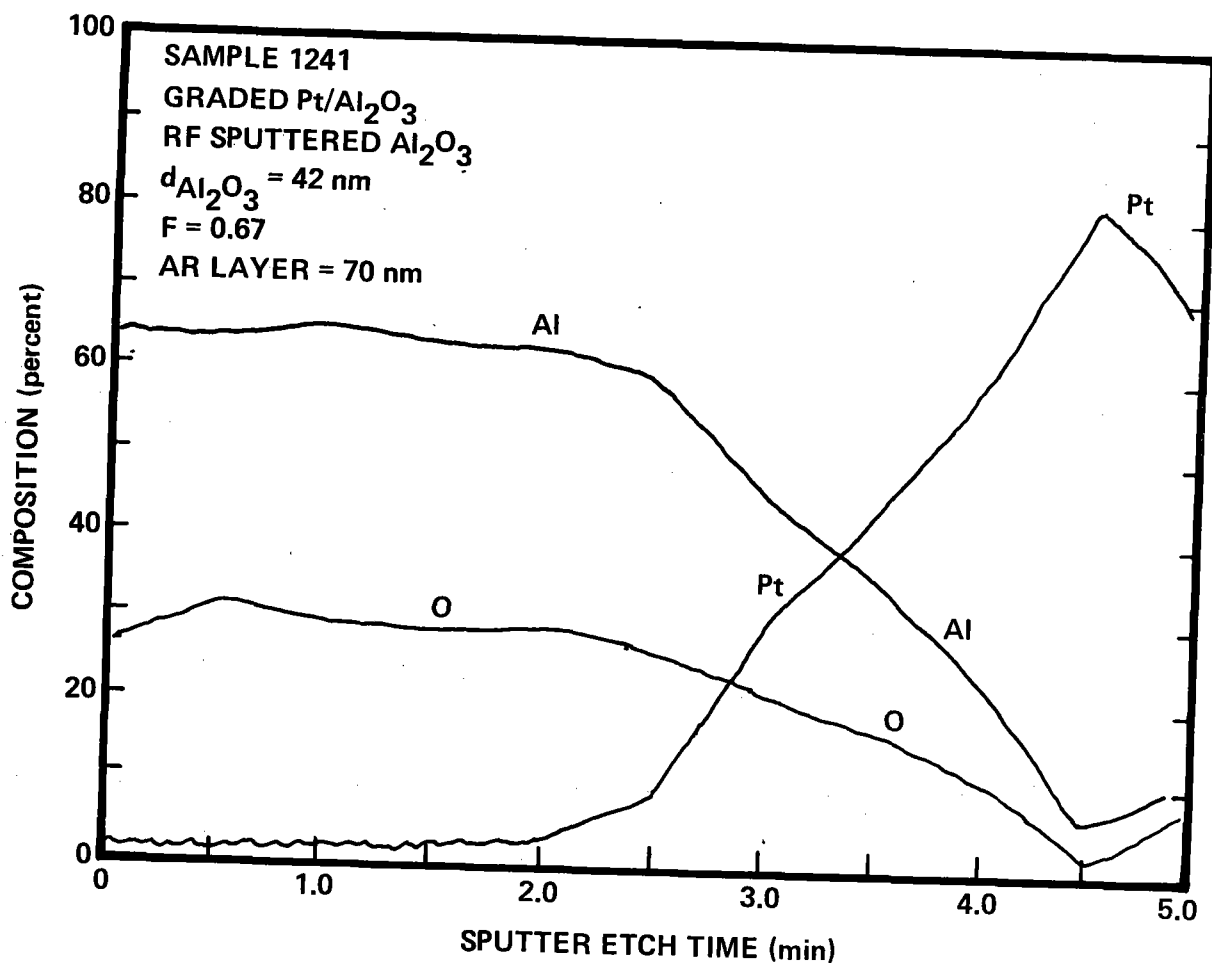


FIG. 8. Auger depth profile composition analysis of graded cermet coating (sample 1241) with $d_{Al_2O_3}$ thickness of 42 nm and F-value at cermet base of 0.67. See Fig. 13 for spectral reflectance data.

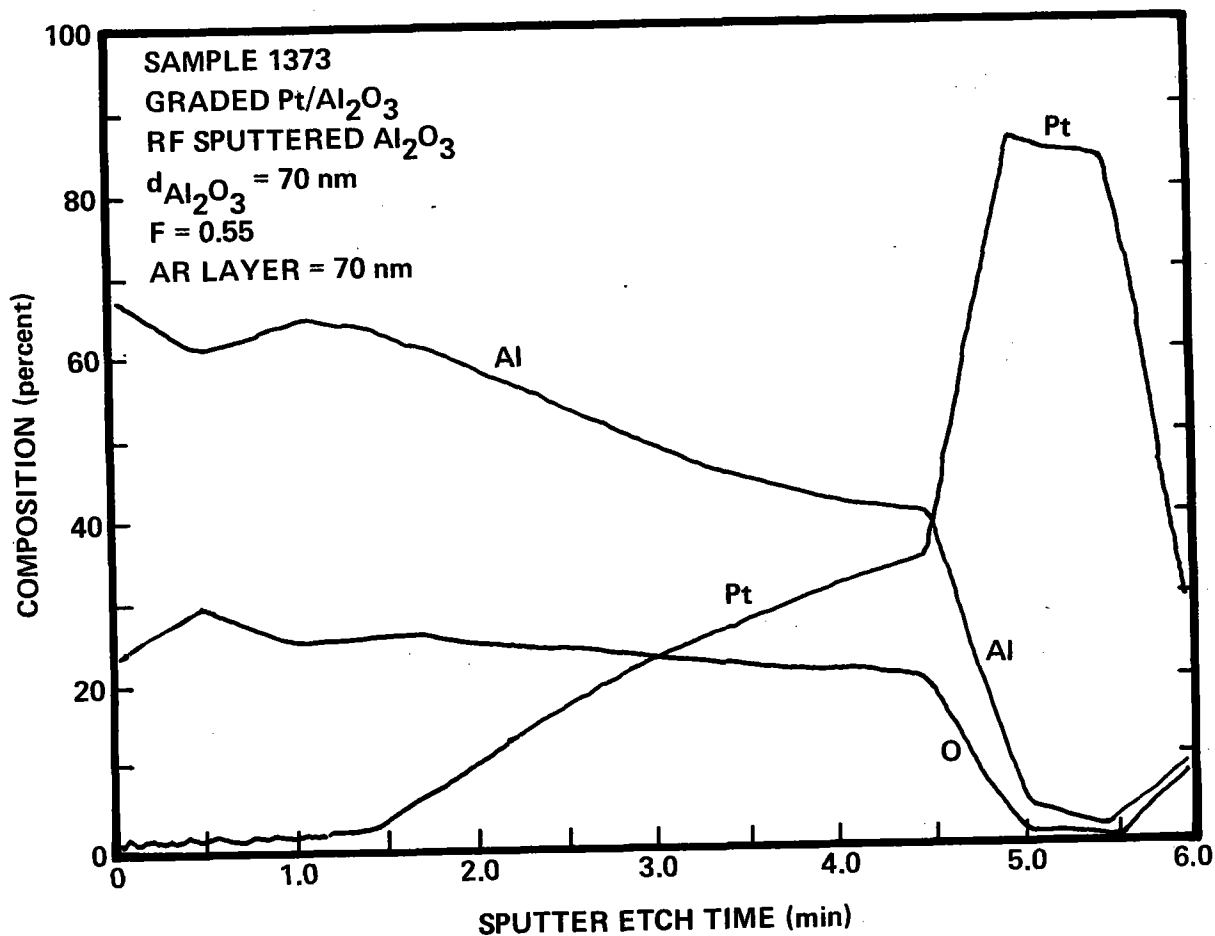


FIG. 9. Auger depth profile composition analysis of graded cermet coating (sample 1373) with $d_{Al_2O_3}$ thickness of 70 nm and F-value at cermet base of 0.55. See Fig. 11 for spectral reflectance data.

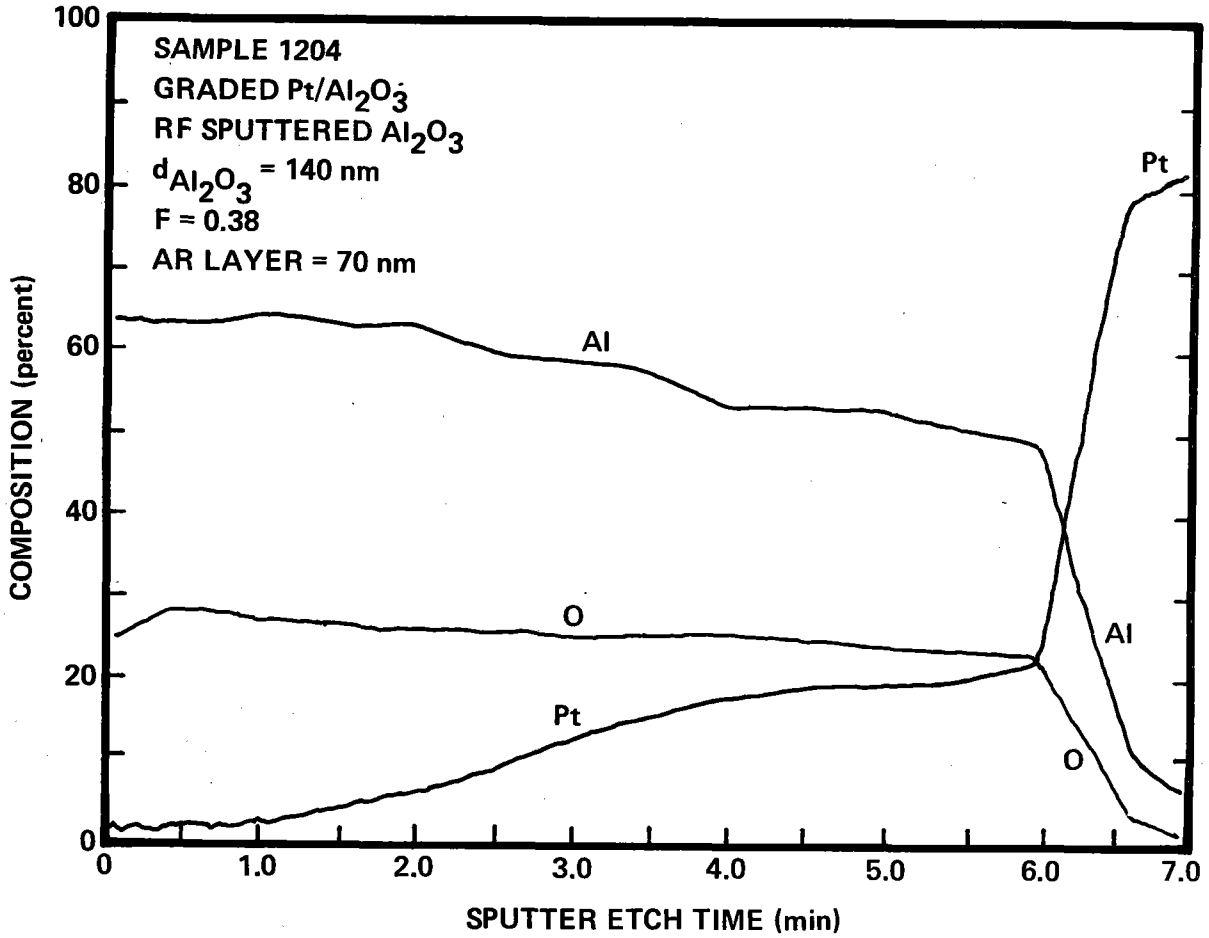


FIG. 10. Auger depth profile composition analysis of graded cermet coating (sample 1204) with $d_{Al_2O_3}$ thickness of 140 nm and F-value at cermet base of 0.38. See Fig. 12 for spectral reflectance data.

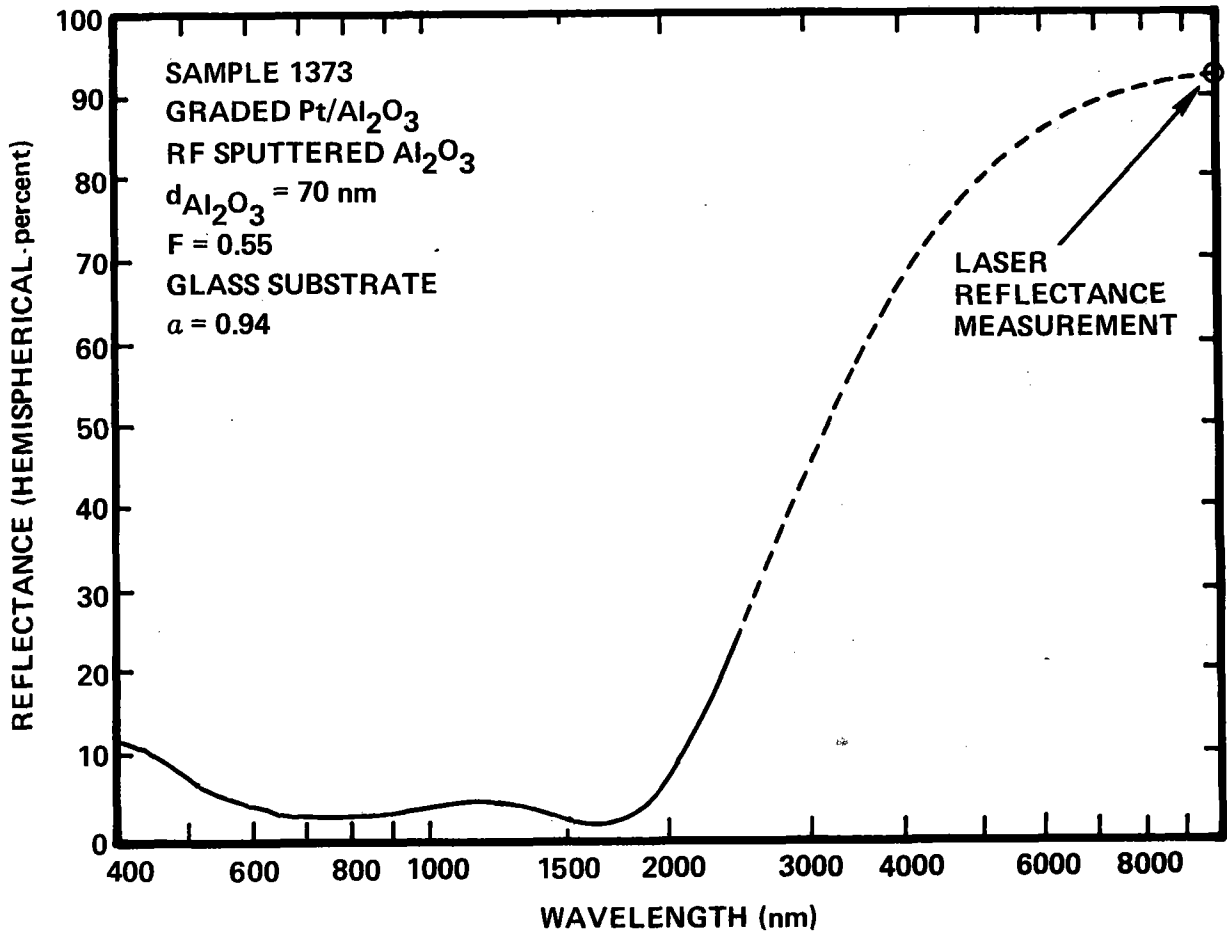


FIG. 11. Spectral reflectance data for graded cermet coating (sample 1373) with $d_{\text{Al}_2\text{O}_3}$ thickness of 70 nm and F-value at cermet base of 0.55. Antireflection layer thickness is 70 nm. Auger depth profile data are given in Fig. 9.

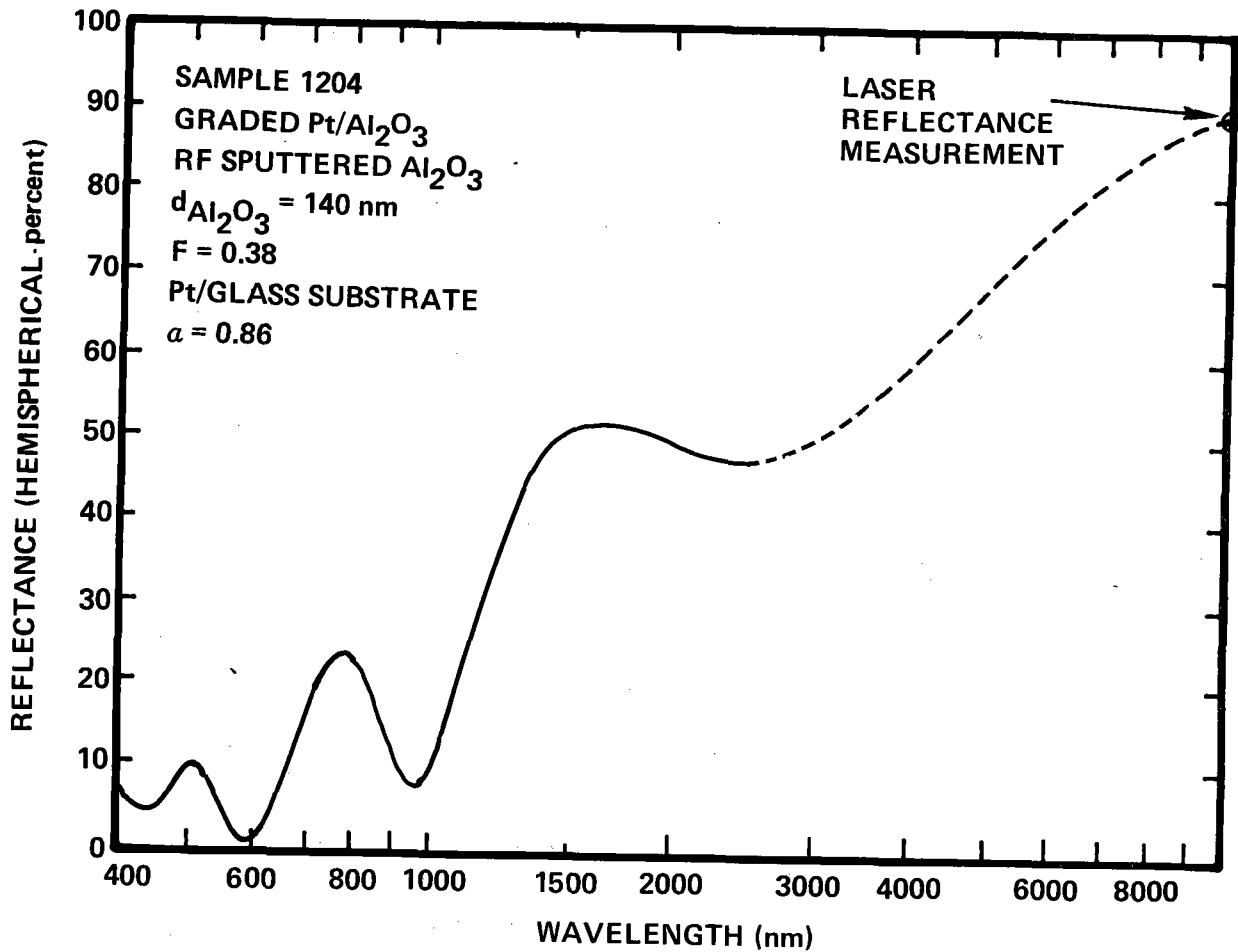


FIG. 12. Spectral reflectance data for graded cermet coating (sample 1204) with $d_{\text{Al}_2\text{O}_3}$ thickness of 140 nm and F-value at cermet base of 0.38. Antireflection layer thickness is 70 nm. Auger depth profile data are given in Fig. 10.

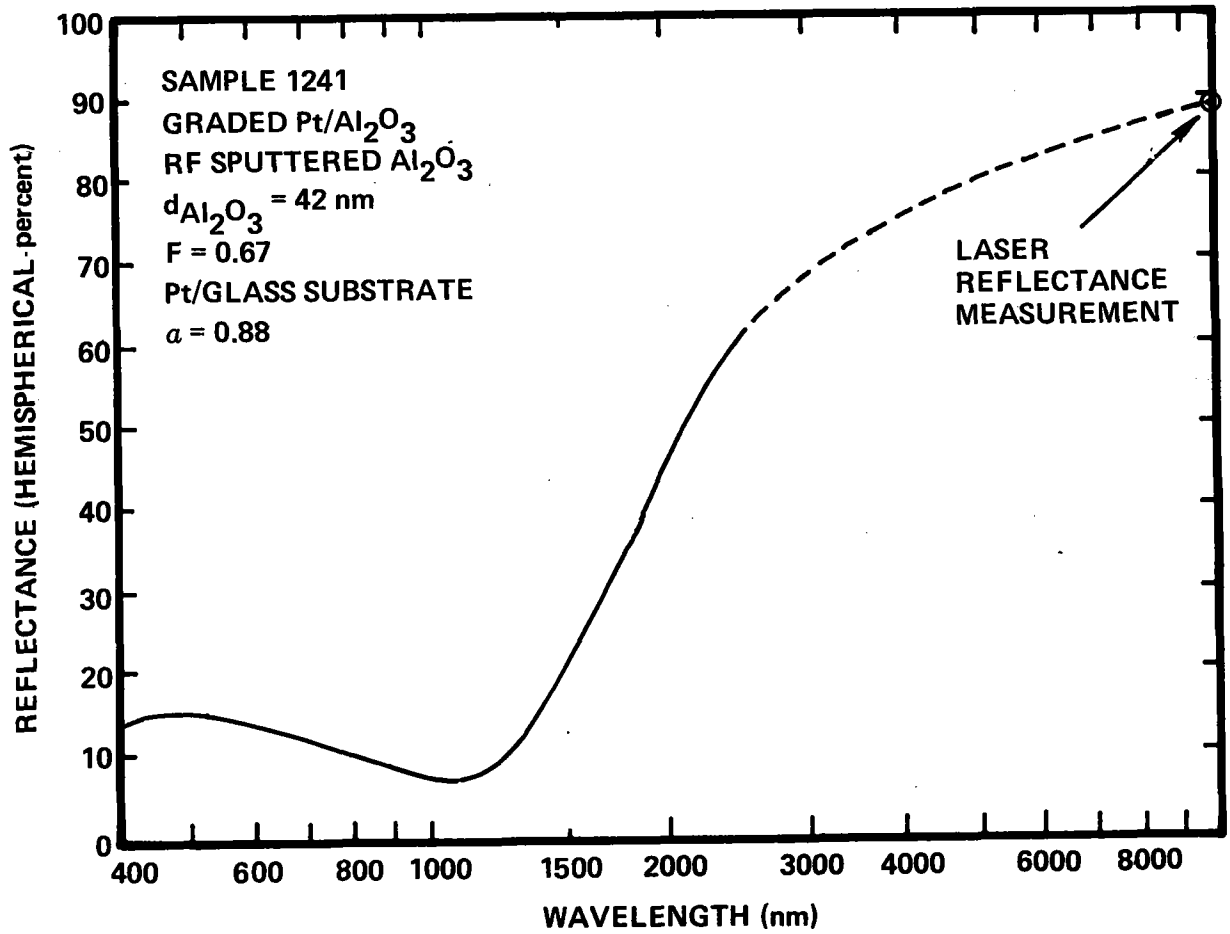


FIG. 13. Spectral reflectance data for graded cermet coating (sample 1241) with $d_{\text{Al}_2\text{O}_3}$ thickness of 42 nm and F-value at cermet base of 0.67. Antireflection layer thickness is 70 nm. Auger depth profile data are given in Fig. 8.

absorptance is 0.94 and the 10.6 μm reflectance implies a room temperature emittance of about 0.07. Figure 12 shows the coating with the thick cermet layer, $d_{\text{Al}_2\text{O}_3} = 140 \text{ nm}$, and low F-value (0.38). Strong interference effects are seen, and, even though the total Pt content matches the sample shown in Fig. 11, the absorptance is considerably lower (0.86). Figure 13 shows the coating with the thin cermet layer, $d_{\text{Al}_2\text{O}_3} = 42 \text{ nm}$, and high F-value (0.67). A reflectance of about 10% is present throughout the visible spectrum. Again, even though the total Pt content matches the sample shown in Fig. 11, the absorptance is lower (0.88).

Thus the new data help to provide limits on the range of validity of the premise in the preceding section (statement 5) that the absorptance is determined primarily by the integrated Pt content in the cermet layer. An increase in the Pt volume fraction appears to increase both the refractive index and the extinction coefficient of the cermet. This is consistent with the general theoretical studies given in Ref. 4. In the case of coatings with low Pt volume fractions, the wave attenuation is insufficient to suppress the interference effects. Consequently, the absorptances that can be obtained are limited. Increasing the cermet thickness to increase the total integrated Pt content causes a slight increase in absorptance because higher order interference fringes are moved into the primary region of the solar spectrum, as can be seen in Fig. 12. However, as is also apparent in the figure, the lower order interference pattern moves to the longer wavelengths and increases the emittance, particularly for operation at elevated temperatures. Consequently, the overall performance of the coating is less than optimum. In the case of coatings with a high Pt volume fraction, the high index of refraction tends to cause light reflections at the front surface. When the cermet layers are made thin, and the F-value at the rear surface is increased to maintain a given total integrated Pt content, the composition profile becomes very steep, as can be seen in Fig. 8. The steep composition profile places material with a relatively high index adjacent to the top surface, with the result that top surface reflec-

tions occur. This can be seen in Fig. 13. The performance of the coating shown in Fig. 13 could probably be improved slightly by optimizing the thickness of the antireflection layer. Nevertheless the steep cermet gradient is expected to limit the ultimate performance.

In the case of the near optimum coating shown in Fig. 11, the composition grading (Fig. 9) is adequate to let light enter the cermet, and the Pt volume fraction within the bulk of the cermet is adequate to suppress the interference effects. In fact, the impedance match of the cermet to the entering light is sufficient so that the thickness of the antireflection layer is not critical. This is seen in Fig. 14, which shows spectral reflection data for a cermet coating that is identical to the one shown in Fig. 11, but where the antireflection layer is about one half as thick and near optimum. The absorptance is increased only slightly to 0.96.

The second group of experiments which were conducted during our optimization studies involved exploring the possibility of using optimized antireflection coating thicknesses to achieve high absorptances from relatively thin cermet layers with low total Pt contents. The objective was to reduce the integrated Pt content and therefore the cost of the coatings. Therefore, a series of coatings were deposited with the same Pt volume fraction ($F = 0.55$) at the rear surface, as in the case of the near optimum coating shown in Fig. 14, but with thinner cermet layers; i.e., $d_{\text{Al}_2\text{O}_3} = 42$ nm, and $d_{\text{Al}_2\text{O}_3} = 25$ nm. In each case the Pt composition was again graded near-linearly from the bottom surface down to zero at the top surface. Figure 15 shows a coating with a 42 nm thick cermet layer and the same antireflection layer thickness as the near optimum coating shown in Fig. 11. The steeper cermet compositional gradient, and the reduced attenuation within the thinner cermet, appear to have increased the interference type reflections and slightly reduced the absorptance. Optimizing the coating by using a thinner antireflection layer regains the high absorptance ($\alpha = 0.95$), as can be seen from the data shown in Fig. 16. The effective Pt thickness, d_{Pt} , for this coating is only about 25 nm. The cost

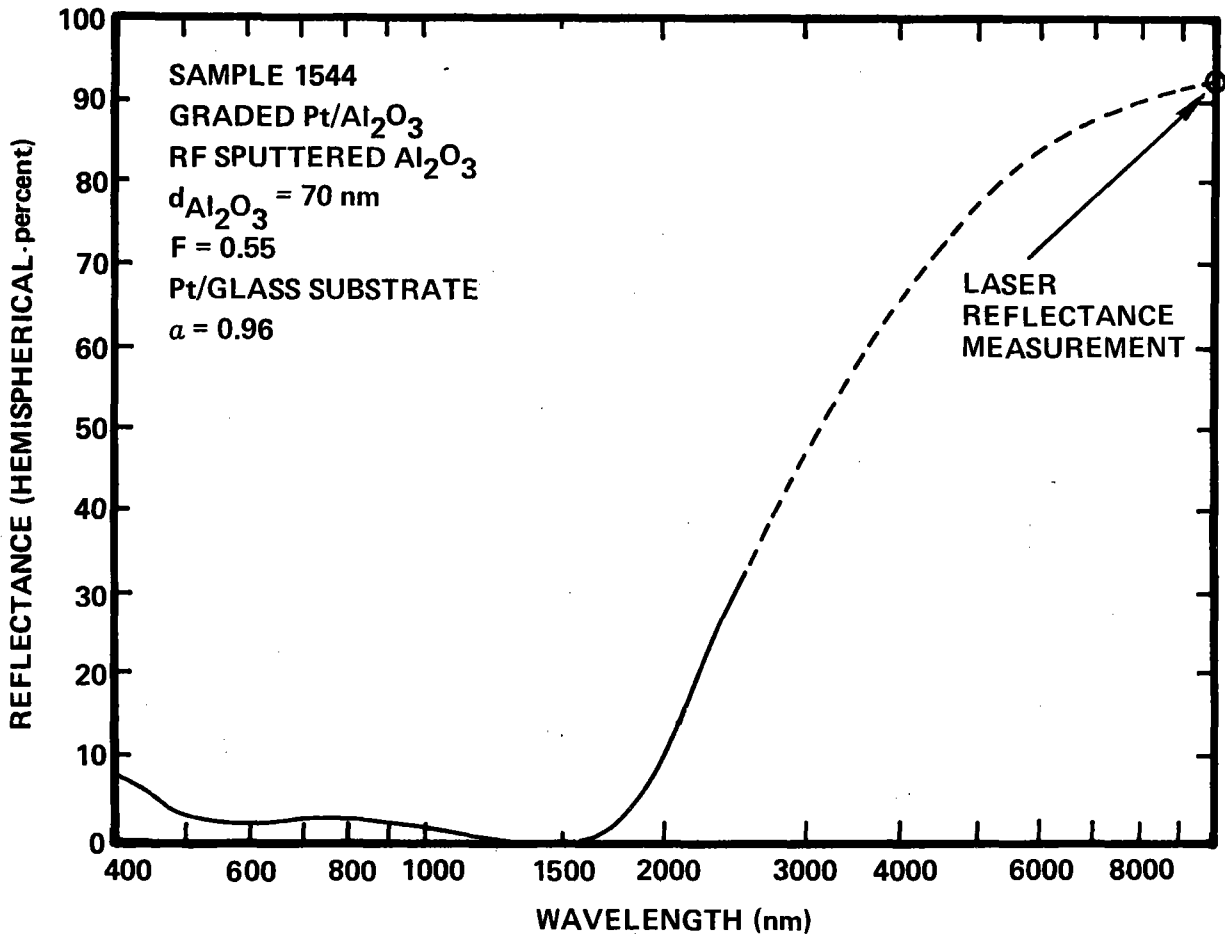


FIG. 14. Spectral reflectance data for graded cermet coating (sample 1544) with $d_{\text{Al}_2\text{O}_3}$ thickness of 70 nm, F-value at base of cermet of 0.55, and near-optimum antireflection layer thickness of 40 nm.

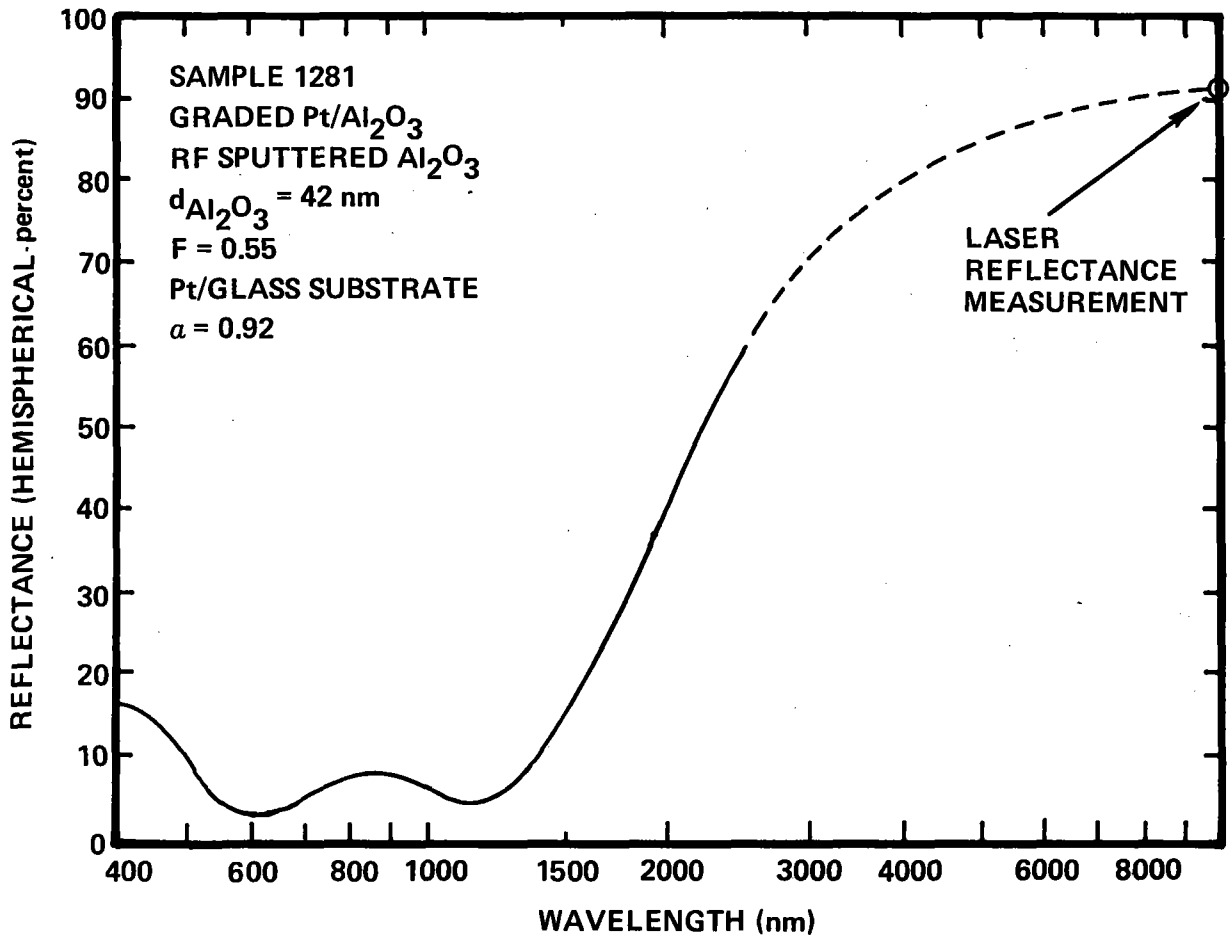


FIG. 15. Spectral reflectance data for graded cermet coating (sample 1281) with $d_{\text{Al}_2\text{O}_3}$ thickness of 42 nm and F-value at the cermet base of 0.55. Antireflection layer thickness is 70 nm.

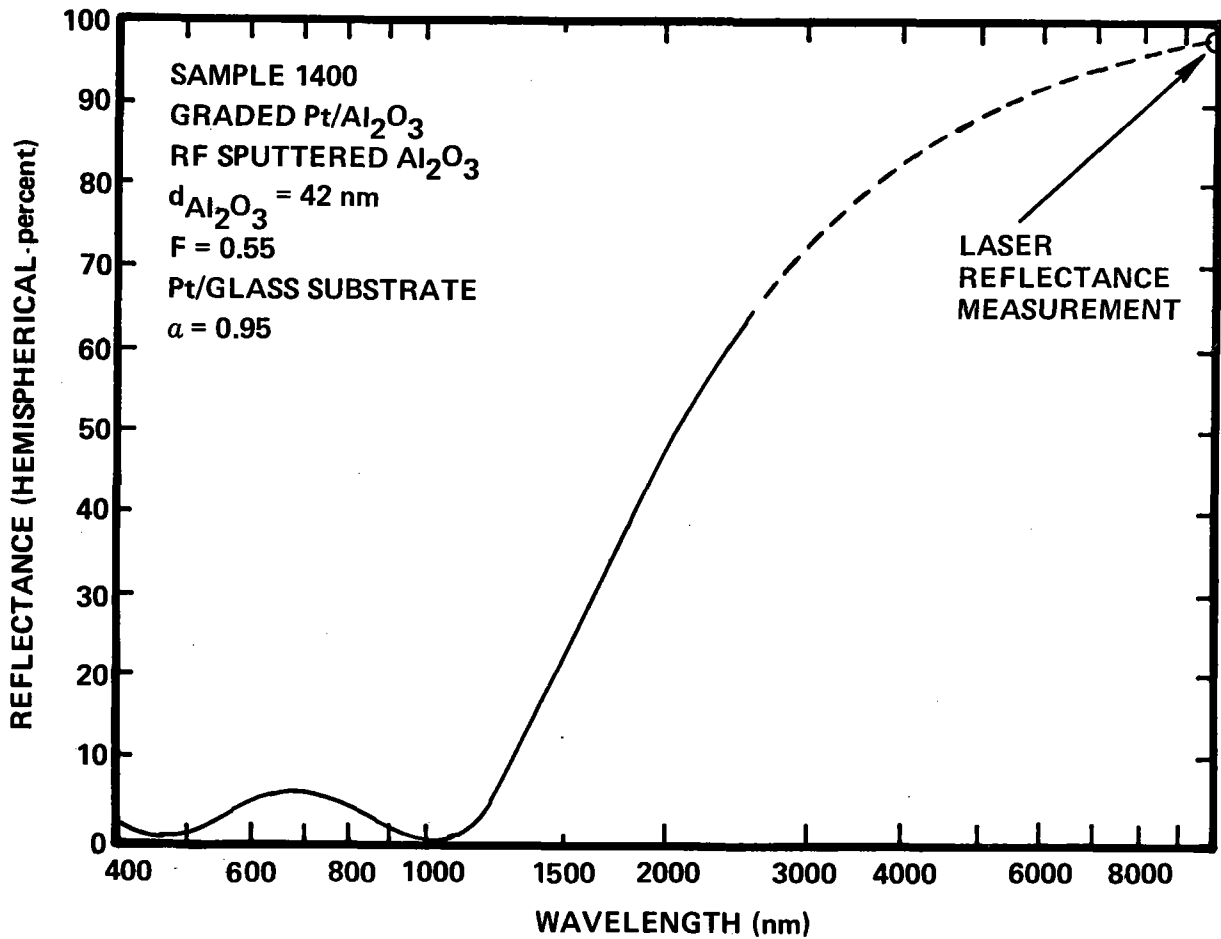


FIG. 16. Spectral reflectance data for graded cermet coating (sample 1400) with $d_{\text{Al}_2\text{O}_3}$ thickness of 42 nm, F-value at base of cermet of 0.55, and near-optimum antireflection layer thickness of 42 nm.

calculations given in Ref. 8 assumed a d_{Pt} value of 50 nm and predicted a cermet Pt cost of about $\$2/\text{ft}^2$, with a projection that high performance graded cermet layers costing about $\$1/\text{ft}^2$ might be possible. These data verify that projection.

Figure 17 shows a coating from the above series with the very thin cermet layer, $d_{Al_2O_3} = 25$ nm, and an optimized antireflection layer thickness. In this case the effective Pt thickness is only about 15 nm. The absorptance is reasonable (0.91), but below the values of 0.95 or above for the coatings shown in Figs. 14 and 16, because the overall coating is too thin to absorb the light in the long wavelength portion of the solar spectrum.

Figure 18 summarizes the effect of antireflection layer thickness in optimizing the absorptance of coatings with various cermet layer thicknesses. In all cases the Pt content of the cermet layers is near-linearly graded with $F = 0.55$ at the base. Two things are apparent from the figure. First, a relatively broad range of antireflection layer thicknesses provide near-optimum performance when used on the 70 nm thick cermet layers. Such a lack of criticality in the antireflection layer thickness is obviously important in production applications involving large areas or complex shaped substrates. When thinner cermet layers are used, the thickness requirements for the antireflection layer become increasingly critical. Second, the graded cermet coatings that had been considered near optimum in our previous work (absorptances of 0.93 to 0.95, see Table I in Ref. 8 and discussion in Section 4.2) actually had antireflection layers (70 nm) that were slightly thicker than the optimum implied by the data shown in Fig. 18. Figure 19 shows spectral reflectance data for a 70 nm thick cermet layer with a near-optimum, 30 nm thick, antireflection layer. The hemispherical absorptance is about 0.97.

Thus the optimization studies on this final phase of the program have shown that graded cermet coatings with absorptances as high as 0.97 can be achieved by optimizing the antireflection layer thicknesses and, that such coatings can be deposited at relatively low substrate temperatures. It has also been shown that

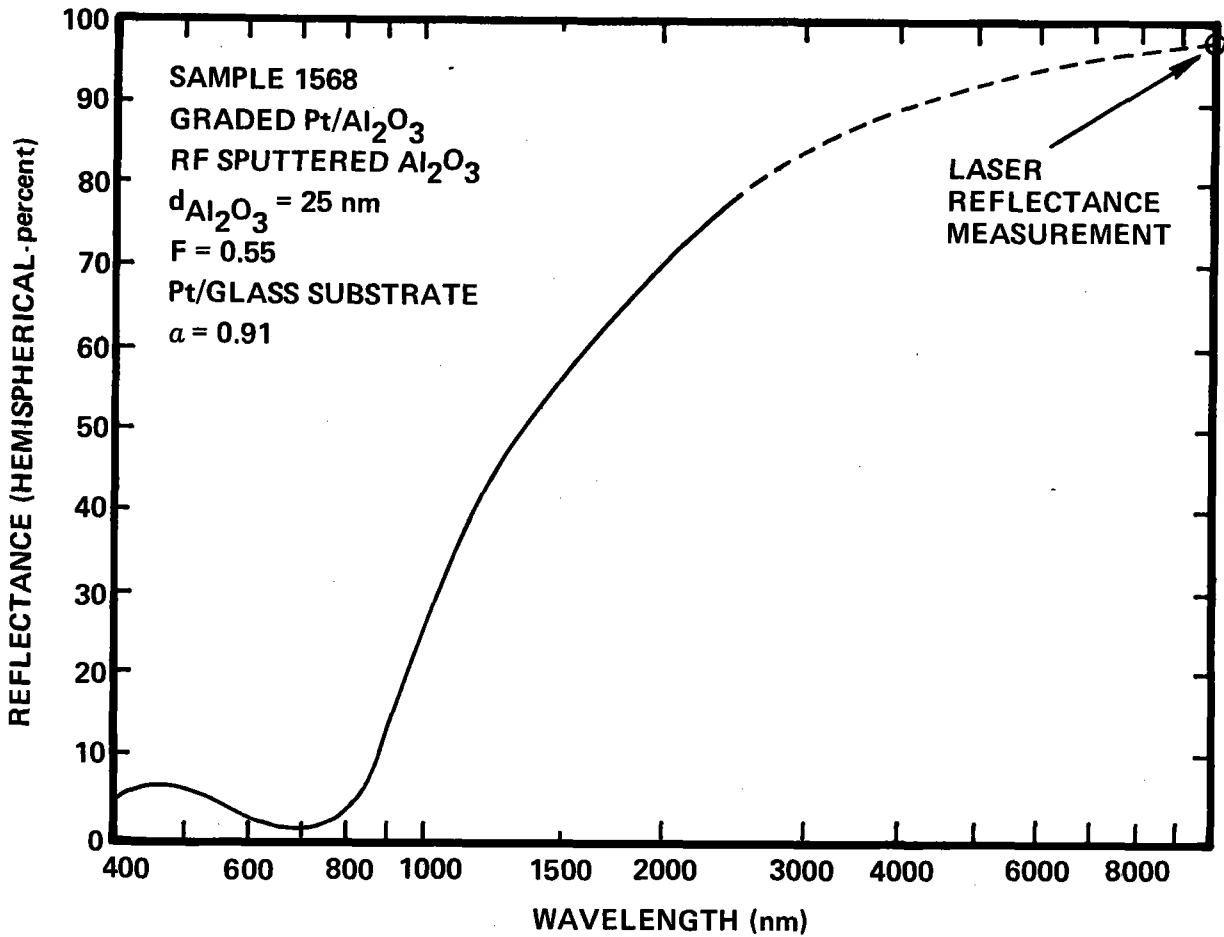


FIG. 17. Spectral reflectance data for graded cermet coating (sample 1568) with $d_{Al_2O_3}$ thickness of 25 nm, F-value at base of cermet of 0.55, and near-optimum antireflection layer thickness of 20 nm.

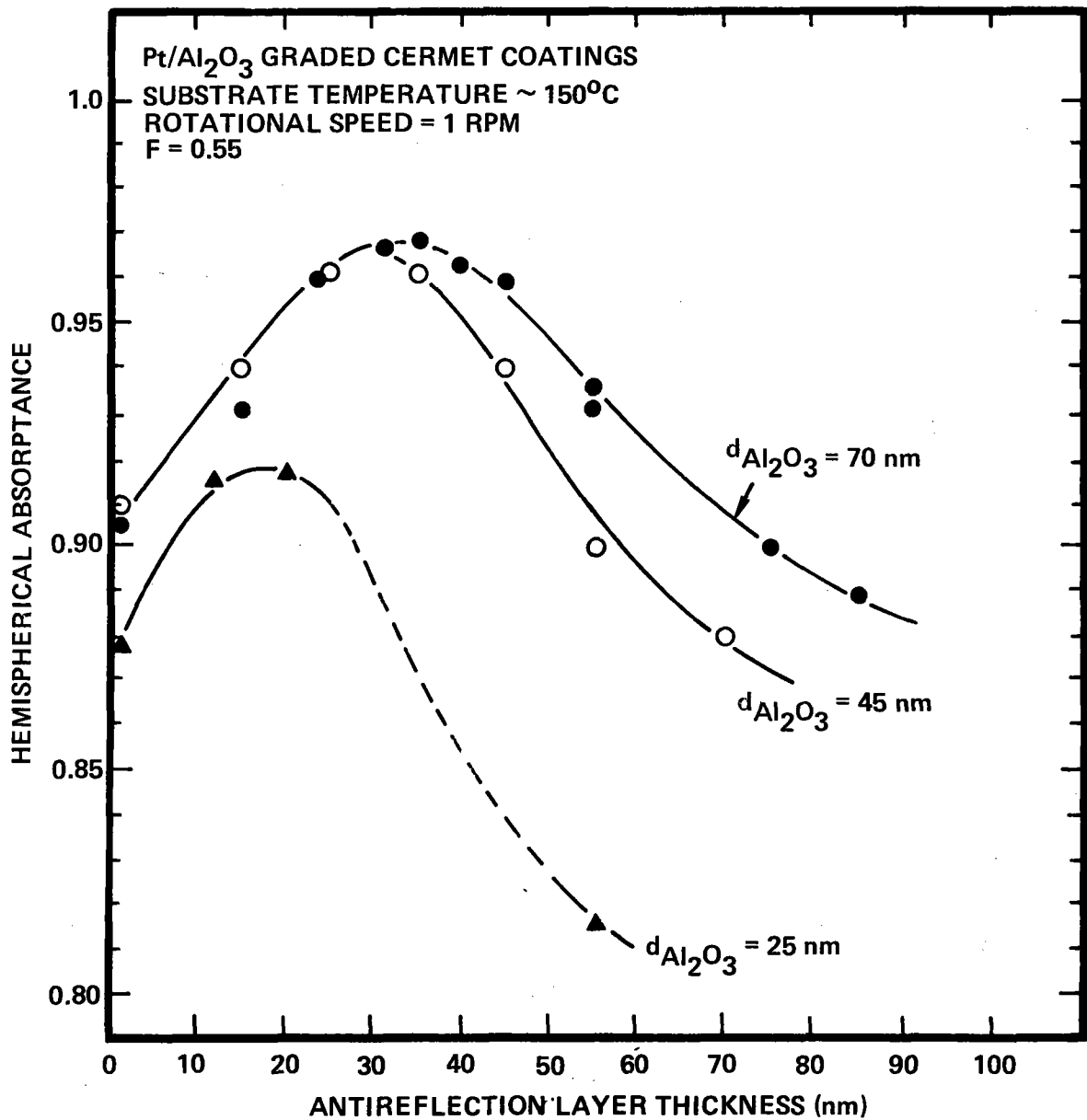


FIG. 18. Hemispherical absorptance versus antireflection layer thickness for graded cermet coatings having cermet layers of various thicknesses.

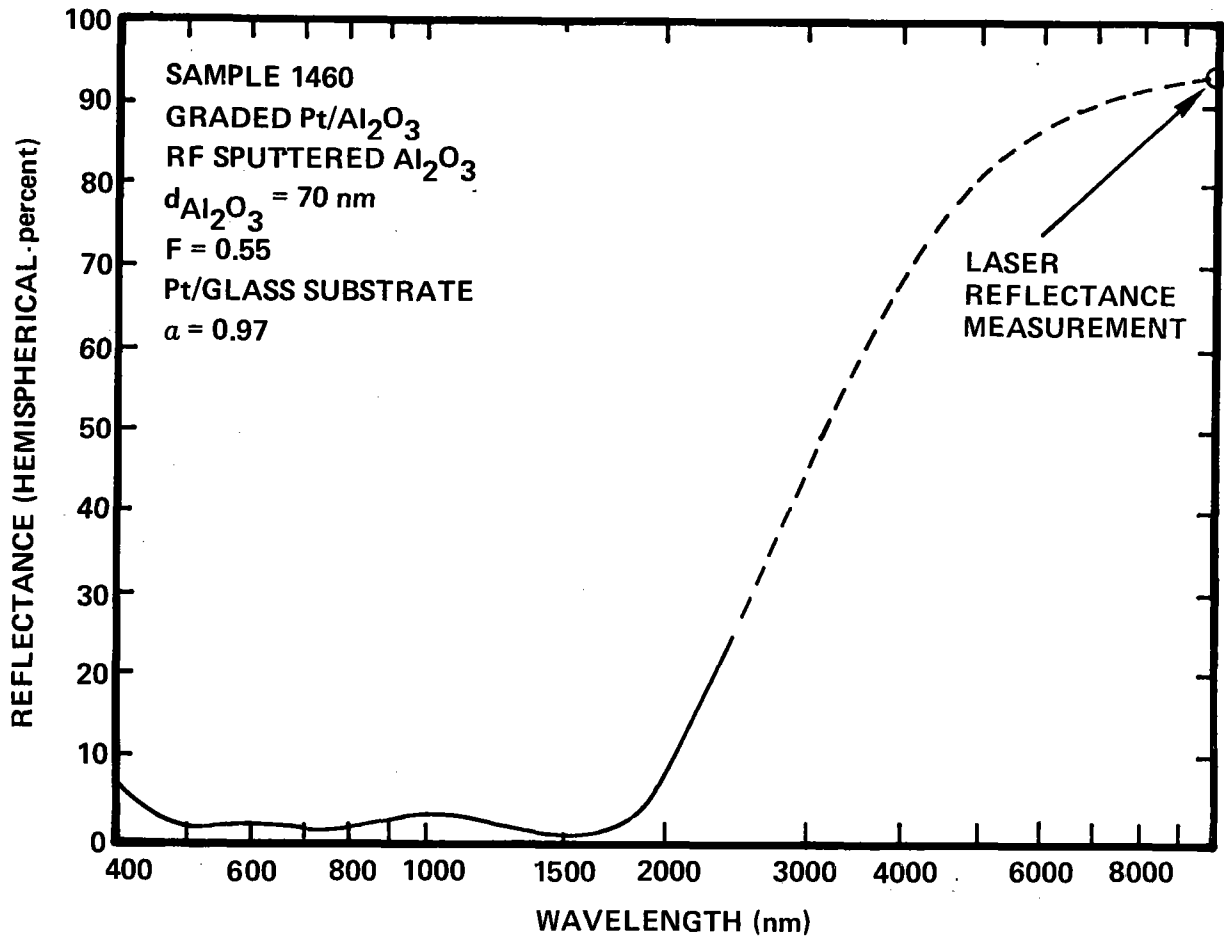


FIG. 19. Spectral reflectance data for graded cermet coating (sample 1460) with $d_{\text{Al}_2\text{O}_3}$ thickness of 70 nm, F-value at base of cermet of 0.55, and near-optimum antireflection layer thickness of 30 nm.

graded cermet coatings with absorptances of greater than 0.90, and with total Pt contents which could reduce the Pt cost of the coatings to less than \$1/ft², can be deposited.

3.4 Thermal Stability Studies

Graded cermet coatings representing the optimum conditions shown in Fig. 18 were tested in air at temperatures of 400°C and 500°C following the procedures described in Section 2.3. Test durations at 400°C ranged from 600 to 1400 hrs. No degradation (change of absorptance >1%) was observed for any of the samples in the 400°C tests. The test duration at 500°C was 684 hrs. At this temperature the coatings with 70 nm thick cermet layers were stable, consistent with the results achieved earlier in the program (see Ref. 8). The data for the thinner coatings was inconclusive, but suggests that these coatings may be less stable. Thus in two cases coatings with cermet layers having $d_{\text{Al}_2\text{O}_3}$ -values of 42 nm underwent absorptance changes of 2 and 10% respectively, while in a third case a very thin coating having a $d_{\text{Al}_2\text{O}_3}$ -value of 25 nm showed no change. The steeper Pt concentration gradients in the thinner coatings may make them more vulnerable to interdiffusion. This is particularly true for coatings deposited at low substrate temperatures. Our previous work indicates that coatings deposited at elevated substrate temperatures ($\geq 350^\circ\text{C}$) are generally more stable than coatings deposited at lower temperatures.⁸

3.5 Cermet Microstructure

A few coatings were deposited onto copper microgrids with carbon support films for analysis by transmission electron microscopy. The microscopy analysis was carried out by Harold Craighead of the Bell Laboratories. The coatings were 25 nm thick. They had a uniform Pt volume fraction F of 0.33, which was selected as being representative of the Pt volume fraction in the bulk of the graded cermet coatings. The effects of three deposition conditions that were thought to influence the Pt phase microstructure were selected for examination. They were

- Substrate drum rotation - Coatings were deposited at drum rotation speeds

of 1.0, 3.3, and 10 rpm. The substrate temperature was about 150°C. The Al₂O₃ phase was deposited by rf sputtering from an alumina target.

- Substrate temperature - Coatings were deposited at substrate temperatures of about 150°C and about 300°C at a substrate rotation speed of 1 rpm. The Al₂O₃ phase was deposited by rf sputtering.
- Reactive versus rf sputtering - Coatings were deposited with the Al₂O₃ phase formed by reactive sputtering from an aluminum target in an Ar+O₂ working gas at substrate temperatures of about 150°C and 300°C. The substrate rotation speed was 1 rpm.

No observable effect on the microstructure was seen which could be attributed to changes in the rotational speed, even though the higher rotational speeds had been found to yield graded cermet coatings with reduced absorptances (see Fig. 7). At 1 rpm the Al₂O₃ deposition per pass is about 8Å. At 1 rpm and F = 0.33 the Pt deposition per pass is estimated to be about 4Å. The Pt grains appear to be of the order of 15 to 20Å in size in a variable density background similar to that reported by Abeles for a Pt/SiO₂ cermet film 200Å thick containing a Pt volume fraction of 21%.¹⁶ The diffraction pattern for our coatings showed only crystalline Pt Debye Scherrer rings.

The rf sputtered coating deposited at 300°C showed no evidence of Pt particles in the transmission micrograph or Pt rings in the electron diffraction image. Energy dispersive X-ray analysis also showed no evidence of Pt. The reason for these observations is not known. In previous work at Cornell University, Craighead examined Pt/Al₂O₃ cermets deposited by co-evaporation at substrate temperatures of about 500°C. Transmission electron microscope examinations of these coatings generally showed no discernable Pt phase particles; however, electron diffraction patterns showed evidence of Pt.⁴

The reactively sputtered coatings clearly showed an effect due to substrate temperature. The transmission micrograph of the coating deposited at about 150°C showed dense particles 15 to 20Å in size which appeared to be embedded in a uniform less dense matrix. The diffraction pattern showed only the most intense Pt diffraction ring (111) and several broad rings of an amorphous phase. The reactively sputtered coating deposited at about 300°C showed larger Pt grains

about 30 to 90 \AA in size embedded in a background material that showed evidence of holes, possibly strain induced from the heating. The diffraction pattern clearly showed FCC Pt diffraction rings.

In all the samples described above, the Al_2O_3 phase appeared to be amorphous in nature.

The transmission electron microscopy examination will be reported in greater detail in a future publication.¹⁹

4. ALTERNATE IR REFLECTOR LAYER MATERIALS

At a typical Pt price of \$500 per troy oz. or \$16/gm, the Pt in a 100 nm thick Pt low emittance base layer costs \$34.40/m² or about \$3.20/ft². For Pt/Al₂O₃ deposited in large production volumes over large areas, this is the single largest contributor to the coating cost. See Section 2 in Ref. 8.

The use of Cr and Mo as alternative base layer materials was examined during the Phase II work described in Ref. 8. In general, Pt/Al₂O₃ selective absorber coatings deposited using these base layer materials were less stable than those which used Pt as a base layer.⁹ Thus uniform cermet and AMA type coatings with rf sputtered Al₂O₃ which were deposited onto Cr or Mo at elevated substrate temperatures (≈350°C) were stable to about 500°C in air but underwent absorptance changes in the 550 to 600°C range. Similar coatings with Pt base layers were stable at 600°C. The use of lower substrate temperatures with Cr and Mo base layers yielded coatings which were stable at 400°C but subject to degradation in the 450-600°C range. The failure mechanisms appear to be oxidation of the base layer material and, in the Cr case, diffusion of Cr from the base layer into the cermet layer.

The objective during the third phase was to concentrate on coatings which could be used at operating temperatures of about 400°C. The data cited above suggest that alternative base layer materials are a realistic possibility at this temperature. Therefore, the objective of this aspect of our Phase III work was to investigate Ta, W, and ZrB₂ as alternative IR reflector layer materials. Zirconium diboride is an example of a compound with high thermal stability and oxidation resistance, along with a remarkably low dc resistivity ($9 \times 10^{-6} \Omega\text{-cm}$)²⁰ and emittance (0.06 to 0.09).²¹ Tungsten and tantalum were selected because of their high melting points and atomic weights, which should limit their tendency to undergo diffusion at the operating temperatures of interest.

Graded cermet coatings were deposited onto Ta, W, and ZrB₂ low emittance base layer coatings as part of the optimization studies described above. This

was possible because the eight-sided substrate mounting drum shown in Fig. 3 permitted a large number of test substrates to be coated in a given deposition run. Glass substrates were used to remove substrate surface roughness effects from consideration. The base layer thicknesses were nominally 100 nm. Table II tabulates the coating configurations and optical properties for the coatings that were deposited during the alternative base layer study and evaluated at the Battelle Northwest Laboratory. The performance of the alternative base layer materials on engineering substrates such as stainless steel and Incoloy 800 is discussed in the next section.

The hemispherical absorptances of graded Pt/Al₂O₃ cermet coatings deposited onto the Ta, W, and ZrB₂ base layers were essentially identical to those for coatings deposited onto Pt base layers during the same run.

The emittances of the coatings deposited onto Ta and W base layers were generally less than 0.12. Figure 20 shows emittance versus temperature relations for graded cermet coatings with W-base layers. The relations were calculated from long wavelength reflectance measurements made at the Lawrence Berkeley Laboratory.

The normal emittances for the coatings deposited onto ZrB₂ were in the range 0.16 to 0.24. The measured emittances for bare sputtered ZrB₂ coatings on glass substrates were about 0.20. These values are to be compared to the published emittances²¹ for ZrB₂ which are in the range of 0.06 to 0.09, as noted above. The resistivities of the sputtered ZrB₂ coatings were about $2 \times 10^{-3} \Omega\text{-cm}$, and therefore more than two orders of magnitude above the published value²⁰ of about $10^{-5} \Omega\text{-cm}$ for the bulk resistivity of ZrB₂. The exact reason for the high resistivity of the sputtered ZrB₂ coatings is not known. The most likely explanation is in the quality of the sputtering target. The ZrB₂ target was formed by hot pressing powders. Hot pressed powder targets have been shown to often be nearly limitless sources of gaseous contamination.²² The major contaminant in these targets appears to be oxygen absorbed onto the raw powder surface prior to hot pressing. Such oxygen evolution could easily explain the

TABLE II

OPTICAL PROPERTIES OF GRADED CERMET COATINGS
WITH ALTERNATIVE IR REFLECTOR LAYERS

Sample Number	AR Thickness	Cermet ⁽¹⁾ Thickness	Pt ⁽²⁾ Content F	Rotation Speed (RPM)	IR Reflectance Layer	Absorptance	Emittance ⁽³⁾ (20°C)
1211	70 nm	140 nm	0.38	1.0	W	0.89	0.10
1251	70 nm	42 nm	0.67	1.0	W	0.89	0.12
1271	70 nm	70 nm	0.55	1.0	Ta	0.95	0.15
1291	70 nm	42 nm	0.55	1.0	Ta	0.94	0.06
1304	70 nm	25 nm	0.55	1.0	Ta	0.90	0.13
1364	70 nm	70 nm	0.55	1.0	ZrB ₂	0.95	0.16
1388	42 nm	42 nm	0.55	1.0	ZrB ₂	0.96	0.18

Substrate - Glass

Substrate temperature $\sim 150^{\circ}\text{C}$

- (1) Effective thickness of Al₂O₃ component of cermet layer. See Section 3.2.
- (2) F refers to Pt content at the base of the cermet layer. F-value is based on the deposition conditions.
- (3) Room temperature emittance estimated from $\epsilon(20^{\circ}\text{C}) = 1-R$, where R is normal reflectance at 10.6 μm measured with CO₂ laser. See Section 2.2.

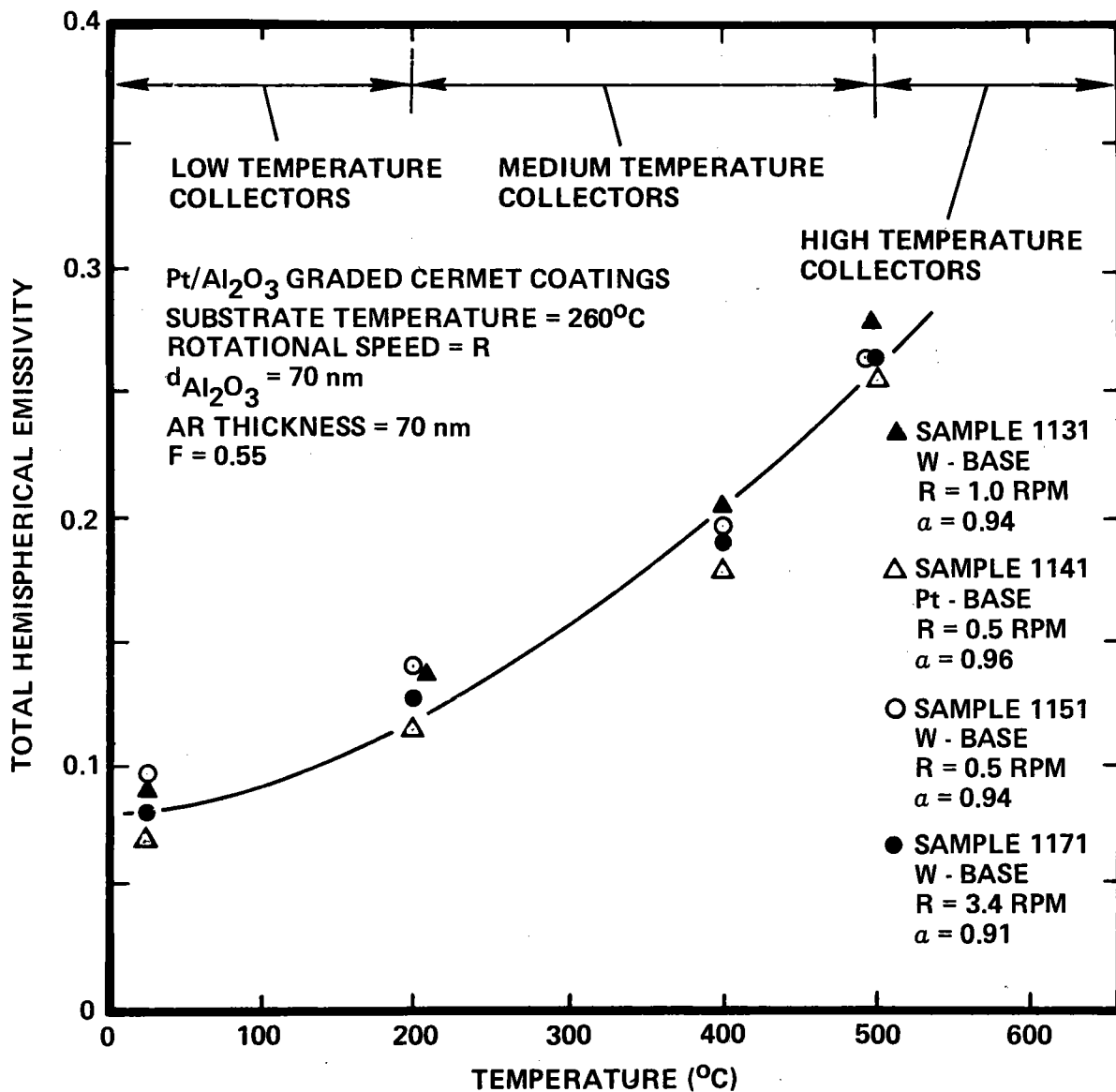


FIG. 20. Temperature dependence of emittance for graded cermet coatings with tungsten low emittance base layers (calculated from reflectance measurements).

high resistivity and emittance values.

Bare coatings of Ta, W, and ZrB₂ about 100 nm thick as well as graded Pt/Al₂O₃ cermet coatings which incorporated these materials as IR reflector layers were tested in air at temperatures of 400°C and 500°C following the procedures described in Section 2.3. The results of these tests are given in Table III and summarized below.

Tantalum - Unprotected Ta coatings about 100 nm thick on glass substrates completely oxidized in about 200 hrs at 350°C in air. Graded Pt/Al₂O₃ cermet coatings deposited onto Ta low emittance base layers on glass substrates exhibited no evidence of degradation after about 800 hrs at 400°C in air. Figure 21 show the spectral reflectance curve for one of these coatings after being subjected to the thermal stability test. A graded Pt/Al₂O₃ coating with a thin cermet layer (see Section 3.3) was tested in air at 500°C. Evidence of degradation (absorptance change >2%) was seen after 260 hrs. However, this degradation may have been a failure of the thin cermet layer and not of the Ta per se. An identical thin cermet coating on a Pt base layer, that was carried as a reference sample in the thermal test, also showed signs of degradation.

Tungsten - Unprotected W coatings about 100 nm thick on glass substrates completely oxidized in from 200 to 400 hrs at 400°C in air. Graded Pt/Al₂O₃ cermet coatings deposited onto W low emittance base layers on glass substrates showed no obvious signs of failure of the coating itself after about 1400 hrs at 400°C in air. However, a large number of pinholes developed because high compressive stresses in the sputter-deposited W ruptured the bond to the glass substrate.²³ A graded Pt/Al₂O₃ cermet coating with a W base layer on a glass substrate was tested in air at 500°C. Nearly complete oxidation of the tungsten layer was observed after 260 hrs of exposure.

Zirconium Diboride - Unprotected ZrB₂ coatings about 70 nm thick on glass substrates developed a very thin oxide layer within the first few hours, but showed no further evidence of change during 280 hr tests conducted in air at 400°C. At 500°C the oxidization was more severe but not catastrophic. Graded Pt/Al₂O₃ cermet coatings deposited onto ZrB₂ low emittance layers on glass substrates showed no change in absorptance after about 600 hrs at 400°C in air. Figure 22 shows the spectral reflectance curve for one of these coatings after the thermal stability test. Thermal stability tests at 500°C in air were encouraging. Thus cermet coatings of normal thickness ($d_{Al_2O_3} \sim 70$ nm) deposited onto ZrB₂ base layers on glass substrates showed no changes in absorptance after almost 1200 hrs of testing (samples 1360 and 1363). In one case (sample 1385), a coating with a thinner cermet layer ($d_{Al_2O_3} = 42$ nm) did show a change in absorptance.

TABLE III

RESULTS OF THERMAL STABILITY TESTS FOR GRADED CERMET COATINGS
WITH ALTERNATE IR REFLECTOR LAYER MATERIALS

Sample	Base Layer	Cermet ⁽¹⁾ Thickness	AR Thickness	Substrate Temp.	Test Temp.	Test Time	Absorptance ⁽²⁾
1115	W	59 nm	59 nm	250°C	- 400°C	- 1407 hrs	0.94 (0.94)*
1126	W	70 nm	70 nm	250°C	- 400°C	- 1407 hrs	0.97 (0.98)*
1154	W	70 nm	70 nm	250°C	- 400°C	- 1132 hrs	0.98 (0.97)*
1134	W	70 nm	70 nm	250°C	- 500°C	- 684 hrs	0.98 (0.96)*†
1266	Ta	70 nm	70 nm	150°C	- 400°C	- 775 hrs	0.96 0.96
1271	Ta	70 nm	70 nm	150°C	-	-	0.96 ⁽³⁾
1270	"	"	"	"	- 400°C	- 775 hrs	0.96 0.96 ⁽⁴⁾
1294	Ta	42 nm	70 nm	150°C	- 500°C	- 684 hrs	0.94 0.88*
1297	Ta	42 nm	70 nm	150°C	- 500°C	- 684 hrs	0.94 0.84*
1361	ZrB ₂	70 nm	70 nm	150°C	- 400°C	- 813 hrs	0.95 0.95
1362	ZrB ₂	70 nm	70 nm	150°C	- 400°C	- 610 hrs	0.96 0.95
1364	ZrB ₂	70 nm	70 nm	150°C	-	-	0.96 ⁽⁵⁾
1365	"	"	"	"	- 400°C	- 610 hrs	0.96 0.95 ⁽⁶⁾
1386	ZrB ₂	42 nm	42 nm	150°C	- 400°C	- 813 hrs	0.96 0.96
1528	ZrB ₂	70 nm	40 nm	150°C	- 400°C	- 813 hrs	0.96 0.96
1554	ZrB ₂	25 nm	20 nm	150°C	- 400°C	- 813 hrs	0.97 0.97

TABLE III (Continued)

RESULTS OF THERMAL STABILITY TESTS FOR GRADED CERMET COATINGS
WITH ALTERNATE IR REFLECTOR LAYER MATERIALS

<u>Sample</u>	<u>Base Layer</u>	<u>Cermet (1) Thickness</u>	<u>AR Thickness</u>	<u>Substrate Temp.</u>	<u>Test Temp.</u>	<u>Test Time</u>	<u>Absorptance (2)</u>
1360	ZrB ₂	70 nm	70 nm	150°C	- 500°C	- 1174 hrs	0.96 0.96
1363	ZrB ₂	70 nm	70 nm	150°C	- 500°C	- 1174 hrs	0.96 0.96
1385	ZrB ₂	42 nm	42 nm	150°C	- 500°C	- 684 hrs	0.97 0.93
1553	ZrB ₂	25 nm	20 nm	150°C	- 500°C	- 684 hrs	0.97 0.96*

Substrate - Glass

(1) Effective thickness of Al₂O₃ component of cermet layer. See Section 3.2.
All cermets have $F \sim 0.55$, where F refers to Pt content at the base of the cermet layer. F-value is based on the deposition conditions.

(2) Absorptance measurements made with International Technology Wiley Alpha Meter.

Comparison measurements made at Battelle Pacific Northwest Laboratories from reflectance data: α = absorptance, ϵ = emittance

- (3) $\alpha = 0.95$ $\epsilon = 0.15$, based on laser reflectance at 10.6 μm
- (4) $\alpha = 0.95$ $\epsilon = 0.14$, based on laser reflectance at 10.6 μm
- (5) $\alpha = 0.95$ $\epsilon = 0.16$, based on laser reflectance at 10.6 μm
- (6) $\alpha = 0.95$ $\epsilon = 0.17$, based on laser reflectance at 10.6 μm

*Pinholes

†Underlayer became transparent

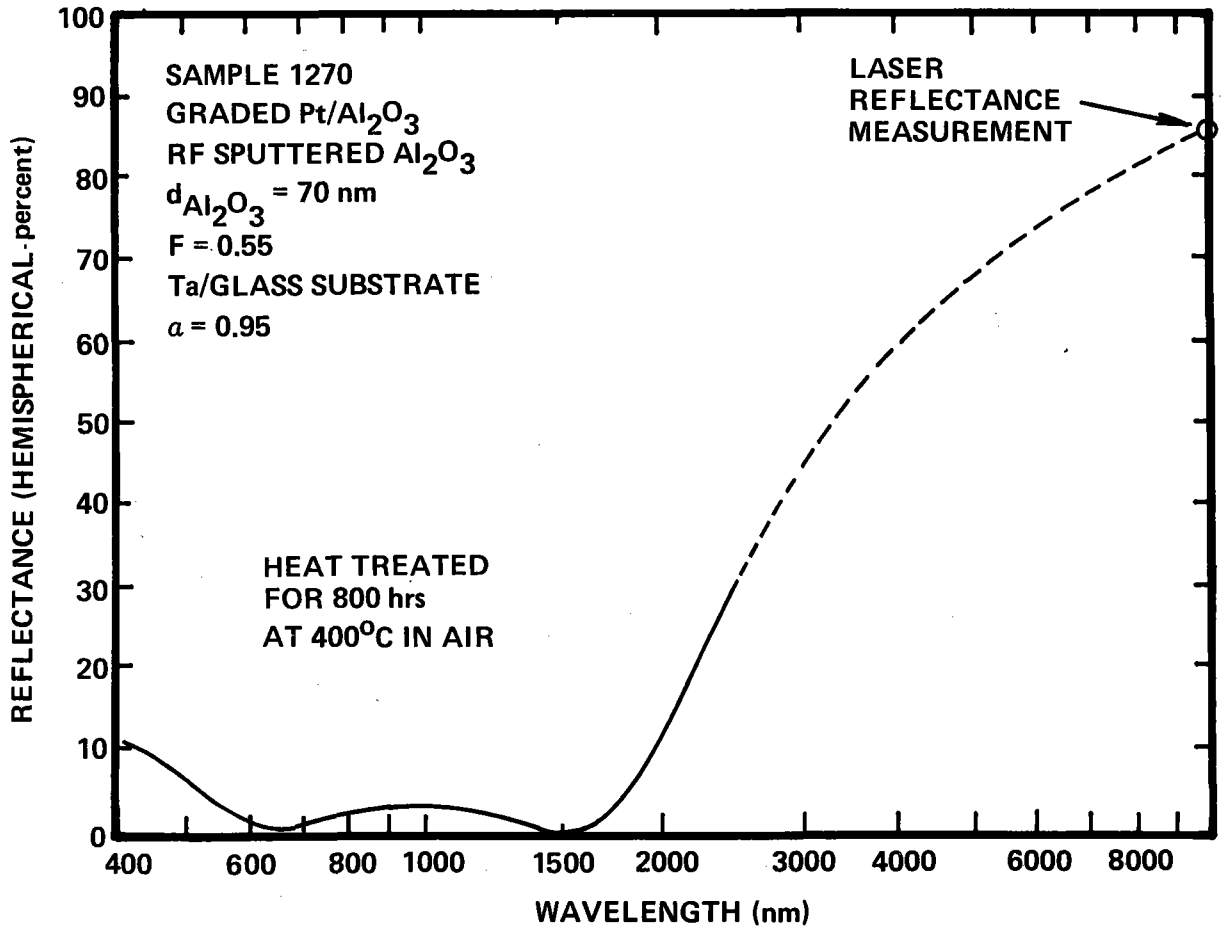


FIG. 21. Spectral reflectance data for graded cermet coating with tantalum low emittance base layer (sample 1270) after heat treatment in air for 800 hrs at 400°C. Antireflection layer thickness is 70 nm.

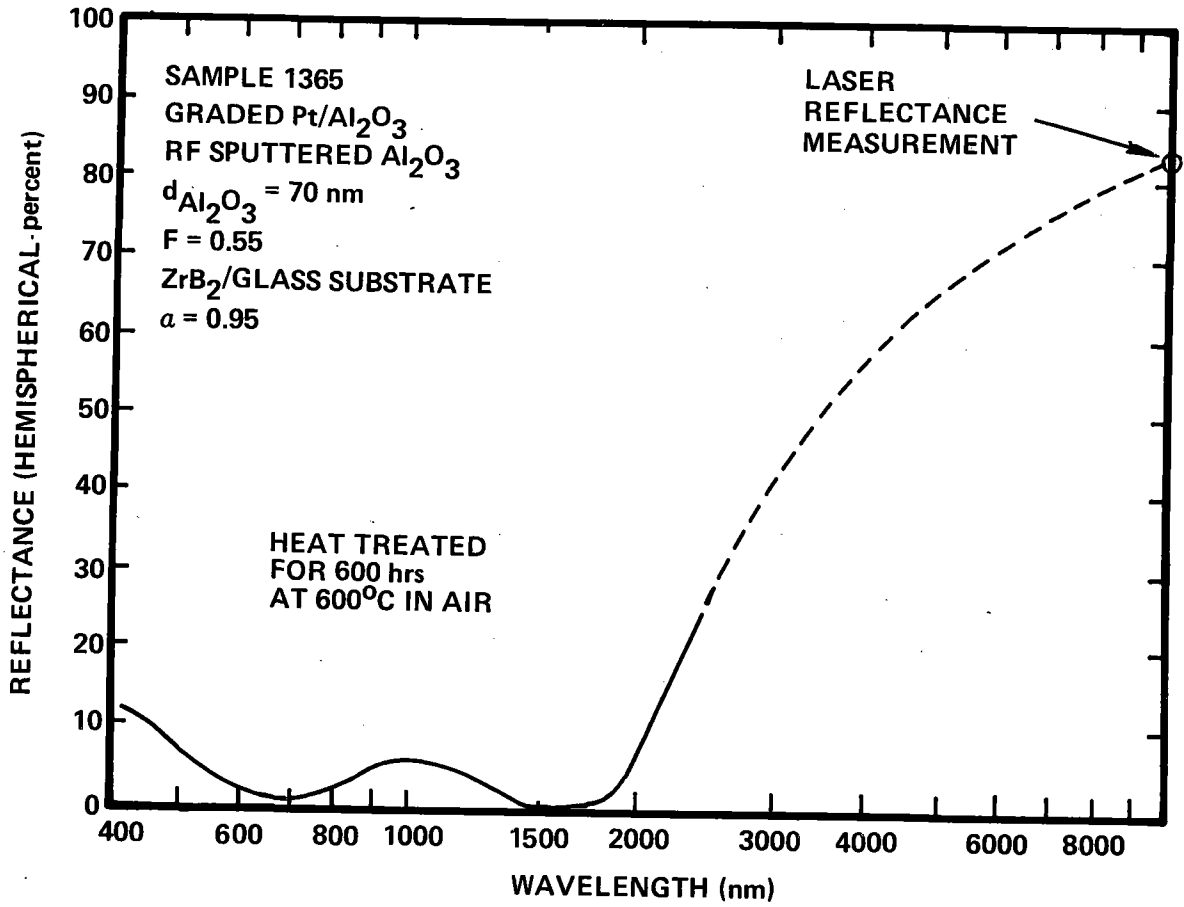


FIG. 22. Spectral reflectance data for graded cermet coating with ZrB₂ low emittance base layer (sample 1365) after heat treatment in air for 600 hrs at 400°C. Antireflection layer thickness is 70 nm.

However, the degradation is believed to be a consequence of the thin cermet layer and not the fact that a ZrB_2 base layer was used (see Section 3.4).

Chromium and Molybdenum - Recent tests have been conducted in which bare coatings of Cr and Mo about 100 nm thick on glass substrates have been tested in air at 350°C for 1000 hrs.⁹ The Cr coating underwent modest oxidation. The Mo coating became severely oxidized.

In summary, ZrB_2 shows promise as a low emittance base material for modest temperature applications. The relatively high emittances which were observed in our sputtered ZrB_2 coatings is believed to be a consequence of the particular sputtering target that was used, and not the fundamental characteristics of ZrB_2 as a base layer material, or sputtering as a deposition method. Although metals such as Cr, Mo, Ta, and W were stable for tests of several hundred hours when overcoated with the cermet layers, the tendency for films of these metals to undergo oxidation when in an unprotected form cast doubt over the long term stability of coatings incorporating IR reflecting layers composed of these materials.

5. EXAMINATION OF ENGINEERING SUBSTRATES

The objective of the engineering substrate task was to optimize graded cermet selective absorber coatings on a variety of metals that are candidates for use in solar thermal receivers. The following substrate materials were selected for investigation:

- Type 316 stainless steel (17% Cr, 12% Ni)
- Incoloy 800 (22% Cr, 32% Ni, 44% Fe)
- Mild steel (type 1020, 0.15% C).

It should be noted again that the coating optimization studies described in Section 3 were conducted using glass substrates. This was done to minimize the effects of variations in surface roughness on the coating optical properties, and the effects of substrate interactions on the coating thermal stability.

A considerable number of cermet coatings were deposited onto type 316 stainless steel substrates during the Phase II research. The stainless steel plates were about 50 mm x 150 mm x 1 mm in size and were attached directly to the substrate mounting reel shown in Fig. 3. They were coated in their as-received state with no polishing. Pre-deposition cleaning consisted of vapor degreasing with trichloroethylene and rinsing with isopropyl alcohol. No sputter cleaning was used. A stainless steel plate of the type described above was mounted at one of the positions on the substrate mounting reel during most of the Phase II deposition runs. In all cases a 50 nm thick Al_2O_3 diffusion barrier was deposited onto the stainless steel prior to depositing a Pt low emittance base layer.⁸ The cermet coatings were deposited at substrate temperatures of about 150°C, 300°C and 400°C using both direct rf sputtering of alumina, and reactive sputtering of aluminum in an Ar+O₂ working gas, to deposit the Al_2O_3 component. Because of the rougher substrate surface the coatings on the stainless steel substrates yielded slightly higher absorptances (typically about 2%) and much larger emittances (typically factor-of-two) than the coatings deposited on glass substrates during the same runs. See Table II in Ref. 8. The higher emittance values are in part a consequence of the method of determination, which was based on normal reflectance measurements and therefore over-

estimates the hemispherical emittance. The hemispherical emittance is the relevant parameter in determining the coating performance. The thermal stability of these coatings depended primarily on the method by which the Al_2O_3 component of the cermet, and the Al_2O_3 diffusion barrier, were deposited. The coatings with rf sputtered Al_2O_3 exhibited the same high thermal stability that was achieved on the glass substrates. Thus one such coating (sample 586 in Table V) showed no change in absorptance after being tested at 600°C in air for about 2000 hrs. Another coating was tested for 2 hrs at 2800 suns (2.8 MW/m^2) at the White Sands Solar furnace by the University of Houston group.¹² The equilibrium temperature was 500°C . No changes in optical properties were found when the coating was re-examined following the exposure. The coatings on stainless steel substrates with reactive sputtered Al_2O_3 appeared to be somewhat less stable than those with direct rf sputtered Al_2O_3 , but still compared favorably with most of the other selective absorber coatings that have been reported in the literature. Thus some of the coatings on stainless steel substrates exhibited increases in absorptance after 100 hr tests in air at 600°C while others showed no change.⁸

During the Phase III optimization studies described in Section 3 graded cermet coatings with rf sputtered Al_2O_3 were deposited onto type 316 stainless steel, Incoloy 800 and mild steel substrates. This was possible because the eight-sided substrate mounting drum allowed a number of substrates to be coated in a given deposition run, as described above. The substrates were flat plates about 50 mm x 50 mm x 1 mm in size. They were clamped onto the larger stainless steel plates which were attached directly to the substrate drum as shown in Fig. 4. The substrate surfaces were coated in their as-received state with no polishing. Pre-deposition cleaning consisted of vapor degreasing with trichloroethylene and rinsing with isopropyl alcohol. In some cases the substrates were sputter cleaned in a separate chamber just prior to being mounted into the deposition chamber (current density of $\sim 1/2 \text{ mA/cm}^2$, at 800V, in an Ar working gas at 0.8 Pa). In most cases the cermet coatings were deposited

without substrate heating. The substrate temperature is estimated to have been about 150°C. In some cases a modest amount of substrate heating was used. The substrate temperature in this case is estimated to have been about 250°C. Because these engineering substrate evaluation studies were conducted in conjunction with the optimization and base layer evaluation studies described in Sections 3 and 4 above, the coatings were deposited using Pt, Ta, W, and ZrB₂ low emittance base layers.

Absorptance and emittance data for typical graded cermet coatings on type 316 stainless steel, low carbon steel, and Incoloy 800 substrates, using W, Ta, Pt, and ZrB₂ base layers, are given in Table IV and compared with similar coatings on glass substrates. It is seen that the data are essentially identical to the Phase II stainless steel results that were described above. Thus the absorptances for the coatings on the metal substrates are equal to, or slightly greater than, the values obtained for glass substrates that were coated during the same deposition run. The implied emittances for the coatings with Pt, W, Ta, and ZrB₂ base layers deposited on the metal substrates are typically about a factor of from 50% (low carbon steel) to 100% (stainless steel and Incoloy) higher than the values for similar coatings on glass substrates. This is believed to be primarily a consequence of the rougher nature of the metal substrates. The low carbon steel substrates were in fact visually smoother than the stainless steel or Incoloy substrates. It should be noted again that the method of measurement somewhat overestimates the emittance for substrates that induce a significant diffuse component to the reflectance. The possible reasons for the high values of the ZrB₂ emittances were discussed in Section 4.

Graded cermet coatings deposited onto the various engineering substrates using Pt, Ta, W, and ZrB₂ base layers were tested in air at 400°C following the procedures described in Section 2.3. Test durations were in the range from 600 to 1700 hrs. In addition selected coatings with Pt and ZrB₂ base layers were tested in air at 500°C for a period of 684 hrs. The results of the thermal tests are summarized in Table V.

TABLE IV
COMPARISON OF OPTICAL PROPERTIES FOR GRADED
CERMET COATINGS ON GLASS AND ENGINEERING SUBSTRATES

Sample Number	Substrate Temperature	Substrate Material (1)	IR Reflector Layer Material	Absorptance (2)	Emittance (3) (20°C)
1107	250°C	Glass	Pt	0.95	0.07
1109	250°C	SS-316	Pt	0.96	0.17
1115	250°C	Glass	W	0.94	0.09
1119	250°C	SS-316	W	0.96	0.22
1316 (4)	150°C	Glass	Pt	0.88	0.08
1300	150°C	SS-316	Pt	0.88	0.24
1322	150°C	Incoloy 800	Pt	0.89	0.20
1301	150°C	Steel	Pt	0.90	0.10
1307 (5)	150°C	Glass	Ta	0.90	0.20
1312	150°C	SS-316	Ta	0.92	0.36
1310	150°C	Incoloy 800	Ta	0.93	0.38
1313	150°C	Steel	Ta	0.92	0.21
1376* (6)	150°C	Glass	Pt	0.95	0.12
1378	150°C	SS-316	Pt	0.96	0.29
1379	150°C	Incoloy 800	Pt	0.96	0.23
1359	150°C	Steel	Pt	0.96	0.14
1361* (7)	150°C	Glass	ZrB ₂	0.95	0.24
1366	150°C	SS-316	ZrB ₂	0.97	0.45
1367	150°C	Incoloy 800	ZrB ₂	0.96	0.42
1371	150°C	Steel	ZrB ₂	0.96	0.29

(1) Material designations are

Glass = Corning Type 7059 Borosilicate Glass.

SS-316 = Type 316 Stainless Steel

Incoloy 800

Steel = Type 1020 Low Carbon Steel.

(2) Absorptance measurements made with International Technology Wiley Alpha Meter.

(3) Emittance measurements made with International Technology Ambient Emisometer.

Comparison measurements made at Battelle Pacific Northwest Laboratories from identical samples:

(4) $\alpha = 0.86$, $\epsilon = 0.04$, based on laser reflectance measurement at 10.6 μm

(5) $\alpha = 0.90$, $\epsilon = 0.13$, based on laser reflectance measurement at 10.6 μm

(6) $\alpha = 0.94$, $\epsilon = 0.07$, based on laser reflectance measurement at 10.6 μm

(7) $\alpha = 0.95$, $\epsilon = 0.16$, based on laser reflectance measurement at 10.6 μm

*After heat treat at 400°C in air for 813 hours (No degradation observed).

TABLE V

RESULTS OF THERMAL STABILITY TESTS FOR GRADED CERMET COATINGS
DEPOSITED ONTO ENGINEERING SUBSTRATE MATERIALS

<u>Sample</u>	<u>(1)</u> <u>Substrate</u>	<u>Base</u> <u>Layer</u>	<u>Cermet (2)</u> <u>Thickness</u>	<u>AR</u> <u>Thickness</u>	<u>Substrate</u> <u>Temp.</u>	<u>Test</u> <u>Temp.</u>	<u>Test</u> <u>Time</u>	<u>Absorp-</u> <u>tance (3)</u>
586	SS	Pt	70 nm	70 nm	350°C	- 600°C	- 1935 hrs	0.96 0.96
870	SS	Pt	70 nm	70 nm	350°C	- 550°C 600°C	- 314 hrs 2011 hrs	0.97 0.97 0.92*
886	SS	Pt	70 nm	70 nm	350°C	- 600°C	- 1935 hrs	0.96 0.95
1289	SS	Ta	42 nm	70 nm	150°C	- 400°C	- 684 hrs	0.96 (0.87)*
1309	SS	Ta	25 nm	70 nm	150°C	- 400°C	- 610 hrs	0.92 0.87
1311	Incoloy	Ta	25 nm	70 nm	150°C	- 400°C	- 610 hrs	0.91 0.87
1314	Steel	Ta	25 nm	70 nm	150°C	- 400°C	- 610 hrs	0.92 0.87
1321	SS	Pt	25 nm	70 nm	150°C	- 400°C	- 610 hrs	0.87 0.87
1369	SS	ZrB ₂	70 nm	70 nm	150°C	- 400°C	- 610 hrs	0.96 0.96
1368	Incoloy	ZrB ₂	70 nm	70 nm	150°C	- 400°C	- 610 hrs	0.96 0.96
1370	Steel	ZrB ₂	70 nm	70 nm	150°C	- 400°C	- 610 hrs	0.96 0.96
1357	SS	Pt	70 nm	70 nm	150°C	- 400°C	- 610 hrs	0.96 0.93
1380	Incoloy	Pt	70 nm	70 nm	150°C	- 400°C	- 610 hrs	0.96 0.94
1358	Steel	Pt	70 nm	70 nm	150°C	- 400°C	- 610 hrs	0.96 0.95

TABLE V (Continued)

RESULTS OF THERMAL STABILITY TESTS FOR GRADED CERMET COATINGS
DEPOSITED ONTO ENGINEERING SUBSTRATE MATERIALS

<u>Sample</u>	<u>(1) Substrate</u>	<u>Base Layer</u>	<u>Cermet (2) Thickness</u>	<u>AR Thickness</u>	<u>Substrate Temp.</u>	<u>Test Temp.</u>	<u>Test Time</u>	<u>Absorp- tance (3)</u>
1390	SS	ZrB ₂	42 nm	42 nm	150°C	- 500°C	- 684 hrs	0.96 0.88
1392	Incoloy	ZrB ₂	42 nm	42 nm	150°C	- 500°C	- 684 hrs	0.96 0.89
1395	Steel	ZrB ₂	42 nm	42 nm	150°C	- 500°C	- 684 hrs	0.96 0.88
1402	SS	Pt	42 nm	42 nm	150°C	- 500°C	- 684 hrs	0.94 0.92
1404	Incoloy	Pt	42 nm	42 nm	150°C	- 500°C	- 684 hrs	0.93 0.92
1383	Steel	Pt	42 nm	42 nm	150°C	- 500°C	- 684 hrs	0.93 0.84
1149	SS	W	70 nm	70 nm	250°C	- 400°C	- 140 hrs	0.98 0.93
1119	SS	W	59 nm	59 nm	250°C	- 400°C	- 409 hrs	0.95 0.89
1109	SS	Pt	59 nm	59 nm	250°C	- 400°C	- 1710 hrs	0.95 0.94

(1) Substrate notation is as follows:

SS = 316 Stainless Steel

Incoloy = Incoloy 800

Steel = Type 1020 Low Carbon Steel

(2) Effective thickness of Al₂O₃ component of cermet layer. See Section 3.2.

All cermets have F = 0.55, where F refers to Pt content at the base of the cermet layer. F-value is based on the deposition conditions.

(3) Absorptance measurements made with International Technology Wiley Alpha Meter.

* Pinholes.

Graded cermet coatings of normal thickness ($d_{\text{Al}_2\text{O}_3} = 70 \text{ nm}$) were stable at 400°C on all three of the engineering substrates (see samples 1368, 1369, and 1370). Absorptance changes were observed at 400°C for the thinner cermet coating, which apparently is inherently less stable (see Section 3.4). The absorptance changes were greatest for the coatings with reactive (Ta) base layers (compare samples 1309, 1311, 1314 and 1321). This suggests oxygen diffusion through the cermet and attacking of the base layers. In some cases (sample 1357) failure was observed even for graded cermets of normal thickness with Pt base layers. This suggests a second failure mechanism. This could be interdiffusion within the cermet or at the cermet-substrate boundary. In both cases the diffusion processes would be enhanced by the presence of columnar growth flaws. The rough engineering substrates would promote the formation of such flaws in both the diffusion barrier and cermet layers.¹⁸

The results of the 500°C tests are somewhat ambiguous because the thin cermet layers that were used for most of the samples. It should also be noted that thin cermet layers would be more vulnerable to the columnar type flaws discussed above.

In summary, the above data are somewhat inconclusive because of the relatively small number of samples that were tested. The data suggest however that the primary difference between the engineering substrates and the glass substrates is in the surface roughness of the metal substrates. This roughness is typically on a size scale that produces a slight, and generally insignificant, increase in the absorptance along with a large, typically factor-of-two, increase in emittance. In addition, there is evidence that the surface roughness can cause columnar growth flaws to develop which significantly degrade the thermal stability of the coatings. Thus surface polishing appears to be an important consideration in improving both the optical properties and the thermal stability of the coatings on engineering substrates. If this is done, and a suitable Al_2O_3 diffusion barrier is used, it appears that the differences between the engineering substrates themselves introduce only second order effects. Thus it should be possible to deposit high performance Pt/ Al_2O_3 selective absorber coatings on all of the engineering substrates that have been examined.

6. TUBE COATING EXPERIMENTS

6.1 Objective and Apparatus Design

The objective of this task was to deposit Pt/Al₂O₃ graded cermet coatings onto a small number of 1 1/4 inch outside diameter by 1 inch inside diameter by 24 inch long receiver tubes, using a bench scale apparatus. Type 316 stainless steel was selected by SERI as the material for the tubes.

A second objective of the tube coating task was to identify problem areas and develop general guidelines for the design of a large scale production apparatus. Thus it was decided that the bench scale coating apparatus should have the same general apparatus configuration that had been envisioned in making the cost calculations described in Ref. 8. In this apparatus a large load of tubes is mounted on a planetary type substrate holder and circulated alternately past long Al₂O₃ and Pt planar magnetron sputtering sources located on the inside wall of a large coating chamber. See Fig. 23.

The bench scale apparatus was identical in concept to the production apparatus, but considerably more complicated because of requirements imposed by the length of the tubes. The general approach in the apparatus design was to replace the substrate mounting drum shown in Figs. 3 and 4 with a planetary system that would circulate the tubes alternately past the rf driven Al₂O₃ sputtering source and the dc driven Pt source. In this sense the bench scale apparatus was identical in concept to the large production apparatus shown in Fig. 23. However, the design of the bench scale apparatus was more complicated because the substrate tubes were longer than the available Al₂O₃ and Pt sputtering sources. (See next section.) Furthermore, the chamber in which the sources were mounted was not deep enough to permit the axial motion required to assure uniform coating thickness along the tube length. Therefore, it was necessary (1) that the entire planetary substrate mounting assembly be designed so that it could be translated axially back and forth in front of the sputtering sources, and (2) that the chamber be lengthened to accommodate this axial tube motion.

The general configuration of the bench scale apparatus is shown schemat-

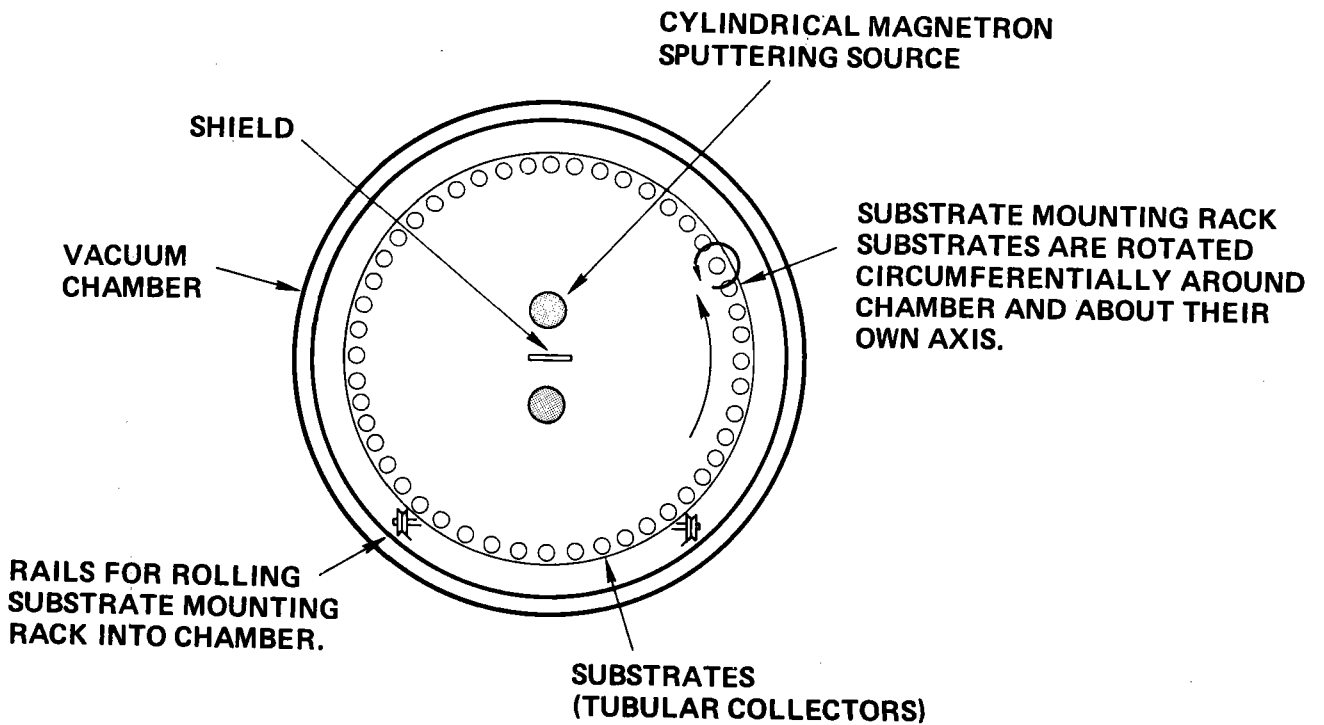


FIG. 23. Schematic illustration of production apparatus envisioned for depositing Pt/Al₂O₃ graded cermet coatings onto tubular substrates.

ically in Fig. 24. The entire planetary assembly was mounted on wheels and attached to a 2m long support rail. A lead screw, running parallel to the rail, was used to apply axial motion to the assembly. Rotary motion to drive the planetary was transmitted to the assembly through a sliding spline type ball bearing. Variable speed electric motors were used to independently drive the lead screw and spline shafts. One end of the rail assembly was attached to an auxiliary vacuum chamber. The auxiliary chamber was designed to be bolted to a 10 inch diameter port in the main chamber. When this was done, the cantilevered rail passed down the axis of the frame assembly shown in Fig. 3. The entire assembly is shown in Fig. 25, with the planetary translated to the end of the cantilevered rail. The auxiliary chamber can be seen at the right. The bearing mounts for the lead screw and spline shafts can be seen at the left along with a conical appendage which became captured in a supporting ring when the assembly was attached to the main chamber. The captured appendage provided leveling and support for the cantilevered rail. The planetary assembly was configured to accommodate twelve substrate tubes on a 16 cm diameter. With this configuration the substrate-to-target distance was about the same as for the apparatus configuration (Fig. 3) that was used for the optimization studies. A load of unpolished tubes is shown on the planetary in Fig. 25.

6.2 Considerations Relating to Coating Uniformity

The deposition flux profiles from the sputtering sources are a critical consideration in the design of apparatuses for coating substrates of large area or complex shape. One of the advantages of magnetron sputtering is that large magnetrons can produce relatively uniform fluxes over long lengths. However, the flux uniformity problem was exacerbated in the present experiments because the relatively small planar magnetron Al_2O_3 and Pt sputtering sources that were available for the project:

- 1) yielded nonuniform coating fluxes at the deposition plane;
- 2) were considerably shorter (factor of two) than the substrate tubes;
- 3) were unequal in length and therefore gave unequal profiles (Al_2O_3 = 15 inches, Pt = 12 inch, see Section 2.1).

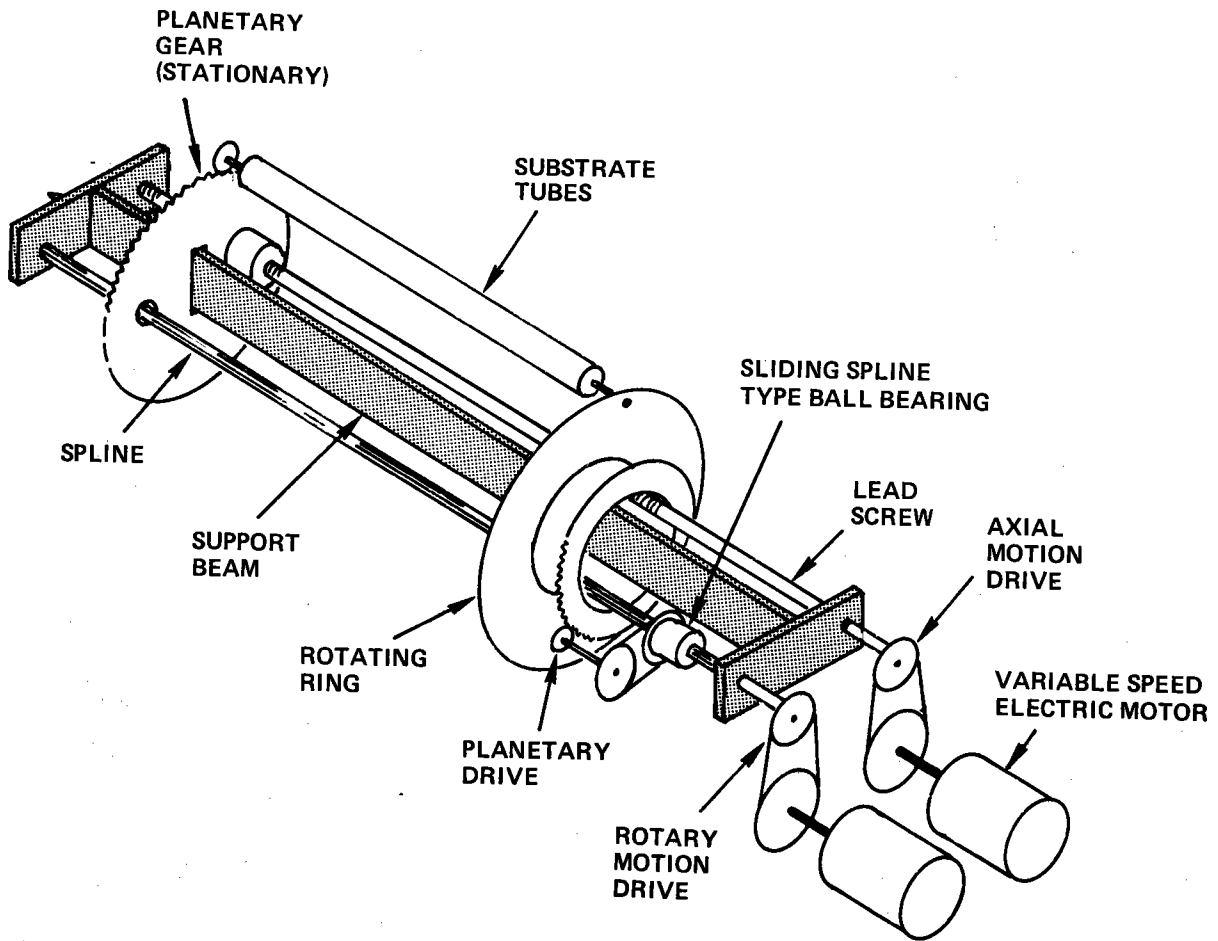


FIG. 24. Schematic illustration of drive mechanism for bench scale apparatus that was used for depositing Pt/Al₂O₃ graded cermet coatings onto tubular substrates.

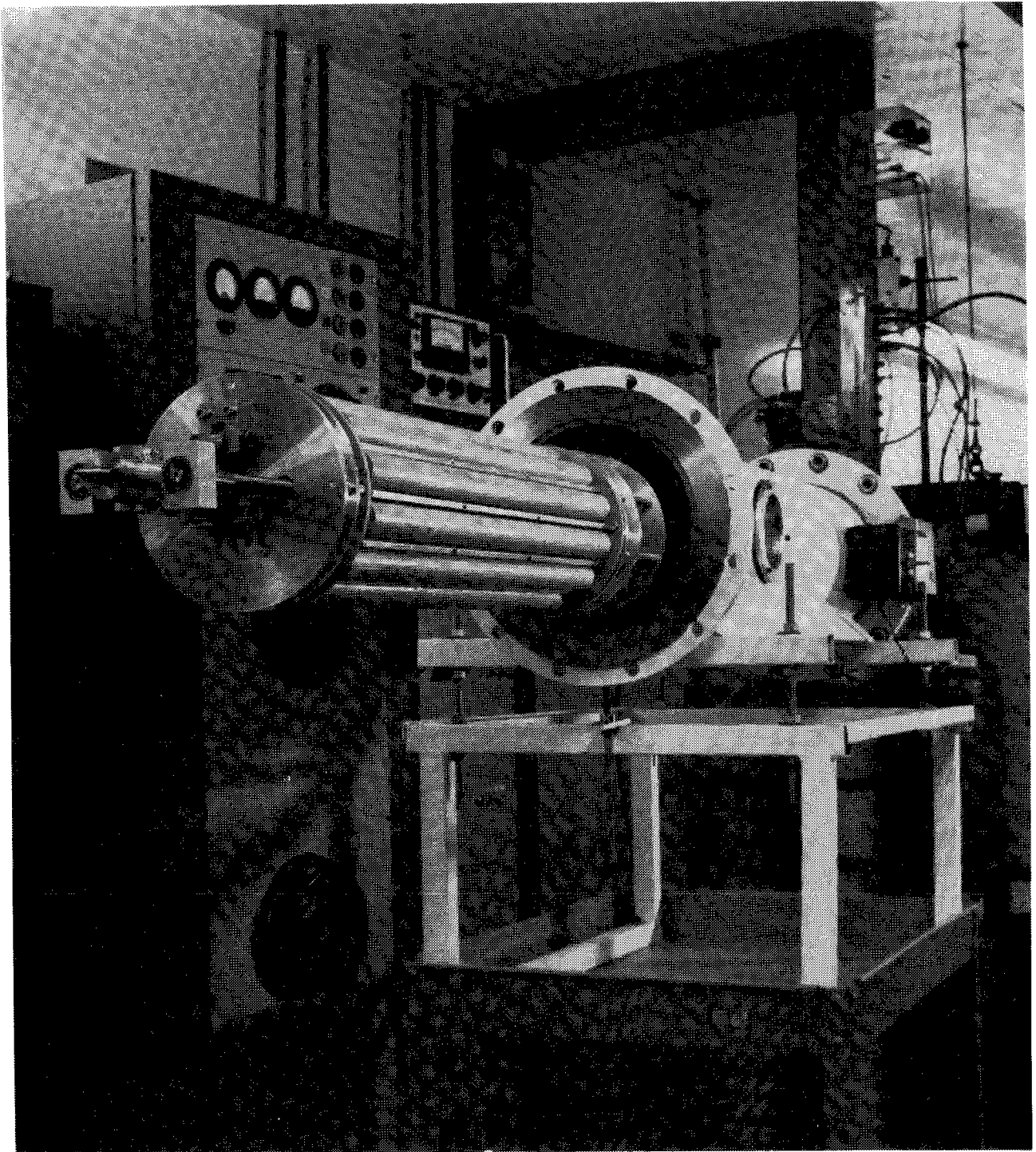


FIG. 25. Photograph of benchscale apparatus that was used for depositing Pt/Al₂O₃ graded cermet coatings onto tubular substrates.

The key factor that allowed these sources to be used was the fact that the Pt composition profile is not critical to the performance of graded cermet coatings (see Section 3.2).

Figures 26 and 27 show the deposition flux profiles at the substrate tube position on the planetary circumference, along the axial (x-x) and transverse (y-y) centerlines, for both the Al_2O_3 and Pt sources under typical operating conditions. These are typical profiles for magnetrons of modest length.

An axial position x along a tube will accumulate a coating flux $G(x)$ given by the integrated flux under the transverse y-y profile as it moves past a sputtering source during the planetary rotation. Thus one can write

$$G(x) = \int_W G(x,y) dy \quad , \quad (3)$$

where $G(x,y)$ is the deposition flux at a position x,y in the substrate plane and the integration is carried out over the width W of the flux profile. Shields such as those shown in Fig. 28 can be used to make the accumulated fluxes constant for all positions x along the tubes. The use of long magnetrons, or a distribution of shorter magnetrons such as is shown in Fig. 29, can, with appropriate shields, produce uniform accumulated fluxes along the length of the tubes. Thus one has:

$$G_{Al_2O_3}(x) = \text{constant} \quad (4)$$

and

$$G_{Pt}(x) = \text{constant} \quad . \quad (5)$$

Under these conditions no axial motion of the tubes is required. This is the envisioned performance for the apparatus shown in Fig. 23. The operating procedure would be essentially identical to that used for the apparatus shown in

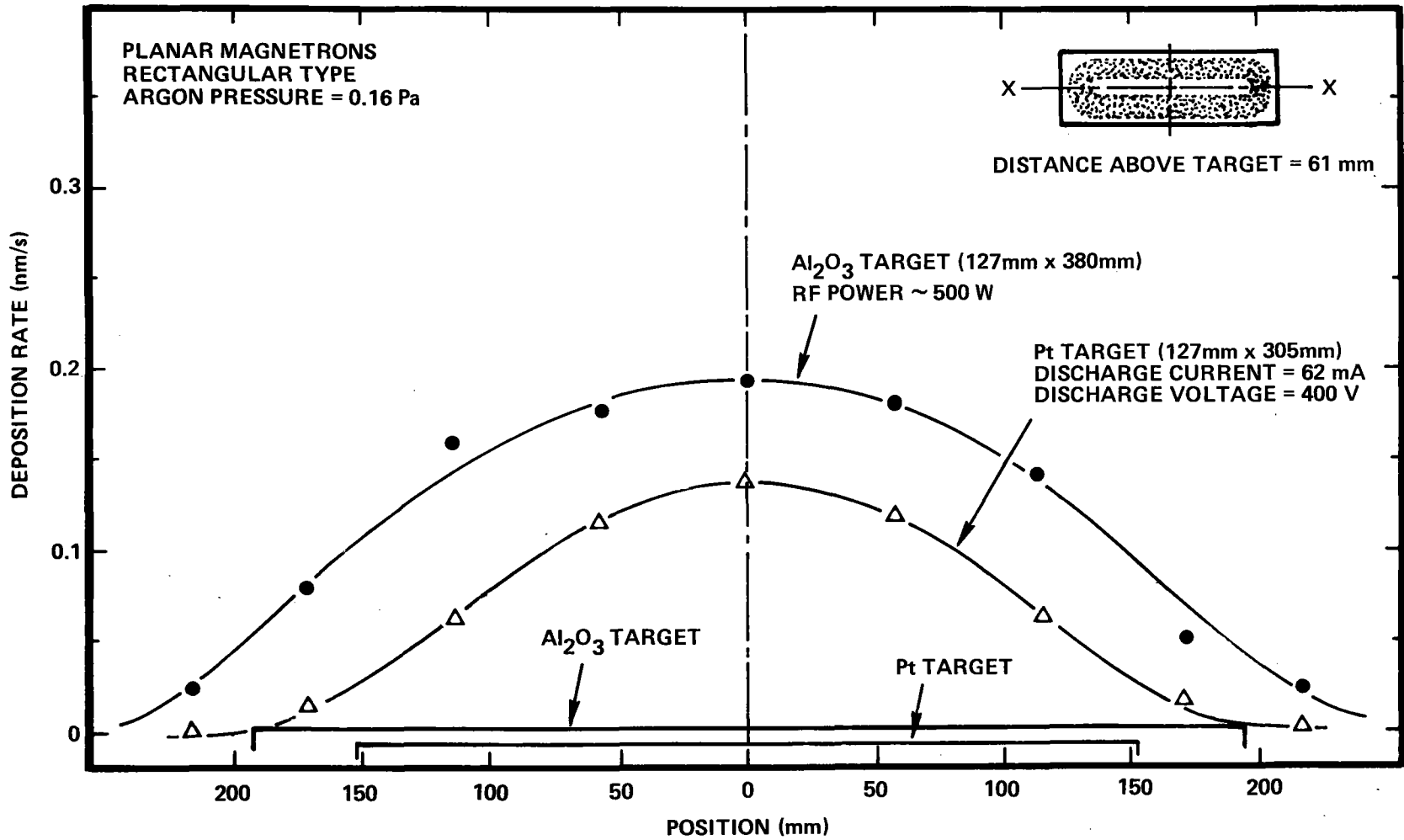


FIG. 26. Deposition rate profiles along the long axis of a 5 inch x 15 inch planar magnetron with an alumina (Al_2O_3) target and a 5 inch x 12 inch planar magnetron with a platinum target.

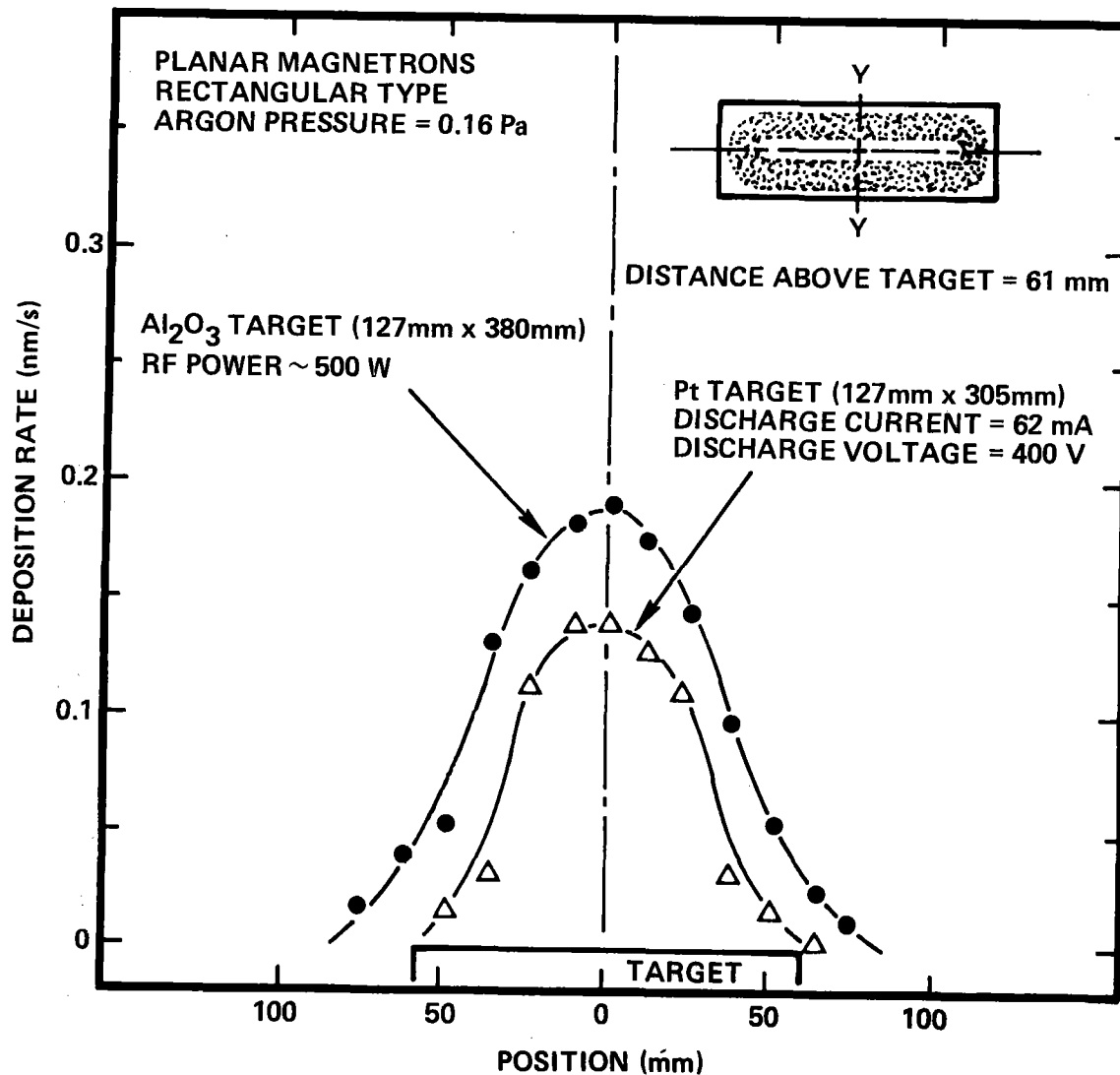


FIG. 27. Deposition rate profiles along the short axis of a 5 inch x 15 inch planar magnetron with an alumina (Al₂O₃) target and a 5 inch x 12 inch planar magnetron with a platinum target.

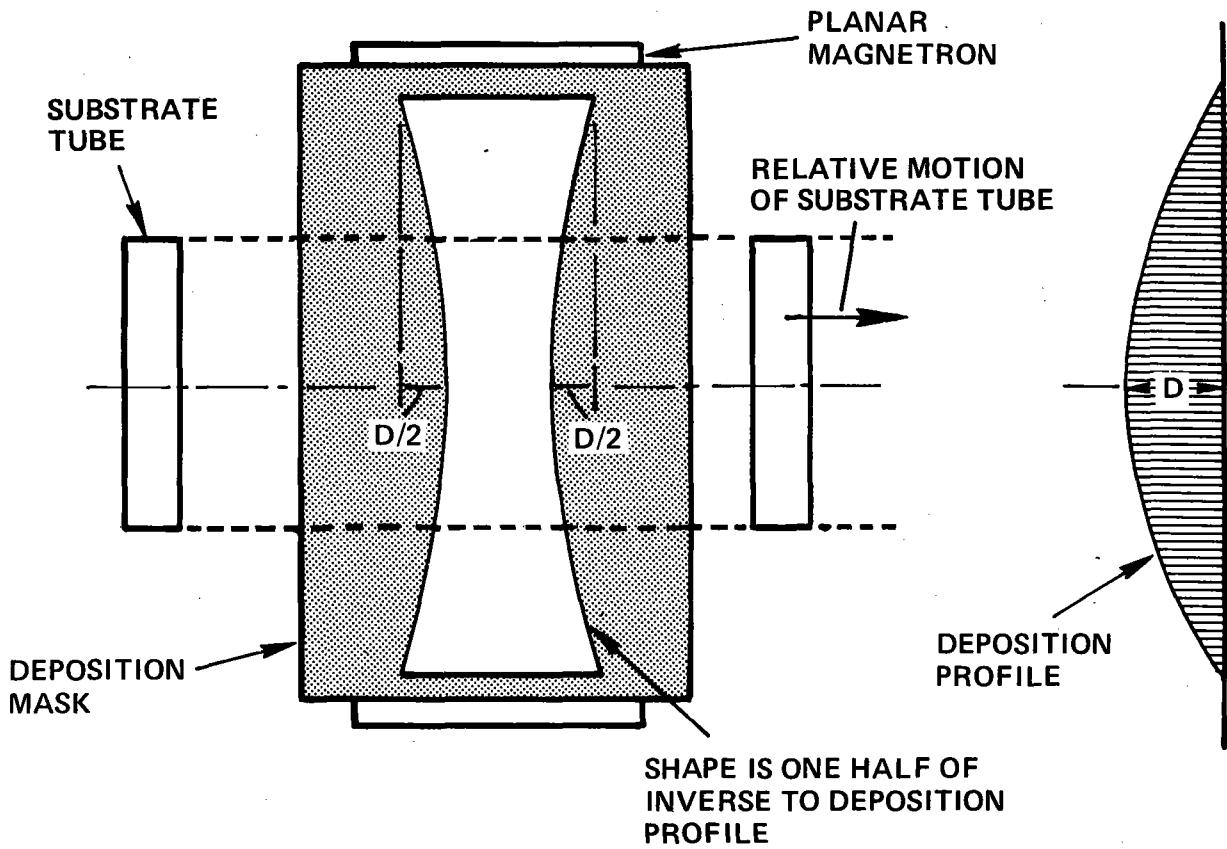


FIG. 28. Shield or mask configuration for producing uniform deposition onto moving substrates.

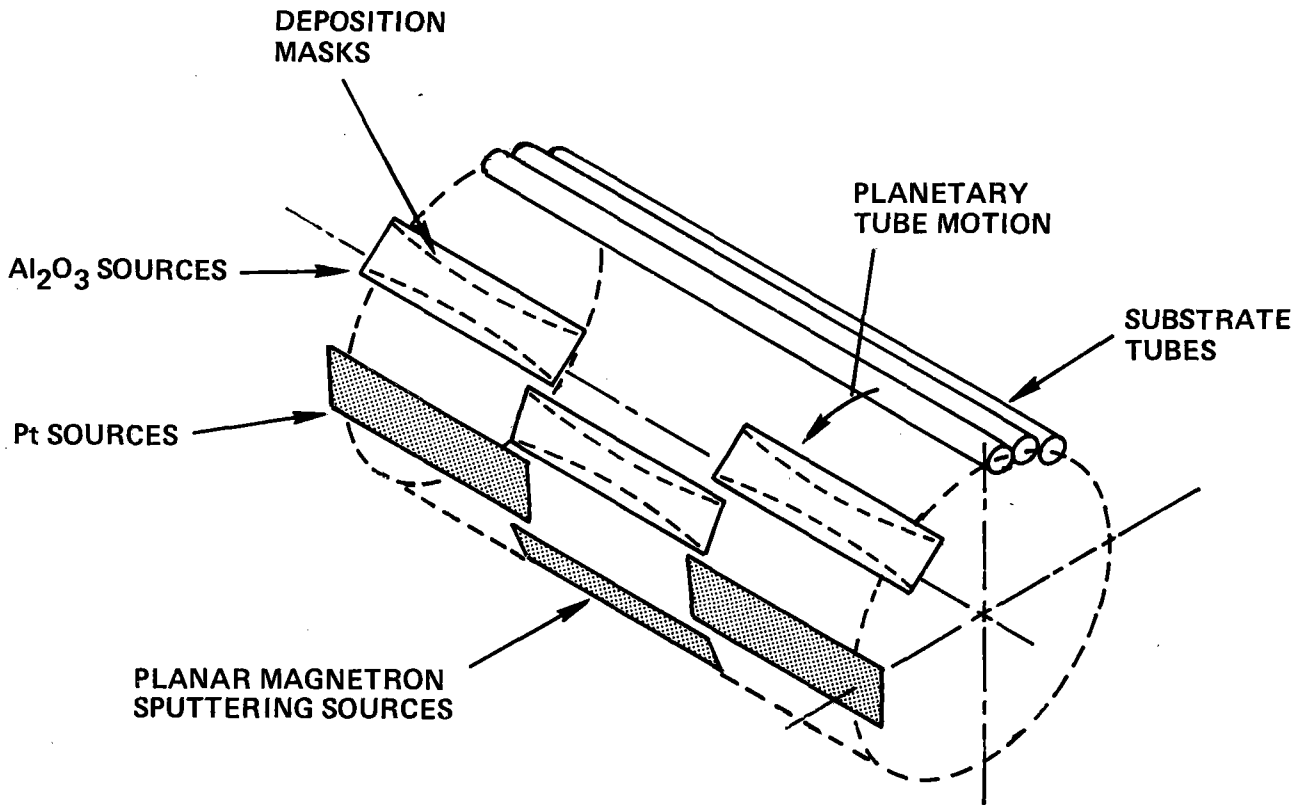


FIG. 29. Production coating configuration which uses a plurality of relatively short magnetron sputtering sources to deposit uniform coatings onto long tubular substrates. See Fig. 23.

Fig. 3 and the optimization studies described in section 3.3. Any desired grading profile could be built into the coating by simply varying the current to the Pt source or sources. The only design requirement is that the tubes make several revolutions as they pass through the alternating regions of Al_2O_3 and Pt flux. This assures that the flux represented by the integrated profiles is spread uniformly around the circumference of the tubes. This requirement establishes the gear ratio of the planetary. The overall rotational speed of the planetary then establishes the number of monolayers of Pt or Al_2O_3 that are accumulated in each passage through the respective fluxes (see Section 3).

If Eqs. (4) and (5) are not satisfied, either because the axial profiles are non-uniform as shown in Fig. 26, or because the tubes are longer than the region of sputtered flux, then axial motion of the tubes is required. The situation would again be relatively simple if one were dealing with a non-graded coating so that co-sputtering would not be required. In such a case, if the planetary rotational speed were made fast compared to the translational speed, and if the entire tube were translated completely past the source, then all points on the tube would accumulate the same integrated axial flux and the coating would be uniform. However, if grading is done, then the rotary and axial motions become coupled and the situation becomes considerably more complicated. This is seen by noting that a given axial position on a tube will undergo a spiral motion as it passes down the tunnel between the Pt and Al_2O_3 sources. The pitch of the spiral motion is determined by the relative magnitudes of the rotation and translation of the planetary assembly.

Consider the idealized case where the Al_2O_3 and Pt deposition profiles are nonuniform in x , but mathematically similar, so that

$$G_{Pt}(x) = K(t) G_{Al_2O_3}(x). \quad (6)$$

We assume that the Al_2O_3 profile has the form of the experimental data shown in Fig. 26. We further assume that K is varied linearly from one to zero, in the time that it takes a substrate element to pass through the axial profile,

in an effort to produce a near-linear grading of F from 0.5 to zero. The solid curve in Fig. 30 shows the calculated F-value as a function of depth in the coating. Part of the distortion from linearity occurs because of the basic nonlinearity of the F-value relationship as discussed in Section 3.2. This contribution is shown by the dashed curve, which corresponds to the F-value variation that would be seen by a stationary substrate, and is essentially identical to the relationship shown in Fig. 5. The additional distortion apparent in the heavy curve results because the substrate point in question experiences various deposition rates at various times during the F-value variation. This component of the distortion could be minimized by making multiple passes with a slow variation in K during a single pass.

The above calculation is idealized, in that it applies to a single point on a tube. Other points on a long tube will pass various points in the profile at different times and will therefore accumulate different F-value grading profiles. Furthermore, when a long tube is passed in front of the sources so that all points on the tube pass entirely through the profiles, a given point on the tube will spend a significant portion of its time outside the coating flux. When it re-enters the coating flux at a later time, a new K value will be operative, with the consequence that an abrupt step will be created in the grading profile. These steps can obviously be minimized by using a large number of axial passes with small K-value variations during each pass. However, the degree to which this can be done is limited by mechanical constraints, since the planetary rotational speed must be large compared to the translational speed, as noted above. The imposition of a requirement between translation and rotational speeds also limits the degree to which the number of monolayers of Al_2O_3 and Pt that are deposited on each cycle can be controlled.

Figure 31 shows a calculated F-value grading profile for a case where the substrate tubes are slightly longer than the deposition profile and where points on the substrate experience six single passes (down or back) in front of the sources during the time that the F-value grading takes place. The conditions

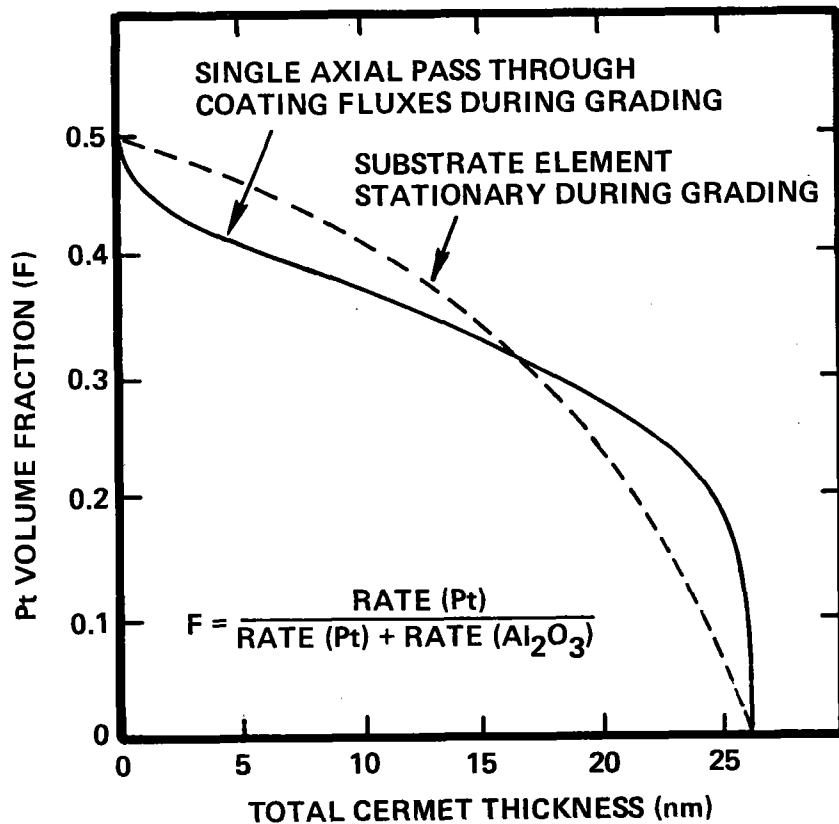


FIG. 30. Calculated Pt volume fraction (F) as a function of depth, showing the effect of the axial variations in the Pt and Al₂O₃ deposition profiles for a substrate element that makes one pass in the axial direction during the time that the F-value grading takes place. Profile for stationary element shown for comparison (see Fig. 5).

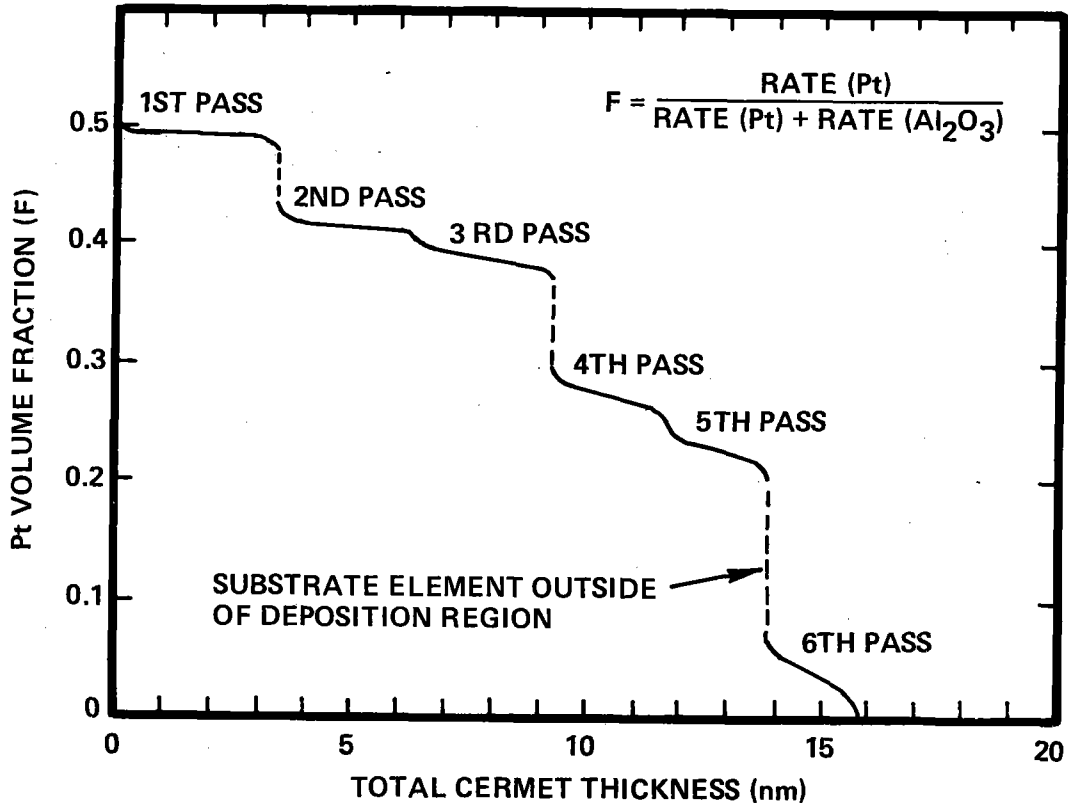


FIG. 31. Calculated Pt volume fraction (F) as a function of depth for an elemental area at one end of a tube which is about equal in length to the deposition sources and makes six single passes (down or back) in front of the sources during the time that the F-value grading takes place.

for this calculation are considered to be a reasonable compromise, and actually approximate the deposition conditions used for the experiments described in the next section. The general departure from linearity and the abrupt steps are not expected to seriously degrade the performance of the coating. This judgement is based on the optimization studies described in Section 3, in which coatings with various grading profiles were examined.

The calculated profile in Fig. 31 is based on the assumption that the Pt and Al_2O_3 deposition profiles are similar--i.e., obey Eq (6). This condition was not satisfied for the experimental equipment that was available on this project, as described in the preceding section. This lack of profile similarity obviously further limits the degree to which a controlled grading profile could be provided at all points along the length of the tubes.

In summary, the use of long sputtering sources, or a suitable array of smaller sources, to produce a uniform axial flux from both the Al_2O_3 and Pt sources will permit uniform graded coatings with controlled composition profiles to be deposited onto long tubular receiver sections in a relatively straightforward manner. The only design requirement is that

- The planetary gear ratio should cause the tubes to make several rotations as they pass respectively through the Pt and Al_2O_3 fluxes.

The situation where the tubes are longer than the sputtering sources, and the sputtering sources are of unequal length, as was the case in the present experiments, introduces complexities that limit the control that can be maintained over the grading profile. These difficulties can be minimized by the following design considerations.

- Shields should be used to make the Pt and Al_2O_3 flux profiles as uniform as possible and of equal length.
- The tubes must be translated so that the entire tube moves completely past the sputtering source.
- The coating must be done with the tubes making many axial cycles past the sputtering sources, so that the variation in Pt and Al_2O_3 sputtering rates (F-value) can be small during one translation past the sources.

- The planetary rotational speed must be large compared to the translational speed.

6.3 Coating Experiments

The substrates were type 316 stainless steel tubes 1 1/4 inch in outside diameter by 1 inch inside diameter, by 24 inches long. A batch of twelve tubes were cleaned and polished using the procedure listed below.

- 1) Isopropyl alcohol scrub and rinse.
- 2) Polish ending with number 320 emery cloth to remove surface oxide and scratches and to smooth surface.
- 3) Isopropyl alcohol rinse.
- 4) Etch for 5.0 min in 25% H_2SO_4 at 28°C.
- 5) Water and isopropyl alcohol rinse.
- 6) Etch for 15 min in 30% HNO_3 at 60°C.
- 7) Water and isopropyl alcohol rinse.
- 8) Cold trichloroethylene rinse.
- 9) Hot trichloroethylene vapor degrease.
- 10) Isopropyl alcohol rinse.

The planetary substrate mounting apparatus was electrically grounded. Therefore, it was not possible to perform in situ sputter cleaning. Accordingly, following the cleaning procedure described above, the substrate tubes were loaded into a separate chamber and sputter-cleaned in an Ar working gas at 1.0 Pa for 12 min at a current density of about 0.8 mA/cm² and voltage of 800V to remove approximately 500 nm of material from the surface. The batch of sputter-cleaned tubes were then stored in a clean room and finally loaded into the planetary assembly, as shown in Fig. 25.

No shielding was used to make the Pt and Al_2O_3 deposition profiles uniform for the preliminary experiment described in this report, since the first objective was to debug the apparatus and the planetary assembly. Two problems were encountered that presented serious difficulties in obtaining uniform coatings over the tubes.

The first problem was not unexpected, but nevertheless was a factor that limited the uniformity that could be achieved over the length of the tubes. The large coating chamber that mounted the sputtering sources was not deep enough to permit the tubes to be moved entirely beyond the sources in the

direction passing into the coating chamber. The problem was minimized by operating the sources for a short time during each translational cycle with no translational motion. Figure 32 shows an approximate axial profile for the final coating that was deposited during the sequence of experiments. The dropoff in thickness at the right is a consequence of the limitation in the available axial motion. The peak adjacent to this dropoff is a consequence of the static operation that was used to compensate for the dropoff effect.

The second problem related to failures of some of the small bearings that were used to mount the spur gears on the planetary assembly. These failures acted in concert to produce a significantly uneven loading on the motor that was driving the rotary motion of the planetary. Consequently, the rotary motion was uneven and resulted in the graded cermet coatings tending to be nonuniform around the circumference of the tubes. The problem was eventually corrected by replacing the bearings.

The procedure during the shakedown experiments was simply to continue depositing coatings, one on top of the other, in order that time be spent on debugging the apparatus and not on repeated cleaning and loading of tubes. Accordingly, coatings on the tubes that were delivered to SERI consisted of a 50 nm thick Al_2O_3 diffusion barrier and about 1000 nm made up of about ten graded cermet coatings, one on top of the other. The final graded cermet coating had the profile shown in Fig. 32 and was optically isolated from the other layers by a 100 nm thick Pt layer for two of the ten tubes that were shipped to SERI. Figure 33 shows a photograph of some of the coated tubes prior to shipment to SERI.

Nominal deposition conditions for the final cermet layer are listed below.

- IR reflecting layer - Pt, 100 nm thick.
- Cermet layer thickness - $d_{\text{Al}_2\text{O}_3} = 90$ nm.
- Cermet layer grading - $F = 0.42$ to 0.
- Al_2O_3 antireflection layer thickness = 30 nm.
- Planetary rotation speed = 0.94 rpm.
- Tube rotation speed = 18 rpm.
- Al_2O_3 deposition rate = 0.19 nm/s.

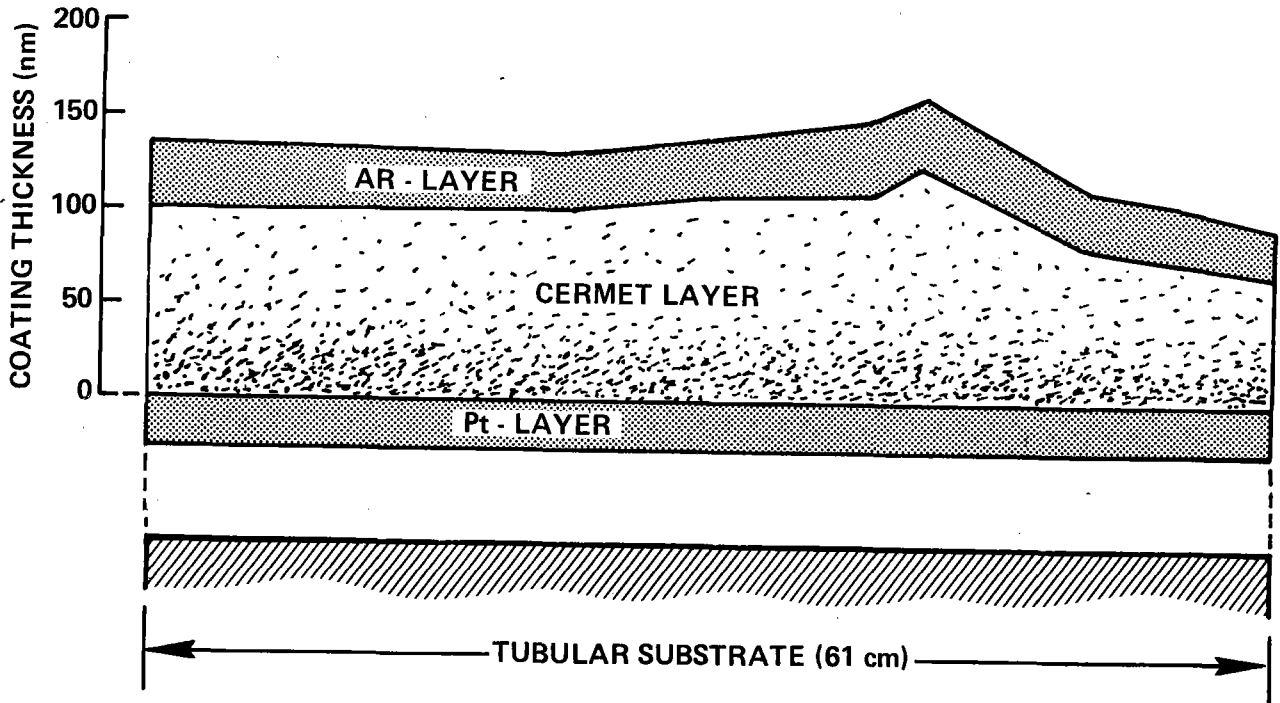


FIG. 32. Approximate axial profiles for the cermet and antireflection layer thicknesses that were deposited in the final sequence of bench type tube coating experiments. The cermet layer was graded with a Pt volume fraction (F) running from about 0.42 at the base to zero at the top surface.

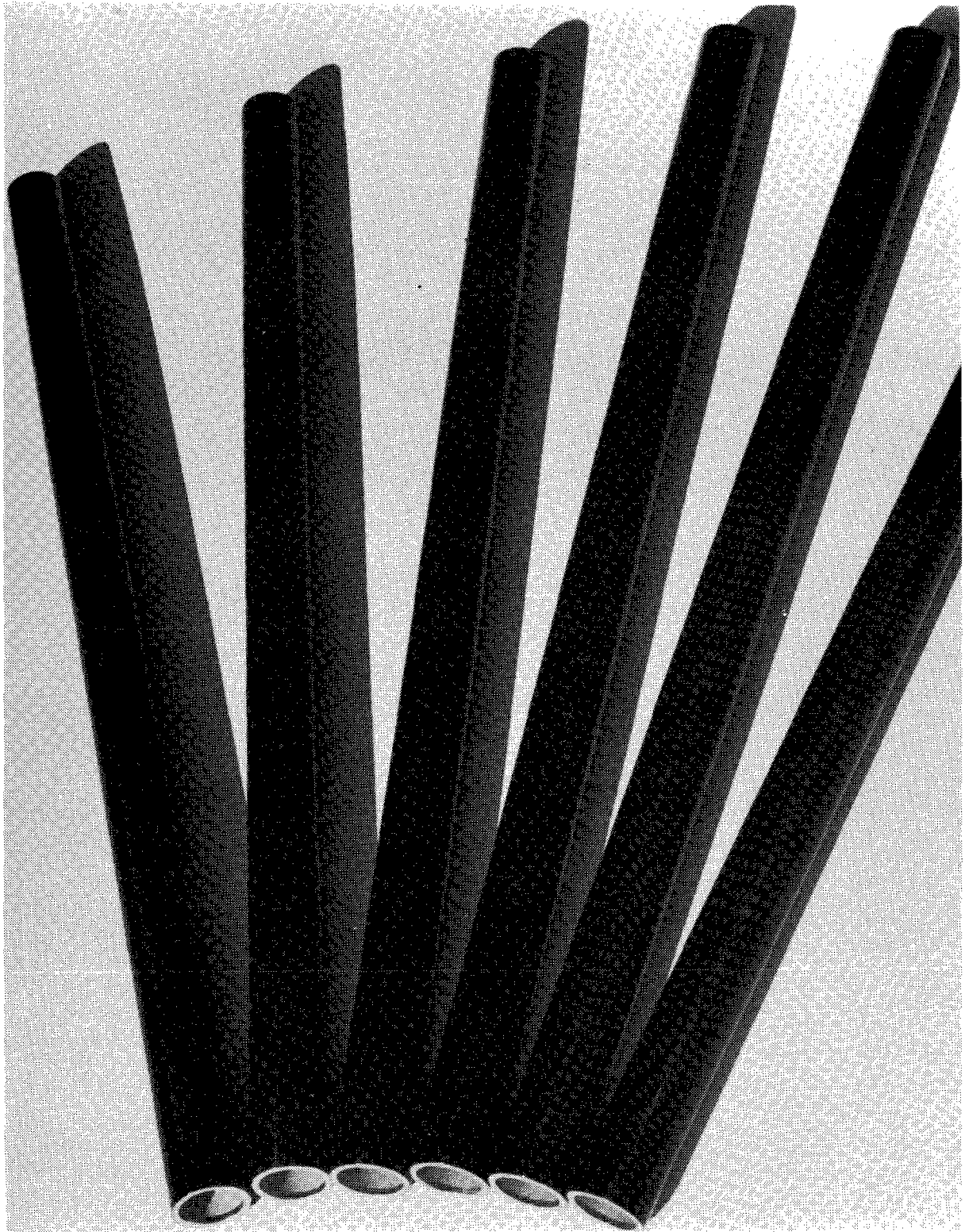


FIG. 33. Photograph showing several of the tubes that were coated during the bench type proof of concept experiments

Ar working pressure = 0.18 Pa.

Planetary translational speed \sim 1 cm/min.

Number of translational passes (down and back) during deposition of cermet layer = 6.

Total time required to deposit cermet layer = 475 min.

7. SUMMARY

The Pt/Al₂O₃ cermet system is extremely stable against oxidation. Therefore, effective high temperature selective absorber coatings can be formed by depositing Pt/Al₂O₃ cermets onto Pt low emittance base layers. Three cermet configurations have been investigated: (1) cermets with graded Pt composition and Al₂O₃ antireflection layers, (2) cermets with uniform Pt compositions and Al₂O₃ antireflection layers, and (3) Al₂O₃-M-Al₂O₃ multilayer coatings where the M-layer is a Pt/Al₂O₃ mixture containing about 20 volume percent Al₂O₃. The coatings were deposited by co-sputtering from Pt and Al₂O₃ sources. Both direct rf sputtering from an alumina target and dc reactive sputtering from an aluminum target in an Ar+O₂ atmosphere were investigated as methods for depositing the Al₂O₃ component of the cermet and the antireflection layers. Approximate cost analyses were made for Pt/Al₂O₃ cermet coatings deposited onto flat plate and tubular shapes in large production volumes. Significant cost reductions can be obtained by replacing the Pt low emittance base layer with a less costly material. Accordingly, Cr, Mo, Ta, W, and ZrB₂ were investigated as alternative base layer materials. The performance of coatings deposited onto flat plates of glass, type 316 stainless steel, type 1020 low carbon steel, and Incoloy 800 were examined. Proof-of-concept experiments were conducted in which graded cermet coatings were deposited onto 24-inch-long type 316 stainless steel receiver tubes.

The coatings in which the Al₂O₃ component of the cermet and antireflection layers was formed by direct rf sputtering of alumina were the most stable. When the Al₂O₃ was deposited by this method, and when elevated substrate temperatures (300-500°C) were used, all three of the coating configurations appeared to be stable at 600°C in air.

The graded cermet coatings appear to be the generally most useful of the three types examined.

The uniform cermet coatings consisted of a Pt/Al₂O₃ cermet about 100 nm thick, with a uniform Pt content of about 40% by volume, and a 70 nm thick

antireflection layer. Hemispherical absorptances were typically about 0.90. However, long wavelength interference effects caused the emittances to be relatively high at room temperature (0.15 to 0.20) and to increase rapidly with increasing temperature. This limits the usefulness of these coatings for high temperature applications.

The multi-layer AMA type coatings consisted of a Pt layer about 5 nm thick, containing about 20% by volume Al_2O_3 , which was sandwiched between two Al_2O_3 layers, about 40 nm thick. These coatings typically yielded hemispherical absorptances of about 0.92 with room temperature emittances of about 0.08. The low Pt content makes these coatings attractive for simple substrate shapes where the individual layer thicknesses could be controlled accurately. However, the critical nature of the coating layer thicknesses and interference effects makes these coatings less attractive for substrates of complex shape.

The graded cermet coatings consist typically of a Pt/ Al_2O_3 cermet layer about 70 to 150 nm thick, with a graded Pt content which varies from about 50% by volume at the rear surface to zero at the top surface. This layer is overcoated with an Al_2O_3 antireflection layer having a thickness in the range of 20 to 40 nm. The exact cermet thickness, Pt content, and grading profile do not appear to be critical. This is an important advantage for coating substrates of complex shape. Coatings with absorptances of 0.93 to 0.95 can be consistently obtained. Optimization of the antireflection layer thickness has yielded hemispherical absorptances as high as 0.97 (tested at independent laboratory). The graded cermet coatings can yield relatively sharp cut-off wavelengths, so that high absorptance to emittance ratios (α/ϵ) can be obtained, even for coatings operating at elevated temperatures. Typical room temperature α/ϵ values are in the range 10 to 17. Emittances for coatings on Pt-coated glass substrates vary from about 0.07 at 20°C to about 0.18 at 500°C.

Graded cermet coatings with direct rf sputtered Al_2O_3 , which were deposited onto Pt coated glass substrates at a temperature of 350°C, exhibited no change

in optical properties after being maintained at 600°C in air for 700 hrs. In general, coatings deposited at lower temperatures are slightly less stable, but adequate for many applications. Thus graded cermet coatings deposited onto Pt coated glass substrates at about 150°C (a convenient temperature for large scale production) showed no change in optical properties after being maintained at 400°C in air for about 1400 hrs.

The Pt cost in a typical Pt/Al₂O₃ graded cermet layer is about \$2/ft. It may be possible to significantly reduce this costs for some applications. The optimization studies have shown that absorptances of about 0.95 can be obtained for cermet layers that are sufficiently thin to reduce the Pt cost to about \$1/ft². Thermal stability test data for these coatings are limited and inconclusive, but suggest that these thin coatings may be less stable than the more typical coatings described above.

The cost of the Pt in a typical Pt low emittance base layer is about \$3/ft². Graded or uniform cermet coatings with Cr, Mo, Ta, and W low emittance base layers, which would considerably reduce the total coating cost, were deposited and tested. The coatings appear to be stable in air at 400°C for tests lasting several hundred hours. However, bare films of these materials underwent significant oxidation in tests at 400°C in air. Therefore, the long term stability of coatings incorporating Cr, Mo, Ta, and W base layers is in doubt. By contrast, bare ZrB₂ coatings were relatively stable in the 400°C air tests. Graded cermet coatings deposited onto ZrB₂ base layers on glass substrates were stable in air at 500°C for tests lasting about 1200 hrs. Unfortunately, the emittances of the sputtered ZrB₂ layers were about 0.20 (glass substrate) and therefore considerably above the expected values (0.06-0.09). However, this behavior is believed to have resulted from a defective sputtering target and not to be a fundamental limitation of ZrB₂ as a base layer material.

An Al₂O₃ diffusion barrier, typically 50 nm thick, was deposited between the substrate and the low emittance base layer when metallic "engineering" substrates were used. When such a diffusion barrier was in place, the graded

cermet coatings exhibited the same thermal stability on metal substrates that was observed on the glass substrates. Thus a graded cermet coating with direct rf sputtered Al_2O_3 , which was deposited onto a type 316 stainless steel plate at a substrate temperature of 350°C , exhibited no change in absorptance after about 2000 hrs at 600°C in air. A similar coating on a small type 316 stainless steel disk substrate showed no change in optical properties after being exposed to a radiation intensity of 2800 suns for 2 hrs.¹² Coatings deposited at 250°C onto type 316 stainless steel were stable during a 1700 hr test at 400°C in air. Similar coatings deposited at 150°C onto type 316 stainless steel, type 1020 low carbon steel, and Incoloy 800 substrates were stable at 400°C in air for tests lasting about 600 hrs.

A primary difference between metal "engineering" substrates and the glass substrates is in the surface roughness of the metal substrates. This roughness is typically on a size scale which produces a slight, and generally insignificant, increase in absorptance along with a large, typically factor of almost two, increase in emittance. In addition, there is evidence that the surface roughness can cause columnar growth flaws to develop within the coating during deposition.¹⁸ These flaws can provide diffusion paths which significantly degrade the thermal stability of the coatings. Thus substrate polishing is recommended for improving both the optical properties and the thermal stability of the coatings on engineering substrates. If this is done, and a suitable Al_2O_3 diffusion barrier is used between the substrate and the low emittance base layer, then the differences between the various engineering substrate materials themselves appear to introduce only second order effects.

A first set of bench type proof-of-concept experiments were completed, in which 24-inch-long receiver tubes were coated with graded cermet type coatings. A set of ten such tubes was shipped to SERI.

It is clear that cermet coating technology offers the solar thermal system designer a wide collection of design options. These options range from coatings with the highest α/ϵ values, and the greatest thermal stability in an

air environment that has been achieved for selective surfaces, to a continuous spectrum of lower performance coatings that can be deposited at lower cost. Thus the Cornell group has recently reported that high substrate temperatures ($\sim 675^{\circ}\text{C}$) can be used to deposit Pt/ Al_2O_3 graded cermet coatings with absorptances as high as 0.985 and emittances of about 0.08.²⁴ Our work described in this report has concentrated on Pt/ Al_2O_3 graded cermet coatings deposited at low substrate temperatures ($\sim 150^{\circ}\text{C}$) for medium temperature applications. Absorptances as high as 0.97 and thermal stability in air at the desired operating temperature ($\sim 400^{\circ}\text{C}$) have been demonstrated for both glass and engineering substrates.

REFERENCES

- 1) R.H. Hahn and B.O. Seraphin, "Spectrally Selective Surfaces for Photo-thermal Solar Energy Conversion," in Physics of Thin Films, Vol. 10, ed. by G. Hass and M.H. Francombe, Academic Press, New York (1978) p. 1.
- 2) O.P. Agnihotri and B.K. Gupta, Solar Selective Surfaces, Wiley, New York (1981).
- 3) S.A. Herzenberg and R. Silberglitt, "Low Temperature Selective Absorber Research," SPIE Vol. 324, "Optical Coatings for Energy Efficiency and Solar Applications," available from SPIE, P. O. Box 10, Bellingham, WA.
- 4) H.G. Craighead, "Optical Properties and Solar Selectivity of Metal-Insulator Composite Films," PhD Thesis, Cornell University, Ithaca, New York (1980).
- 5) H.G. Craighead, R. Bartynski, R.A. Buhrman, L. Wojcik and A.J. Sievers, "Metal/Insulator Composite Selective Absorbers," Solar Energy Materials, Vol. 1, p. 105 (1979).
- 6) J.A. Thornton, "High Rate Sputtering Techniques," Thin Solid Films, Vol. 80, p. 1 (1981).
- 7) J.A. Thornton, "Sputter Deposited Selective Absorber Coatings," Plating and Surface Finishing, Vol. 67, p. 48 (1980).
- 8) J.A. Thornton and J.L. Lamb, "Evaluation of Vacuum Deposition - Sputter Deposited Cermet Selective Absorber Coatings," Interim Technical Process Report, Jan. 15, 1980 to April 30, 1981, SERI Contract XP-9-8260-1, Telic Publication No. 82-1, Telic Company, Santa Monica, CA (July 1982).
- 9) J.A. Thornton and J.L. Lamb, "Sputter-Deposited Pt-Al₂O₃ Selective Absorber Coatings," Thin Solid Films, Vol. 83, p. 377 (1981).
- 10) J.A. Thornton and J.M. Lefferdo, "Selective Absorber Research," paper presented at STTFUA High Temperature Materials Workshop, Cocoa Beach, FL (January 1982).
- 11) J.A. Thornton, "Research on Sputter Deposited Selective Absorber Coatings," Proceedings 1982 ASTM MiCon Symposium, Houston, TX (Jan. 1982). Available from ASTM, Metals Park, OH.
- 12) Private communication, Professor Alex Ignatiev, Physics Department, University of Houston, Houston, TX (January 1982).

- 13) J.A. Thornton, A.S. Penfold and J.L. Lamb, "Sputter Deposited Al_2O_3 - $\text{Mo-Al}_2\text{O}_3$ Selective Absorber Coatings," Thin Solid Films, Vol. 72, p. 101 (1980).
- 14) J.A. Thornton and J.L. Lamb, "Thermal Stability Studies of Sputter-Deposited Multilayer Selective Absorber Coatings," Thin Solid Films, Vol. 96, 175 (1982).
- 15) R.W. Waits, "Planar Magnetron Sputtering," in Thin Film Processes, ed. by J.L. Vossen and W. Kern, Academic Press, New York (1978) p. 75.
- 16) B. Abeles, P. Sheng, M.D. Coutts and Y. Arie, "Structural and Electrical Properties of Granular Metal Films," Advances in Physics, Vol. 24, 407 (1975).
- 17) C.G. Granquist, "Selective Absorption of Solar Energy in Ultrafine Metal Particles: Model Calculations," J. Appl. Phys. Vol. 50, 1058 (1979).
- 18) J.A. Thornton, "High Rate Thick Film Growth," Ann. Rev. Mater. Sci. Vol. 7, 239 (1977).
- 19) H.G. Craighead, J.A. Thornton and J.L. Lamb, to be published.
- 20) P. Schwarzkopf and R. Kieffer, Refractory Materials, McGraw Hill, New York (1953) p. 283.
- 21) E. Randich and D.D. Allred, "Chemically Vapor-Deposited ZrB_2 As a Selective Solar Absorber," Thin Solid Films, Vol. 83, 393 (1981).
- 22) J.L. Vossen and J.J. Cuomo, "Glow Discharge Sputter Deposition," in Thin Film Processes, ed. by J.L. Vossen and W. Kern, Academic Press, New York (1978) p. 1.
- 23) J.A. Thornton and D.W. Hoffman, "Internal Stresses in Titanium, Nickel, Molybdenum, and Tantalum Films Deposited by Cylindrical Magnetron Sputtering," J. Vac. Sci. Technol. 14, 164 (1977).
- 24) G.A. Nyberg, H.G. Craighead and R.A. Buhrman, "Surface Roughness and Thermal Stability of Graded Cermet Photothermal Absorber Coatings with very High Absorptivities," Thin Solid Films, Vol. 96, 185 (1982).

SELECTED DISTRIBUTION LIST

ARCO Solar, Inc.
9315 Deering
Chatsworth, CA 91311
Mr. Jim Caldwell

Acurex Solar Corporation
485 Clyde Ave.
Mt. View, CA 94042
Mr. Don Duffy

Arizona Public Service Company
P.O. Box 21666
Phoenix, AZ 85036
Mr. Eric Weber

Babcock and Wilcox
91 Stirling Ave.
Barberton, OH 44203
Mr. Paul Elsbree

Barber-Nichols Engineering Co.
6325 W. 55th Ave.
Arvada, CO 80002
Mr. Robert Barber

Bechtel Corporation
P.O. Box 3965
San Francisco, CA 94119
Mr. Pascal DeLaquil

Black and Veatch Consulting
Engineers
1500 Meadow Lake Parkway
Kansas City, MO 64114
Dr. Charles Grosskreutz

Cornell University
Department of Physics
Ithaca, NY 14853
Dr. A. Sievers

Department of Energy/ALO
P.O. Box 1500
Albuquerque, NM 87115
Mr. Dean Graves

Department of Energy/HQ
Forrestal Building
1000 Independence Ave., SW
Washington, DC 20585
Dr. H. Coleman
Mr. S. Gronich
Mr. M. Scheve
Mr. Frank Wilkins

Department of Energy/SAN
1333 Broadway
Oakland, CA 94536
Mr. William Lambert

Department of Energy/SAO
1617 Cole Blvd.
Golden, CO 80401
Mr. Jerry Bellows

Electric Power Research Institute
P.O. Box 10412
Palo Alto, CA 94303
Mr. Donald Augenstein

Entech, Incorporated
P.O. Box 612246
DFW Airport, TX 75261
Mr. Walter Hesse

Farmland Industries
P.O. Box 69
Lawrence, KS 66044
Mr. John Prijatel

Foster Wheeler Solar Development
Corp.
12 Peach Tree Hill Road
Livingston, NJ 07070
Mr. Robert J. Zoschak

Gas Research Institute
8600 West Bryn Mawr Ave.
Chicago, IL 60631
Mr. Keith Davidson

Georgia Institute of Technology
Atlanta, GA 30332
Dr. Dan O'Neill

Georgia Power Company
7 Solar Circle
Shenandoah, GA 30265
Mr. Ed Ney

LaJet Energy Company
P.O. Box 3599
Abilene, TX 79604
Mr. Monte McGlaun

Luz Engineering Corp.
15720 Ventura Blvd.
Suite 504
Encino, CA 91436
Dr. David Kearney

Pacific Gas and Electric Company
3400 Crow Canyon Rd.
San Ramon, CA 94583
Mr. Gerry Braun

Power Kinetics, Inc.
1223 Peoples Ave.
Troy, NY 12180
Mr. Bob Rogers

Rockwell International
Energy Systems Group
8900 DeSoto Ave.
Canoga Park, CA 91304
Mr. Tom H. Springer

Sanders Associates, Inc.
95 Canal Street
Nashua, NH 03010
Mr. Daniel J. Shine

Sandia National Laboratories
Solar Energy Department 6220
P.O. Box 5800
Albuquerque, NM 87185
Mr. John Otts
Mr. James Leonard
Dr. Donald Schuler

Science Applications, Inc.
10401 Rosselle Street
San Diego, CA 92121
Dr. Barry Butler

Solar Energy Industries Association
1717 Massachusetts Ave. NW No. 503
Washington, DC 20036
Mr. Carlo La Porta

Solar Energy Research Institute
1617 Cole Blvd.
Golden, CO 80401
Mr. B. P. Gupta
Dr. D. Blake
Mr. G. Gross

Solar Kinetics, Inc.
P.O. Box 47045
Dallas, TX 75247
Mr. Gus Hutchison

Stirling Thermal Motors, Inc.
2841 Boardwalk
Ann Arbor, MI 48104
Mr. Benjamin Ziph

University of Illinois
Dept. of Mechanical and Industrial
Engineering
1206 W. Green Street
Urbana, IL 61801
Dr. Art Clausing

University of Illinois
Department of Physics
1206 W. Green Street
Urbana, IL 61801
Dr. John Thornton

Document Control Page	1. SERI Report No. SERI/STR-255-3040	2. NTIS Accession No.	3. Recipient's Accession No.
4. Title and Subtitle Evaluation of Cermet Selective Absorber Coatings Deposited by Vacuum Sputtering		5. Publication Date October 1986	
7. Author(s) John A. Thornton and James A. Lamb, Telic		8. Performing Organization Rept. No. Telic 82-4	
9. Performing Organization Name and Address Telic Company 1631 Colorado Avenue Santa Monica, California 90404		10. Project/Task/Work Unit No.	
		11. Contract (C) or Grant (G) No. (C) XP-9-8260-1 (G)	
12. Sponsoring Organization Name and Address Solar Energy Research Institute A Division of Midwest Research Institute 1617 Cole Boulevard Golden, Colorado 80401-3393		13. Type of Report & Period Covered Technical Report	
15. Supplementary Notes		14.	
16. Abstract (Limit: 200 words) This report describes a project undertaken to investigate the use of sputtering. The study describes experiments in which 24-inch long receiver tubes were coated with Pt/Al ₂ O ₃ graded cermet coatings by sputtering. Three coatings were examined: (1) cermets with graded Pt composition and Al ₂ O ₃ antireflection layers; (2) cermets with uniform Pt compositions and Al ₂ O ₃ antireflection layers; and (3) Al ₂ O ₃ -M-Al ₂ O ₃ type coatings with Pt/Al ₂ O ₃ M-layers. Sputter codeposition was used to form the cermet layers. Direct rf-sputtering of alumina and dc-reactive sputtering of aluminum were investigated as methods for depositing the Al ₂ O ₃ . The rf-sputtered Al ₂ O ₃ was found to yield coatings with superior thermal stability. Thus, all three coating configurations were stable in air at 600°C. Absorptances were in the range from 0.90 to 0.95. The study concluded that graded cermet coatings were the most useful of the three types examined; optimized coatings on Pt-coated glass substrates yield absorptances of 0.97 and room-temperature emittances of about 0.08; alternative IR reflector layer materials were limited to low-temperature applications; substrate surface polishing is important in affecting the optical properties and thermal stability of coatings deposited onto engineering substrates; and an Al ₂ O ₃ diffusion barrier was required to achieve maximum thermal stability for coatings deposited onto the engineering substrates.			
17. Document Analysis			
a. Descriptors Antireflection Coatings ; Cermets ; Solar Absorbers ; Solar Receivers ; Surface Coating ; Vacuum Coating ; Vacuum Deposition ; Vacuum Evaporation			
b. Identifiers/Open-Ended Terms			
c. UC Categories 59a, 62b, c			
18. Availability Statement National Technical Information Service U.S. Department of Commerce 5285 Port Royal Road Springfield, Virginia 22161		19. No. of Pages 100	
		20. Price A05	